Protein tyrosine phosphatases in zebrafish development and regeneration

Maaike Allers

Protein tyrosine phosphatases in zebrafish development and regeneration

Proteïne tyrosine fosfatases in zebravis ontwikkeling en regeneratie
(met een samenvatting in het Nederlands)

Proefschrift

ter verkrijging van de graad van doctor aan de
Universiteit Utrecht
op gezag van de
rector magnificus, prof. dr. H.R.B.M. Kummeling,
ingevolge het besluit van het college voor promoties
in het openbaar te verdedigen op

dinsdag 30 januari 2024 des ochtends te 10.15 uur

door

Maaike Allers

geboren op 4 januari 1993
te Nieuwegein

Colofon
The work described in this thesis was performed at the Hubrecht Institute for Developmental Biology and Stem Cell Research (Royal Netherlands Academy of Arts and Sciences, KNAW), within the framework of the research school Cancer, Stem Cells and Developmental Biology (CS&D), which is part of the Utrecht Graduate School of Life Sciences (Utrecht University).

The work was funded by a grant from the Dutch Research Council to Jeroen den Hertog (ALW OP.234).

MIX
Paper from responsible sources
FSC
www.fsc.org

Cover design and layout: © evelienjagtman.com
Printed by: Ipskamp Printing

ISBN/EAN: 978-94-6473-311-2
DOI: https://doi.org/10.33540/2092

Promotoren:
Prof. dr. J.P.W.M. Bakkers
Prof. dr. J. den Hertog

Beoordelingscommissie:
Prof. dr. ir. B.M.T. Burgering (voorzitter)
Prof. dr. H.C. Korswagen
Prof. dr. R.J. Pasterkamp
Prof. dr. E. van Rooij
Prof. dr. H.P. Spaink

Dit proefschrift werd (mede) mogelijk gemaakt met financiële steun van de Nederlandse organisatie voor Wetenschappelijk Onderzoek aan Jeroen den Hertog (ALW OP.234).

Table of contents

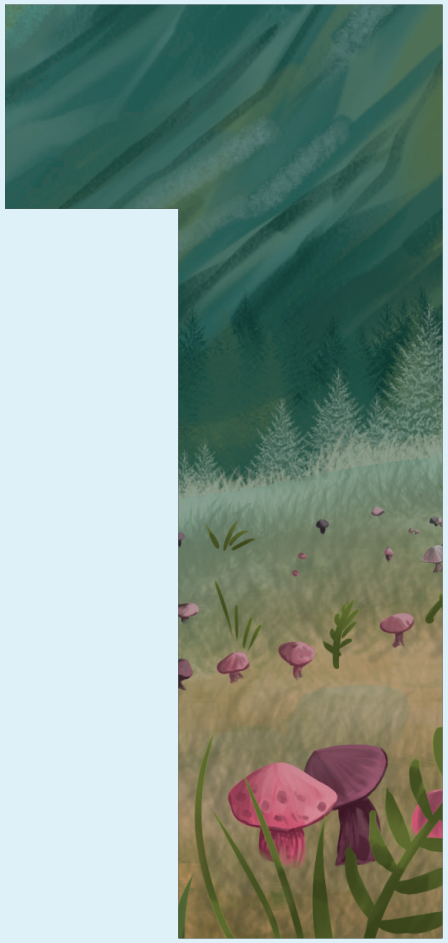

Introduction

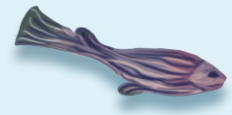

Introduction

Protein tyrosine phosphatases have an essential role in cell signaling

Protein tyrosine phosphatases (PTPs) have a central role in cell signaling with diverse functions in cell proliferation, migration, differentiation and apoptosis. These enzymes regulate a multitude of functions by dephosphorylating their target proteins, thereby balancing the activity of kinases. Together, kinases and PTPs guard a balance in innumerable cell signaling pathways. Loss of this balance has been linked to a plethora of human diseases, including cancer (Hendriks *et al*., 2013; Tautz *et al*., 2013; Tonks, 2006; T. Wang *et al*., 2022).

The human superfamily of PTPs is composed of 125 genes and can be subdivided into four classes. The largest class consists of the class I cysteine-based members (Andres Alonso *et al*., 2004; Andrés Alonso *et al*., 2016). This class can be further specified as classical and dual specificity PTPs. This thesis will focus on several members of the classical PTP subfamily. Classical PTPs can only dephosphorylate tyrosine residues. The phosphate on the target tyrosine is attacked by the catalytic cysteine, in the middle of the active site. This cysteine has a low pKa and is conserved in all PTPs. The reaction is supported by an invariant arginine that stabilizes the transition. Subsequently, the phosphate gets released from the cysteine by hydrolysis, with assistance from a catalytic aspartate and a water molecule that gets positioned by a conserved glutamate (Denu *et al*., 1996; Z. Y. Zhang *et al*., 1994). The positions of these supporting amino acids are strongly conserved across all class I classical PTPs. Even though the PTPs all share a highly similar active site, there are differences in efficiencies and target proteins. These differences are caused by small differences between the active sites, as well as different protein binding domains, and most likely differences in subcellular localization.

Box 1: **The nomenclature of genes and proteins in humans, mice and zebrafish.**
Gene and protein names are written in a different manner for humans, mice and zebrafish. In this way we can distinguish what species is being discussed. Only the protein name for humans and mice is identical. Gene names for zebrafish are written in lowercase, unless they are the starting word of a sentence, in which case they will start with an uppercase letter and therefore resemble a mouse gene.

Human: *GENE* / PROTEIN
Mouse: *Gene* / PROTEIN
Zebrafish: *gene* / Protein

Zebrafish are a highly useful model organism

We investigated PTPs in zebrafish development and regeneration. Due to their easy maintenance and short generation times, zebrafish are a widely popular model organism. A single pair of fish can generate hundreds of embryos every week. These embryos are transparent, which makes them highly useful for developmental biology research. Zebrafish embryos are also easily manipulated, with a range of methods available to mutate the genome, induce a certain gene expression, generate a knock-down or infect embryos. Over the years, many transgenic zebrafish lines have been generated, which are highly useful to investigate the development and function of certain cell types. The evolutionary conservation between zebrafish and humans is strong, however zebrafish have undergone one additional round of genome duplication (Postlethwait *et al.*, 1998; Taylor *et al.*, 2001). This causes many genes to be present in duplicate, compared to the human genome.

In addition to the previously mentioned characteristics, zebrafish possess a remarkable capacity to regrow tissues or organs after damage, called regeneration. Upon injury of many organs, including the heart, or even amputation of fins, zebrafish will regenerate the lost structures within days or weeks (reviewed in Marques *et al.*, 2019). Both embryonic and adult zebrafish possess the capacity to regenerate. A lot is still unknown about how the process of regeneration takes place. Many signaling pathways have already been implicated, which shows that a very complex signaling program organizes regeneration.

One of the earliest signaling events upon injury, in many - if not all - species, is the production of a burst of reactive oxygen species. This production of reactive oxygen species (ROS), such as H_2O_2, plays an extensive role in wound healing in mice and drosophila embryos and it has been shown to be essential for correct regeneration in zebrafish, planarians, axolotls and xenopus (Carbonell-M *et al.*, 2022; Ferreira *et al.*, 2016; Gauron *et al.*, 2013; Hunter *et al.*, 2018; Love *et al.*, 2013; Niethammer *et al.*, 2009; Pirotte *et al.*, 2015; Roy *et al.*, 2006). It is known that the gradient of H_2O_2 plays a role in the attraction of macrophages, but this cannot be its only function, since depletion of macrophages does not abolish regeneration (L. Li *et al.*, 2012). One of the other possible functions is that this burst of H_2O_2 functions to oxidize certain target proteins.

Specific PTPs get oxidized during zebrafish tail fin regeneration

PTPs are highly susceptible to oxidation, due to the low pKa of their active sites (Denu & Tanner, 1998; Meng *et al.*, 2002; Östman *et al.*, 2011; Peters *et al.*, 1998). Their reactive cysteine gets oxidized, which leads to the temporary inactivation of the PTP. The exact susceptibility of a PTP to oxidation depends on the circumstances and the kind of reactive oxygen species that is causing the oxidation.

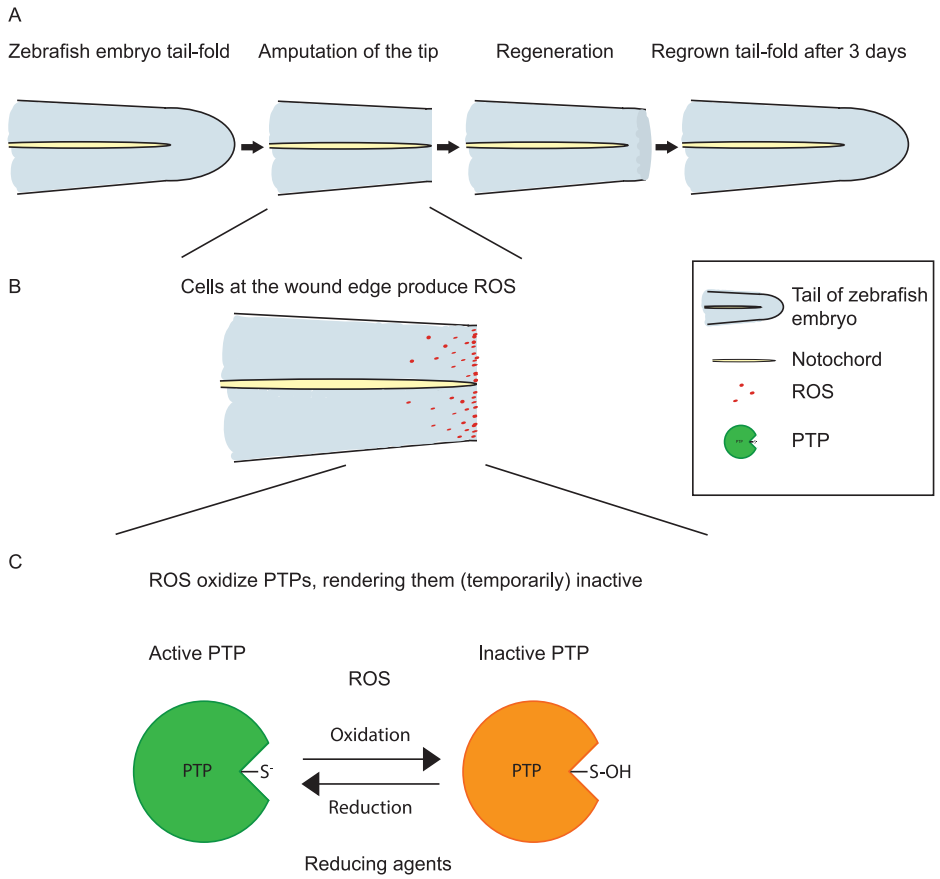

Figure 1: Schematic representation of regeneration after amputation of tail-fold from zebrafish embryo. A: Schematic representation of the tail-fold from a zebrafish embryo before amputation of the tip, directly after amputation, during regeneration and 3 days post amputation, when the tail-fold has regrown. The notochord is indicated in yellow. B: Schematic overview of the tail-fold of a zebrafish embryo several hours after amputation of the tip, when the cells at the wound edge produce ROS (indicated in red) that diffuse inside the embryo. C: Schematic representation of PTPs that are oxidized by ROS at their active site, hence rendering them inactive until they are reduced again by reducing agents.

It was hypothesized that oxidation of certain PTPs by the burst of H_2O_2 might play a role in causing specific signaling programs initiating regeneration. To challenge this hypothesis, mass-spec experiments were performed on tail clips of zebrafish before and after amputation of the tail fin. PTPs were isolated using an oxPTP antibody and mass-spec was performed to determine which PTPs were present in the sample. Using a specific set of alkylating and oxidizing circumstances, the authors were able to distinguish which PTPs were oxidized at the time of collection and which were not.

Eight PTPs were specifically oxidized after amputation of the caudal fin. These PTPs were *ptpn11a* (Shp2a), *ptpn11b* (Shp2b), *ptpn1* (PTP-1b), *ptpn2a* (TC-PTPa), *ptpn4b* (PTP-Meg1b), *ptpn9a* (PTP-Meg2a), *ptprea* and *ptprh1* (Wu *et al*., 2017). It was discovered that one of these PTPs, *ptpn11a*, was essential for regeneration to proceed. Embryos without a functional variant of *ptpn11a* were unable to regenerate their caudal fin after the blastema stage (Hale & den Hertog, 2018).

SHP2 is a protein implicated in many diseases

The gene *ptpn11a* encodes the protein Src homology 2 (SH2) domain containing protein tyrosine phosphatase 2a (Shp2a). In zebrafish, a paralog of *ptpn11a* is present, due to the aforementioned genome duplication, which is called *ptpn11b*. *ptpn11b* encodes the protein Shp2b, which is very similar to Shp2a, however it shows a different expression pattern. Shp2b is not essential for regeneration to proceed in zebrafish.

Besides regeneration, Shp2a is essential for the embryonic survival of zebrafish and its paralog Shp2 is essential for the survival of mouse embryos (Bonetti, Rodriguez-Martinez, *et al*., 2014; Yang *et al*., 2006). In humans, gain-of-function mutations in SHP2, that lead to increased SHP2 activity, are involved in the developmental disorders Noonan syndrome and Noonan syndrome with multiple lentigines (Bonetti, Overman, *et al*., 2014; Digilio *et al*., 2002; Fragale *et al*., 2004; Legius *et al*., 2002; Tartaglia *et al*., 2002). Mutation of Shp2a in zebrafish has recapitulated symptoms seen in humans with these disorders (Bonetti, Rodriguez-Martinez, *et al*., 2014; Jopling *et al*., 2007; Solman *et al*., 2022). Children with these disorders are more susceptible to specific kinds of cancer, like juvenile myelomonocytic leukemia. In addition, activating mutations in SHP2 are linked to the development of several other kinds of cancer, like breast, lung, gastric, and neuroblastoma tumors and adult acute myeloid leukemia (Bentires-Alj *et al*., 2004; H. Chen *et al*., 2020).

This indicates that SHP2 is a highly important and conserved player in cell signaling in embryonic development, regeneration and cancer across species. In many circumstances, it has been shown that SHP2 functions by activating the SRC/RAS/ERK pathway (Cai *et al*., 2011; Easton *et al*., 2006; Hale & den Hertog, 2018; Yang *et al*., 2006; S. Q. Zhang *et al*., 2004; Zhu *et al*., 2020).

Shp2a is thus essential for regeneration in zebrafish and most likely functions by activating the Src/Ras/Erk pathway. The oxidation of Shp2a at the beginning of the regeneration process, that temporarily inactivates Shp2a, seems paradoxical to its function in regeneration. We will investigate this further in this thesis.

PTPs are implicated in many different processes

The other PTPs that were implicated to be oxidized upon amputation, range from being extensively studied to hardly known. Here we give an overview of the current state of knowledge for the other PTPs that will be discussed in this thesis. Too much work has been done to describe all knowledge in this brief summary, so a select number of findings is discussed.

PTP1B, encoded by *Ptpn1,* was discovered to be pivotal in regulation of the insulin receptor and the generation of obesity as a result of a high fat diet in mice (Bence *et al*., 2006; Cheng *et al*., 2002; Elchebly *et al*., 1999; Klaman *et al*., 2000). In humans, PTPN1 polymorphisms have been associated with lower obesity (Salazar-Tortosa *et al*., 2022). Recently, it has been shown that mice depleted from PTP1B show a shorter lifespan and increased development of acute myeloid leukemia (Le Sommer *et al*., 2018). Macrophages of both mice and human origin show less viability and increased inflammation, when PTPN1 is depleted (Heinonen *et al*., 2009; Pike *et al*., 2014; Través *et al*., 2017). These data indicate that while PTP1B plays an essential role in developing obesity and diabetes in response to a high fat diet, it is also essential in macrophages to prevent excessive inflammation.

Besides regulation of insulin signaling, PTP1B is involved in inhibiting the JAK2-STAT3 pathway, the PI3/Akt pathway in HepG2 cells and VEGF signaling in endothelial cells in mice, while in human cells PTP1B is implicated in inhibiting the JNK-MAPK pathway (Gu *et al*., 2003; Lanahan *et al*., 2014; H. Li *et al*., 2014; Moon *et al*., 2017; Myers *et al*., 2001; Tsunekawa *et al*., 2017).

TCPTP, encoded by *Ptpn2* has been shown to be essential for the development of T-cells, by inhibiting IL7-recepter - Stat signaling in stromal cells (Pike *et al*., 2017; Wiede *et al*., 2014; You-Ten *et al*., 1997). Depletion of TCPTP in the T-cells themselves, results in increased expansion and survival (Flosbach *et al*., 2020; Wiede *et al*., 2014). *In vitro*, JAK1-STAT3, JAK3-STAT5 and STAT1 signaling were affected by TCPTP (Shields *et al*., 2008; Simoncic *et al*., 2002; ten Hoeve *et al*., 2002). In addition, TCPTP was found to control insulin signaling supplementary to PTP1B *in vitro* (Galic *et al*., 2005).

Ptpn4a is known to play a role at the synapses by dephosphorylating the NMDAR subunits GluN2A and GluN2B (Espinoza *et al*., 2020). In addition, deletion of the *Drosophila* homolog of *PTPN4*, called *ptpmeg*, affects the maintenance of the mushroom body axon branches (Whited *et al*., 2007). *In vitro*, Ptpn4 has been implicated in affecting cell growth and motility by interacting with CrkI (Zhou *et al*., 2013). In addition, Ptpn4 has been shown *in vitro* to interact with TRAM and TCR ζ in immune cells (Huai *et al*., 2015; Young *et al*., 2008). However, there is no effect of *ptpn4* deletion on the development of T-cells (Young *et al*., 2008).

PTP-MEG2, encoded by *PTPN9* is essential for expansion of human erythroid cells and *ptpn9a* is essential for the correct development of erythroid cells in zebrafish (Bu *et al*., 2014; Xu *et al*., 2003). Both in the zebrafish, as well as in breast and colorectal cancer cells, PTP-MEG2 has been shown to act by dephosphorylation of STAT3 (Su *et al*., 2012; D. Wang *et al*., 2019). Finally, PTP-MEG2 has been shown to inhibit VEGF signaling in endothelial cells (Hao *et al*., 2012).

The different roles of PTPRE in different cell types were accurately reviewed by Liang *et al* (Liang *et al*., 2019). Briefly, PTPRE has been shown to inhibit signaling by the insulin receptor (Moller *et al*., 1995). In addition, both osteoclasts and macrophages with deletion of Ptpre showed deficiencies in their functional activity (Chiusaroli *et al*., 2004; Finkelshtein *et al*., 2014; Sully *et al*., 2001). Finally, mice lacking *Ptpre* also show hypomyelination (Peretz *et al*., 2000).

Not much is known about *ptprh.* PTPRH dephosphorylates the EGFR directly, both in general and in asthmatic lung cells (F. J. Chen *et al*., 2022; Swiatnicki *et al*., 2022; Yao *et al*., 2017). In addition, PTPRH was found as an inhibitor of hyperactive STAT3 *in vitro* (Parri *et al*., 2020).

These data together indicate that there is some overlap in the pathways that are affected by the PTPs discussed in this thesis. However, deletion of each PTP leads to very specific disturbances in model organisms. This indicates that each PTP has its own specific role in specific cell types. In this thesis we investigate if these PTPs play a role during fin regeneration or development in zebrafish.

Finally, this thesis also concerns one additional PTP, namely *ptpn6*. The non-receptor protein tyrosine phosphatase SHP1 encoded by the *PTPN6* gene is a key regulator of immune cell function. SHP1 is, as the name suggests, highly similar to SHP2. As a result, we were interested in investigating the role of SHP1 in development and regeneration. SHP1 is mainly expressed in hematopoietic cells (Neel, Gu and Pao, 2003). Because of its important role in regulating immune cell function, SHP1 has become an interesting target for treatment of auto-immune diseases and cancer in recent years (Watson *et al.*, 2016).

Scope of this thesis

In this thesis we discuss the role of 11 specific PTPs in regeneration and zebrafish development. These PTPs were chosen due to their oxidation status in a mass spectrometry screen, that was performed previously. In addition, we investigate the role of another PTP, Shp1, in zebrafish development. Finally, we also created a tool for inhibiting the oxidation of PTPs, which we used to investigate the role of oxidation of Shp2a during regeneration.

Outline of this thesis

In **chapter 2** we discuss the generation of 22 knock-out lines, 2 for each chosen PTP. We show that regeneration was not affected in zebrafish missing *ptpn1, ptpn2a, ptpn2b, ptpn4a, ptpn4b, ptpn9a, ptpn9b, ptprea, ptpreb, ptprh1* or *ptprh2.* We also show that in cases where there are two paralogs, regeneration was not affected in zebrafish missing both paralogs. In addition, we found that embryonic development was not affected in any of these zebrafish lines, which was unexpected, given the function of some of these genes in other model systems. However, we did notice juvenile mortality in the *ptpn4a* mutant line, which we further explored in **chapter 3**. In this chapter we confirm the essential role that *PTPN4* played in neurodevelopment across species. We show that zebrafish missing *ptpn4a* suffered from deadly epileptic seizures during juvenile development. However, we also show that some zebrafish compensated for the loss of *ptpn4a* and survived. In **chapter 4** we switched to the investigation of another PTP, *ptpn6*. We show that knockout of *ptpn6* in zebrafish resulted in severe inflammation and death of juvenile zebrafish. We show that the development and behavior of immune cells and hematopoietic stem cells was already affected during embryonic development. Finally, in **chapter 5** we describe a variant of Shp2a that prevented oxidation of Shp2a *in vivo*. Using this variant, we show that oxidation of Shp2 is required for caudal fin-fold regeneration in embryos. In **chapter 6** we discuss the findings from the different experimental chapters.

Literature list

Alonso, Andrés, Nunes-Xavier, C. E., Bayón, Y., & Pulido, R. (2016). The Extended Family of Protein Tyrosine Phosphatases. *Methods in Molecular Biology (Clifton, N.J.)*, *1447*, 1–23. https://doi.org/10.1007/978-1-4939-3746-2_1

Alonso, Andres, Sasin, J., Bottini, N., Friedberg, I., Friedberg, I., Osterman, A., Godzik, A., Hunter, T., Dixon, J., & Mustelin, T. (2004). Protein tyrosine phosphatases in the human genome. *Cell*, *117*(6), 699–711. https://doi.org/10.1016/j.cell.2004.05.018

Bence, K. K., Delibegovic, M., Xue, B., Gorgun, C. Z., Hotamisligil, G. S., Neel, B. G., & Kahn, B. B. (2006). Neuronal PTP1B regulates body weight, adiposity and leptin action. *Nature Medicine*, *12*(8), 917–924. https://doi.org/10.1038/nm1435

Bentires-Alj, M., Paez, J. G., David, F. S., Keilhack, H., Halmos, B., Naoki, K., Maris, J. M., Richardson, A., Bardelli, A., Sagarbaker, D. J., Richards, W. G., Du, J., Girard, L., Minna, J. D., Loh, M. L., Fisher, D. E., Velculescu, V. E., Vogelstein, B., Meyerson, M., … Neel, B. G. (2004). Activating mutations of the noonan syndrome-associated SHP2/PTPN11 gene in human solid tumors and adult acute myelogenous leukemia. *Cancer Research*, *64*(24), 8816–8820. https://doi.org/10.1158/0008-5472.CAN-04-1923

Bonetti, M., Overman, J. P., Tessadori, F., Noël, E., Bakkers, J., & den Hertog, J. (2014). Noonan and LEOPARD syndrome Shp2 variants induce heart displacement defects in zebrafish. *Development (Cambridge, England)*, *141*(9), 1961–1970. https://doi.org/10.1242/DEV.106310

Bonetti, M., Rodriguez-Martinez, V., Paardekooper Overman, J., Overvoorde, J., van Eekelen, M., Jopling, C., & Hertog, J. den. (2014). Distinct and Overlapping Functions of ptpn11 Genes in Zebrafish Development. *PLoS ONE*, *9*(4), e94884. https://doi.org/10.1371/journal.pone.0094884

Bu, Y., Su, F., Wang, X., Gao, H., Lei, L., Chang, N., Wu, Q., Hu, K., Zhu, X., Chang, Z., Meng, K., & Xiong, J.-W. (2014). Protein tyrosine phosphatase PTPN9 regulates erythroid cell development through STAT3 dephosphorylation in zebrafish. *Journal of Cell Science*, *127*(Pt 12), 2761–2770. https://doi.org/10.1242/jcs.145367

Cai, Z., Simons, D. L., Fu, X.-Y., Feng, G.-S., Wu, S. M., & Zhang, X. (2011). Loss of Shp2-mediated mitogen-activated protein kinase signaling in Muller glial cells results in retinal degeneration. *Molecular and Cellular Biology*, *31*(14), 2973–2983. https://doi.org/10.1128/MCB.05054-11

Carbonell-M, B., Zapata Cardona, J., & Delgado, J. P. (2022). Post-amputation reactive oxygen species production is necessary for axolotls limb regeneration. *Frontiers in Cell and Developmental Biology*, *0*, 1690. https://doi.org/10.3389/FCELL.2022.921520

Chen, F. J., Du, L. J., Zeng, Z., Huang, X. Y., Xie, C. M., Liang, Y. X., Guo, Y. B., Xu, C. Y., & Tan, W. P. (2022). PTPRH Alleviates Airway Obstruction and Th2 Inflammation in Asthma as a Protective Factor. *Journal of Asthma and Allergy*, *15*, 133–144. https://doi.org/10.2147/JAA.S340059

Chen, H., Libring, S., Ruddraraju, K. V., Miao, J., Solorio, L., Zhang, Z. Y., & Wendt, M. K. (2020). SHP2 is a multifunctional therapeutic target in drug resistant metastatic breast cancer. *Oncogene*, *39*(49), 7166–7180. https://doi.org/10.1038/s41388-020-01488-5

Cheng, A., Uetani, N., Simoncic, P. D., Chaubey, V. P., Lee-Loy, A., McGlade, C. J., Kennedy, B. P., & Tremblay, M. L. (2002). Attenuation of leptin action and regulation of obesity by protein tyrosine phosphatase 1B. *Developmental Cell*, *2*(4), 497–503. http://www.ncbi.nlm.nih.gov/pubmed/11970899

Chiusaroli, R., Knobler, H., Luxenburg, C., Sanjay, A., Granot-Attas, S., Tiran, Z., Miyazaki, T., Harmelin, A., Baron, R., & Elson, A. (2004). Tyrosine phosphatase epsilon is a positive regulator of osteoclast function in vitro and in vivo. *Molecular Biology of the Cell*, *15*(1), 234–244. https://doi.org/10.1091/MBC.E03-04-0207

Denu, J. M., Lohse, D. L., Vijayalakshmi, J., Saper, M. A., & Dixon, J. E. (1996). Visualization of intermediate and transition-state structures in protein-tyrosine phosphatase catalysis. *Proceedings of the National Academy of Sciences of the United States of America*, *93*(6), 2493. https://doi.org/10.1073/PNAS.93.6.2493

Denu, J. M., & Tanner, K. G. (1998). Specific and reversible inactivation of protein tyrosine phosphatases by hydrogen peroxide: Evidence for a sulfenic acid intermediate and implications for redox regulation. *Biochemistry*, *37*(16), 5633–5642. https://doi.org/10.1021/BI973035T/ASSET/IMAGES/LARGE/BI973035TH00002.JPEG

Digilio, M. C., Conti, E., Sarkozy, A., Mingarelli, R., Dottorini, T., Marino, B., Pizzuti, A., & Dallapiccola, B. (2002). Grouping of multiple-lentigines/LEOPARD and Noonan syndromes on the PTPN11 gene. *American Journal of Human Genetics*, *71*(2), 389–394. https://doi.org/10.1086/341528

Easton, J. B., Royer, A. R., & Middlemas, D. S. (2006). The protein tyrosine phosphatase, Shp2, is required for the complete activation of the RAS/MAPK pathway by brain-derived neurotrophic factor. *Journal of Neurochemistry*, *97*(3), 834–845. https://doi.org/10.1111/J.1471-4159.2006.03789.X

Elchebly, M., Payette, P., Michaliszyn, E., Cromlish, W., Collins, S., Loy, A. L., Normandin, D., Cheng, A., Himms-Hagen, J., Chan, C. C., Ramachandran, C., Gresser, M. J., Tremblay, M. L., & Kennedy, B. P. (1999). Increased Insulin Sensitivity and Obesity Resistance in Mice Lacking the Protein Tyrosine Phosphatase-1B Gene. *Science*, *283*(5407), 1544–1548. https://doi.org/10.1126/SCIENCE.283.5407.1544

Espinoza, S., Arredondo, S. B., Barake, F., Carvajal, F., Guerrero, F. G., Segovia-Miranda, F., Valenzuela, D. M., Wyneken, U., Rojas-Fernández, A., Cerpa, W., Massardo, L., Varela-Nallar, L., & González, A. (2020). Neuronal surface P antigen (NSPA) modulates postsynaptic NMDAR stability through ubiquitination of tyrosine phosphatase PTPMEG. *BMC Biology*, *18*(1). https://doi.org/10.1186/s12915-020-00877-2

Ferreira, F., Luxardi, G., Reid, B., & Zhao, M. (2016). Early bioelectric activities mediate redox-modulated regeneration. *Development*, *143*(24), 4582–4594. https://doi.org/10.1242/dev.142034

Finkelshtein, E., Lotinun, S., Levy-Apter, E., Arman, E., den Hertog, J., Baron, R., & Elson, A. (2014). Protein tyrosine phosphatases and perform nonredundant roles in osteoclasts. *Molecular Biology of the Cell*, *25*(11), 1808–1818. https://doi.org/10.1091/mbc.E14-03-0788

Flosbach, M., Oberle, S. G., Scherer, S., Zecha, J., von Hoesslin, M., Wiede, F., Chennupati, V., Cullen, J. G., List, M., Pauling, J. K., Baumbach, J., Kuster, B., Tiganis, T., & Zehn, D. (2020). PTPN2 Deficiency Enhances Programmed T Cell Expansion and Survival Capacity of Activated T Cells. *Cell Reports*, *32*(4). https://doi.org/10.1016/J.CELREP.2020.107957

Fragale, A., Tartaglia, M., Wu, J., & Gelb, B. D. (2004). Noonan syndrome-associated SHP2/PTPN11 mutants cause EGF-dependent prolonged GAB1 binding and sustained ERK2/MAPK1 activation. *Human Mutation*, *23*(3), 267–277. https://doi.org/10.1002/HUMU.20005

Galic, S., Hauser, C., Kahn, B. B., Haj, F. G., Neel, B. G., Tonks, N. K., & Tiganis, T. (2005). Coordinated Regulation of Insulin Signaling by the Protein Tyrosine Phosphatases PTP1B and TCPTP. *Molecular and Cellular Biology*, *25*(2), 819. https://doi.org/10.1128/MCB.25.2.819-829.2005

Gauron, C., Rampon, C., Bouzaffour, M., Ipendey, E., Teillon, J., Volovitch, M., & Vriz, S. (2013). Sustained production of ROS triggers compensatory proliferation and is required for regeneration to proceed. *Scientific Reports*, *3*(1), 2084. https://doi.org/10.1038/srep02084

Gu, F., Dubé, N., Kim, J. W., Cheng, A., Ibarra-Sanchez, M. de J., Tremblay, M. L., & Boisclair, Y. R. (2003). Protein tyrosine phosphatase 1B attenuates growth hormone-mediated JAK2-STAT signaling. *Molecular and Cellular Biology*, *23*(11), 3753–3762. http://www.ncbi.nlm.nih.gov/pubmed/12748279

Hale, A. J., & den Hertog, J. (2018). Shp2-Mitogen-Activated Protein Kinase Signaling Drives Proliferation during Zebrafish Embryo Caudal Fin Fold Regeneration. *Molecular and Cellular Biology*, *38*(4), e00515-17. https://doi.org/10.1128/MCB.00515-17

Hao, Q., Samten, B., Ji, H.-L., Zhao, Z. J., & Tang, H. (2012). Tyrosine phosphatase PTP-MEG2 negatively regulates vascular endothelial growth factor receptor signaling and function in endothelial cells. *American Journal of Physiology-Cell Physiology*, *303*(5), C548–C553. https://doi.org/10.1152/ajpcell.00415.2011

Heinonen, K. M., Bourdeau, A., Doody, K. M., & Tremblay, M. L. (2009). Protein tyrosine phosphatases PTP-1B and TC-PTP play nonredundant roles in macrophage development and IFN- signaling. *Proceedings of the National Academy of Sciences*, *106*(23), 9368–9372. https://doi.org/10.1073/pnas.0812109106

Hendriks, W. J. A. J., Elson, A., Harroch, S., Pulido, R., Stoker, A., & Den Hertog, J. (2013). Protein tyrosine phosphatases in health and disease. *The FEBS Journal*, *280*(2), 708–730. https://doi.org/10.1111/FEBS.12000

Huai, W., Song, H., Wang, L., Li, B., Zhao, J., Han, L., Gao, C., Jiang, G., Zhang, L., & Zhao, W. (2015). Phosphatase PTPN4 Preferentially Inhibits TRIF-Dependent TLR4 Pathway by Dephosphorylating TRAM. *The Journal of Immunology*, *194*(9), 4458–4465. https://doi.org/10.4049/jimmunol.1402183

Hunter, M. V, Willoughby, P. M., Bruce, A. E. E., & Fernandez-Gonzalez, R. (2018). Oxidative Stress Orchestrates Cell Polarity to Promote Embryonic Wound Healing. *Developmental Cell*, *47*(3), 377-387.e4. https://doi.org/10.1016/j.devcel.2018.10.013

Jopling, C., Van Geemen, D., & Den Hertog, J. (2007). Shp2 knockdown and noonan/LEOPARD mutant Shp2-induced gastrulation defects. *PLoS Genetics*, *3*(12), 2468–2476. https://doi.org/10.1371/journal.pgen.0030225

Klaman, L. D., Boss, O., Peroni, O. D., Kim, J. K., Martino, J. L., Zabolotny, J. M., Moghal, N., Lubkin, M., Kim, Y. B., Sharpe, A. H., Stricker-Krongrad, A., Shulman, G. I., Neel, B. G., & Kahn, B. B. (2000). Increased energy expenditure, decreased adiposity, and tissue-specific insulin sensitivity in protein-tyrosine phosphatase 1B-deficient mice. *Molecular and Cellular Biology*, *20*(15), 5479–5489. http://www.ncbi.nlm.nih.gov/pubmed/10891488

Lanahan, A. A., Lech, D., Dubrac, A., Zhang, J., Zhuang, Z. W., Eichmann, A., & Simons, M. (2014). PTP1b Is a Physiologic Regulator of Vascular Endothelial Growth Factor Signaling in Endothelial Cells. *Circulation*, *130*(11), 902–909. https://doi.org/10.1161/CIRCULATIONAHA.114.009683

Le Sommer, S., Morrice, N., Pesaresi, M., Thompson, D., Vickers, M. A., Murray, G. I., Mody, N., Neel, B. G., Bence, K. K., Wilson, H. M., & Delibegović, M. (2018). Deficiency in Protein Tyrosine Phosphatase PTP1B Shortens Lifespan and Leads to Development of Acute Leukemia. *Cancer Research*, *78*(1), 75–87. https://doi.org/10.1158/0008-5472.CAN-17-0946

Legius, E., Schrander-Stumpel, C., Schollen, E., Pulles-Heintzberger, C., Gewillig, M., & Fryns, J. P. (2002). PTPN11 mutations in LEOPARD syndrome. *Journal of Medical Genetics*, *39*(8), 571–574. https://doi.org/10.1136/JMG.39.8.571

Li, H., Dusseault, J., & Larose, L. (2014). Nck1 depletion induces activation of the PI3K/Akt pathway by attenuating PTP1B protein expression. *Cell Communication and Signaling*, *12*(1), 71. https://doi.org/10.1186/s12964-014-0071-9

Li, L., Yan, B., Shi, Y. Q., Zhang, W. Q., & Wen, Z. L. (2012). Live imaging reveals differing roles of macrophages and neutrophils during zebrafish tail fin regeneration. *Journal of Biological Chemistry*, *287*(30), 25353–25360. https://doi.org/10.1074/JBC.M112.349126/ATTACHMENT/F834DDA9-9B59-43E0-ABB3-59B983EEF484/MMC1.ZIP

Liang, J., Shi, J., Wang, N., Zhao, H., & Sun, J. (2019). Tuning the Protein Phosphorylation by Receptor Type Protein Tyrosine Phosphatase Epsilon (PTPRE) in Normal and Cancer Cells. *Journal of Cancer*, *10*(1), 105–111. https://doi.org/10.7150/jca.27633

Love, N. R., Chen, Y., Ishibashi, S., Kritsiligkou, P., Lea, R., Koh, Y., Gallop, J. L., Dorey, K., & Amaya, E. (2013). Amputation-induced reactive oxygen species are required for successful Xenopus tadpole tail regeneration. *Nature Cell Biology*, *15*(2), 222–228. https://doi.org/10.1038/ncb2659

Marques, I. J., Lupi, E., & Mercader, N. (2019). Model systems for regeneration: Zebrafish. *Development (Cambridge)*, *146*(18). https://doi.org/10.1242/DEV.167692/224198

Meng, T. C., Fukada, T., & Tonks, N. K. (2002). Reversible Oxidation and Inactivation of Protein Tyrosine Phosphatases In Vivo. *Molecular Cell*, *9*(2), 387–399. https://doi.org/10.1016/S1097-2765(02)00445-8

Moller, N. P. H., Moller, K. B., Lammers, R., Kharitonenkov, A., Hoppe, E., Wiberg, F. C., Sures, I., & Ullrich, A. (1995). Selective down-regulation of the insulin receptor signal by protein-tyrosine phosphatases alpha and epsilon. *The Journal of Biological Chemistry*, *270*(39), 23126–23131. https://doi.org/10.1074/JBC.270.39.23126

Moon, J., Ha, J., & Park, S.-H. (2017). Identification of PTPN1 as a novel negative regulator of the JNK MAPK pathway using a synthetic screening for pathway-specific phosphatases. *Scientific Reports*, *7*(1), 12974. https://doi.org/10.1038/s41598-017-13494-x

Myers, M. P., Andersen, J. N., Cheng, A., Tremblay, M. L., Horvath, C. M., Parisien, J.-P., Salmeen, A., Barford, D., & Tonks, N. K. (2001). TYK2 and JAK2 Are Substrates of Protein-tyrosine Phosphatase 1B. *Journal of Biological Chemistry*, *276*(51), 47771–47774. https://doi.org/10.1074/jbc.C100583200

Niethammer, P., Grabher, C., Look, A. T., & Mitchison, T. J. (2009). A tissue-scale gradient of hydrogen peroxide mediates rapid wound detection in zebrafish. *Nature*, *459*(7249), 996–999. https://doi.org/10.1038/nature08119

Östman, A., Frijhoff, J., Sandin, Å., & Böhmer, F.-D. (2011). Regulation of protein tyrosine phosphatases by reversible oxidation. *The Journal of Biochemistry*, *150*(4), 345–356. https://doi.org/10.1093/jb/mvr104

Parri, E., Kuusanmäki, H., van Adrichem, A. J., Kaustio, M., & Wennerberg, K. (2020). Identification of novel regulators of STAT3 activity. *PLoS ONE*, *15*(3). https://doi.org/10.1371/JOURNAL.PONE.0230819

Peretz, A., Gil-Henn, H., Sobko, A., Shinder, V., Attali, B., & Elson, A. (2000). Hypomyelination and increased activity of voltage-gated K(+) channels in mice lacking protein tyrosine phosphatase epsilon. *The EMBO Journal*, *19*(15), 4036–4045. https://doi.org/10.1093/emboj/19.15.4036

Peters, G. H., Frimurer, T. M., & Olsen, O. H. (1998). Electrostatic evaluation of the signature motif (H/V)CX5R(S/T) in protein-tyrosine phosphatases. *Biochemistry*, *37*(16), 5383–5393. https://doi.org/10.1021/BI971187I

Pike, K. A., Hatzihristidis, T., Bussières-Marmen, S., Robert, F., Desai, N., Miranda-Saavedra, D., Pelletier, J., & Tremblay, M. L. (2017). TC-PTP regulates the IL-7 transcriptional response during murine early T cell development. *Scientific Reports*, *7*(1), 13275. https://doi.org/10.1038/s41598-017-13673-w

Pike, K. A., Hutchins, A. P., Vinette, V., Theberge, J.-F., Sabbagh, L., Tremblay, M. L., & Miranda-Saavedra, D. (2014). Protein Tyrosine Phosphatase 1B Is a Regulator of the Interleukin-10-Induced Transcriptional Program in Macrophages. *Science Signaling*, *7*(324), ra43–ra43. https://doi.org/10.1126/scisignal.2005020

Pirotte, N., Stevens, A. S., Fraguas, S., Plusquin, M., Van Roten, A., Van Belleghem, F., Paesen, R., Ameloot, M., Cebrià, F., Artois, T., & Smeets, K. (2015). Reactive oxygen species in planarian regeneration: An upstream necessity for correct patterning and brain formation. *Oxidative Medicine and Cellular Longevity*. https://doi.org/10.1155/2015/392476

Postlethwait, J. H., Yan, Y. L., Gates, M. A., Horne, S., Amores, A., Brownlie, A., Donovan, A., Egan, E. S., Force, A., Gong, Z., Goutel, C., Fritz, A., Kelsh, R., Knapik, E., Liao, E., Paw, B., Ransom, D., Singer, A., Thomson, M., … Talbot, W. S. (1998). Vertebrate genome evolution and the zebrafish gene map. *Nature Genetics*, *18*(4), 345–349. https://doi.org/10.1038/NG0498-345

Roy, S., Khanna, S., Nallu, K., Hunt, T. K., & Sen, C. K. (2006). Dermal wound healing is subject to redox control. *Molecular Therapy*, *13*(1), 211–220. https://doi.org/10.1016/j.ymthe.2005.07.684

Salazar-Tortosa, D. F., Labayen, I., González-Gross, M., Seral-Cortes, M., Moreno, L. A., G. Zapico, A., Widhalm, K., Meirhaeghe, A., Enard, D., & R. Ruiz, J. (2022). Association between PTPN1 polymorphisms and obesity-related phenotypes in European adolescents: influence of physical activity. *Pediatric Research*. https://doi.org/10.1038/s41390-022-02377-1

Shields, B. J., Court, N. W., Hauser, C., Bukczynska, P. E., & Tiganis, T. (2008). Cell cycle-dependent regulation of SFK, JAK1 and STAT3 signaling by the protein tyrosine phosphatase TCPTP. *Cell Cycle*, *7*(21), 3405–3416. https://doi.org/10.4161/cc.7.21.6950

Simoncic, P. D., Lee-Loy, A., Barber, D. L., Tremblay, M. L., & McGlade, C. J. (2002). The T cell protein tyrosine phosphatase is a negative regulator of janus family kinases 1 and 3. *Current Biology : CB*, *12*(6), 446–453. http://www.ncbi.nlm.nih.gov/pubmed/11909529

Solman, M., Blokzijl-Franke, S., Piques, F., Yan, C., Yang, Q., Strullu, M., Kamel, S. M., Ak, P., Bakkers, J., Langenau, D. M., Cavé, H., & Den Hertog, J. (2022). Inflammatory response in hematopoietic stem and progenitor cells triggered by activating SHP2 mutations evokes blood defects. *ELife*, *11*. https://doi.org/10.7554/ELIFE.73040

Su, F., Ren, F., Rong, Y., Wang, Y., Geng, Y., Wang, Y., Feng, M., Ju, Y., Li, Y., Zhao, Z. J., Meng, K., & Chang, Z. (2012). Protein tyrosine phosphatase Meg2 dephosphorylates signal transducer and activator of transcription 3 and suppresses tumor growth in breast cancer. *Breast Cancer Research*, *14*(2), R38. https://doi.org/10.1186/bcr3134

Sully, V., Pownall, S., Vincan, E., Bassal, S., Borowski, A. H., Hart, P. H., Rockman, S. P., & Phillips, W. A. (2001). Functional Abnormalities in Protein Tyrosine Phosphatase ε-Deficient Macrophages. *Biochemical and Biophysical Research Communications*, *286*(1), 184–188. https://doi.org/10.1006/bbrc.2001.5360

Swiatnicki, M. R., Rennhack, J. P., Ortiz, M. M. O., Hollern, D. P., Perry, A. V., Kubiak, R., Riveria Riveria, S. M., OReilly, S., & Andrechek, E. R. (2022). Elevated phosphorylation of EGFR in NSCLC due to mutations in PTPRH. *PLoS Genetics*, *18*(9). https://doi.org/10.1371/JOURNAL.PGEN.1010362

Tartaglia, M., Kalidas, K., Shaw, A., Song, X., Musat, D. L., Van der Burgt, I., Brunner, H. G., Bertola, D. R., Crosby, A., Ion, A., Kucherlapati, R. S., Jeffery, S., Patton, M. A., & Gelb, B. D. (2002). PTPN11 mutations in Noonan syndrome: molecular spectrum, genotype-phenotype correlation, and phenotypic heterogeneity. *American Journal of Human Genetics*, *70*(6), 1555–1563. https://doi.org/10.1086/340847

Tautz, L., Critton, D. A., & Grotegut, S. (2013). Protein Tyrosine Phosphatases: Structure, Function, and Implicationin Human Disease. *Methods in Molecular Biology (Clifton, N.J.)*, *1053*, 179. https://doi.org/10.1007/978-1-62703-562-0_13

Taylor, J. S., Van de Peer, Y., Braasch, I., & Meyer, A. (2001). Comparative genomics provides evidence for an ancient genome duplication event in fish. *Philosophical Transactions of the Royal Society of London. Series B, Biological Sciences*, *356*(1414), 1661–1679. https://doi.org/10.1098/RSTB.2001.0975

ten Hoeve, J., de Jesus Ibarra-Sanchez, M., Fu, Y., Zhu, W., Tremblay, M., David, M., & Shuai, K. (2002). Identification of a nuclear Stat1 protein tyrosine phosphatase. *Molecular and Cellular Biology*, *22*(16), 5662–5668. http://www.ncbi.nlm.nih.gov/pubmed/12138178

Tonks, N. K. (2006). Protein tyrosine phosphatases: from genes, to function, to disease. *Nature Reviews. Molecular Cell Biology*, *7*(11), 833–846. https://doi.org/10.1038/NRM2039

Través, P. G., Pardo, V., Pimentel-Santillana, M., González-Rodríguez, Á., Mojena, M., Rico, D., Montenegro, Y., Calés, C., Martín-Sanz, P., Valverde, A. M., & Boscá, L. (2017). Pivotal role of protein tyrosine phosphatase 1B (PTP1B) in the macrophage response to pro-inflammatory and anti-inflammatory challenge. *Cell Death & Disease*, *5*(3), e1125–e1125. https://doi.org/10.1038/cddis.2014.90

Tsunekawa, T., Banno, R., Mizoguchi, A., Sugiyama, M., Tominaga, T., Onoue, T., Hagiwara, D., Ito, Y., Iwama, S., Goto, M., Suga, H., Sugimura, Y., & Arima, H. (2017). Deficiency of PTP1B Attenuates Hypothalamic Inflammation via Activation of the JAK2-STAT3 Pathway in Microglia. *EBioMedicine*, *16*, 172–183. https://doi.org/10.1016/j.ebiom.2017.01.007

Wang, D., Cheng, Z., Zhao, M., Jiao, C., Meng, Q., Pan, H., Xie, Y., Li, L., Zhu, Y., Wang, W., Qu, C., & Liang, D. (2019). PTPN9 induces cell apoptosis by mitigating the activation of Stat3 and acts as a tumor suppressor in colorectal cancer. *Cancer Management and Research*, *11*, 1309–1319. https://doi.org/10.2147/CMAR.S187001

Wang, T., Ba, X., Zhang, X., Zhang, N., Wang, G., Bai, B., Li, T., Zhao, J., Zhao, Y., Yu, Y., & Wang, B. (2022). Pan-cancer analyses of classical protein tyrosine phosphatases and phosphatase-targeted therapy in cancer. *Frontiers in Immunology*, *13*. https://doi.org/10.3389/FIMMU.2022.976996

Whited, J. L., Robichaux, M. B., Yang, J. C., & Garrity, P. A. (2007). Ptpmeg is required for the proper establishment and maintenance of axon projections in the central brain of Drosophila. *Development*, *134*(1), 43–53. https://doi.org/10.1242/dev.02718

Wiede, F., La Gruta, N. L., & Tiganis, T. (2014). PTPN2 attenuates T-cell lymphopenia-induced proliferation. *Nature Communications*, *5*, 3073. https://doi.org/10.1038/ncomms4073

Wu, W., Hale, A. J., Lemeer, S., & den Hertog, J. (2017). Differential oxidation of protein-tyrosine phosphatases during zebrafish caudal fin regeneration. *Scientific Reports*, *7*(1), 8460. https://doi.org/10.1038/s41598-017-07109-8

Xu, M. -j., Sui, X., Zhao, R., Dai, C., Krantz, S. B., & Zhao, Z. J. (2003). PTP-MEG2 is activated in polycythemia vera erythroid progenitor cells and is required for growth and expansion of erythroid cells. *Blood*, *102*(13), 4354–4360. https://doi.org/10.1182/blood-2003-04-1308

Yang, W., Klaman, L. D., Chen, B., Araki, T., Harada, H., Thomas, S. M., George, E. L., & Neel, B. G. (2006). An Shp2/SFK/Ras/Erk signaling pathway controls trophoblast stem cell survival. *Developmental Cell*, *10*(3), 317–327. https://doi.org/10.1016/J.DEVCEL.2006.01.002

Yao, Z., Darowski, K., St-Denis, N., Wong, V., Offensperger, F., Villedieu, A., Amin, S., Malty, R., Aoki, H., Guo, H., Xu, Y., Iorio, C., Kotlyar, M., Emili, A., Jurisica, I., Neel, B. G., Babu, M., Gingras, A.-C., & Stagljar, I. (2017). A Global Analysis of the Receptor Tyrosine Kinase-Protein Phosphatase Interactome. *Molecular Cell*, *65*(2), 347–360. https://doi.org/10.1016/j.molcel.2016.12.004

You-Ten, K. E., Muise, E. S., Itié, A., Michaliszyn, E., Wagner, J., Jothy, S., Lapp, W. S., & Tremblay, M. L. (1997). Impaired bone marrow microenvironment and immune function in T cell protein tyrosine phosphatase-deficient mice. *The Journal of Experimental Medicine*, *186*(5), 683–693. http://www.ncbi.nlm.nih.gov/pubmed/9271584

Young, J. A., Becker, A. M., Medeiros, J. J., Shapiro, V. S., Wang, A., Farrar, J. D., Quill, T. A., van Huijsduijnen, R. H., & van Oers, N. S. C. (2008). The protein tyrosine phosphatase PTPN4/PTP-MEG1, an enzyme capable of dephosphorylating the TCR ITAMs and regulating NF-κB, is dispensable for T cell development and/or T cell effector functions. *Molecular Immunology*, *45*(14), 3756–3766. https://doi.org/10.1016/j.molimm.2008.05.023

Zhang, S. Q., Yang, W., Kontaridis, M. I., Bivona, T. G., Wen, G., Araki, T., Luo, J., Thompson, J. A., Schraven, B. L., Philips, M. R., & Neel, B. G. (2004). Shp2 regulates SRC family kinase activity and Ras/Erk activation by controlling Csk recruitment. *Molecular Cell*, *13*(3), 341–355. https://doi.org/10.1016/S1097-2765(04)00050-4

Zhang, Z. Y., Wang, Y., & Dixon, J. E. (1994). Dissecting the catalytic mechanism of protein-tyrosinephosphatases. *Proceedings of the National Academy of Sciences of the United States of America*, *91*(5), 1624. https://doi.org/10.1073/PNAS.91.5.1624

Zhou, J., Wan, B., Shan, J., Shi, H., Li, Y., & Huo, K. (2013). PTPN4 negatively regulates CrkI in human cell lines. *Cellular & Molecular Biology Letters*, *18*(2), 297–314. https://doi.org/10.2478/s11658-013-0090-3

Zhu, G., Xie, J., Kong, W., Xie, J., Li, Y., Du, L., Zheng, Q., Sun, L., Guan, M., Li, H., Zhu, T., He, H., Liu, Z., Xia, X., Kan, C., Tao, Y., Shen, H. C., Li, D., Wang, S., … Zhu, J. (2020). Phase Separation of Disease-Associated SHP2 Mutants Underlies MAPK Hyperactivation. *Cell*, *183*(2), 490-502.e18. https://doi.org/10.1016/J.CELL.2020.09.002

A panel of ptp knock-out lines does not show defects during regeneration or embryonic development

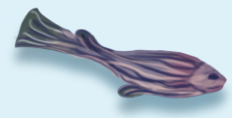

Maaike Allers[1], Danielle T.J. Woutersen[1], Fereshte Dadkhodaie[1] and Jeroen den Hertog[1,2‡]

1. Hubrecht Institute-KNAW and University Medical Center Utrecht, Utrecht, the Netherlands
2. Institute Biology Leiden, Leiden University, Leiden, the Netherlands

Abstract

One of the earliest signaling events upon injury, in many if not all species, is the production of a burst of reactive oxygen species (ROS). This production of ROS plays an extensive role in wound healing in mice and it has been shown to be essential for correct regeneration in zebrafish and planarians. Due to their susceptibility to oxidation, PTPs may be affected by the burst of ROS upon injury and play a role in signaling. A mass spectrometry-based screening of the oxidation status of PTPs before and after amputation of the caudal fin in zebrafish, identified 8 PTPs that are specifically oxidized in reaction to the amputation. Of these PTPs, Shp2a is required for regeneration of the amputated caudal fin-fold in embryos. We hypothesized that some of the other PTPs would be essential for regeneration too. In this chapter we describe the generation of knock-out mutants using CRISPR-Cas9 of 6 PTPs and their 5 homologs. None of the 11 generated knock-out mutants showed regeneration defects or embryonic developmental defects. The phenotypes we expected to find for *ptpn2* and *ptpn9* mutants based on previously reported defects were not found in zebrafish mutants. We did find a high mortality rate of *ptpn4a* mutant fish late during juvenile development, but only with partial penetrance. In conclusion, we did not find the phenotypes we expected in knock-out mutants that we generated, lacking functional PTPs, which we believe may be due to genetic compensation in these mutants.

2

Introduction

Zebrafish possess the ability to regenerate tissues upon injury throughout their lifetime. This is strikingly different from many other species, including humans, which can only regenerate a few specific tissues during the adult stages (Devarajan *et al*., 2003; Mao *et al*., 2014; Salamonsen, 2003). Many signaling pathways have been shown to play a role in the caudal fin regeneration pathway in zebrafish, the most important pathways seem to be Wnt, Retinoic Acid and FGF signaling (Banu *et al*., 2022; Blum & Begemann, 2012; Lee *et al*., 2005; Poss *et al*., 2000; Stoick-Cooper *et al*., 2007; Tal *et al*., 2010). However, the initial signal that triggers regeneration is still unclear. Experiments have shown that if regeneration is inhibited, a subsequent small skin injury is sufficient to induce regeneration of the missing tissue, thus indicating that the trigger signal is produced even in reaction to small injuries and it is diffusible (Owlarn *et al*., 2017).

One of the earliest signaling events upon injury, in many - if not all - species, is the production of a burst of reactive oxygen species. This production of reactive oxygen species (ROS), such as H_2O_2, plays an extensive role in wound healing in mice and it has been shown to be essential for correct regeneration in zebrafish and planarians (Gauron *et al*., 2013; Niethammer *et al*., 2009; Pirotte *et al*., 2015; Roy *et al*., 2006). This burst of ROS is a likely candidate for the signal that triggers regeneration, however it has not yet been found how this burst initiates the regeneration process.

In zebrafish the burst of H_2O_2 has been shown to be generated by dual oxidase. Inhibition or knock-down of dual oxidase inhibits the recruitment of both neutrophils and macrophages to the wound edge (Niethammer *et al*., 2009; Tauzin *et al*., 2014). However, significantly diminishing neutrophils, by a mutation in *runx1*, does not inhibit regeneration, and depletion of macrophages by morpholino-induced knockdown of *irf8,* results in affected, but still progressing, regeneration (Li *et al*., 2012). In Drosophila embryos, inhibition of ROS leads to a strongly reduced wound closure rate (Hunter *et al*., 2018). This indicates that the ROS burst upon injury has several effects, which accumulate to the essential role of the ROS burst in regeneration across species.

Protein tyrosine phosphatases are a widely expressed super-family of proteins that are involved in many different processes by acting in different signaling pathways. Together with protein tyrosine kinases, they determine the balance in signaling pathways that affect cell proliferation, differentiation and growth. Among the PTPs, 38 belong to the classical PTP family, categorized by the presence of the catalytic motif [I/V]HCSXGXGR[S/T]G. Within this motif, the cysteine is the active site residue. In catalysis, it acts by binding to phosphate groups and forming a phosphocysteinyl intermediate prior to hydrolysis.

For this to be possible, the cysteine exists in the thiolate anion form, due to the low pKa (between 4.5 and 5.5) in the active site. Because it exists as a thiolate anion, the active site cysteine of classical PTPs is highly susceptible to oxidation. Oxidation of the active site cysteine to a sulphenic acid state will temporarily and transiently inactivate the phosphatase. It can be reactivated by reduction for instance by glutathione or thioredoxin. Further oxidation will oxidize the cysteine to a sulphinic or sulphonic state, which is non-reducible and hence results in irreversible inactivation.

Oxidation of PTPs has been shown to act as a post-translational method of controlling phosphatase activity. For example, PDGF stimulation of fibroblasts and T-cell receptor activation of T-cells leads to specific oxidation of SHP2 (Jang *et al*., 2014; T.-C. Meng *et al*., 2002; Weibrecht *et al*., 2007), whereas stimulation of rat cells with insulin leads to specific oxidation of PTP1b and TC-PTP (T. C. Meng *et al*., 2004).

Due to their susceptibility to oxidation, PTPs could be affected by the burst of ROS upon injury and play a role in signaling. A mass spectrometry-based screening method of the oxidation status of PTPs before and after amputation of the caudal fin in zebrafish, led to the identification of 8 PTPs that are specifically oxidized in response to amputation. These PTPs are Shp2a (*ptpn11a*), Shp2b (*ptpn11b*), Ptp1b (*ptpn1*), TC-Ptpa (*ptpn2a*), PTP-Meg1b (*ptpn4b*), PTP-Meg2a (*ptpn9a*), Ptpɛa (*ptprea)* and Sap1 (*ptprh1*) (Wu *et al*., 2017). Of these oxidized PTPs, Shp2a is essential for regeneration, because homozygous zebrafish embryos carrying a knockout mutation in *ptpn11a* are not able to regrow their caudal fin fold after amputation, whereas tail development is normal (Hale & den Hertog, 2018). However, the closely related homolog Shp2b is not required for regeneration in zebrafish embryos, which is probably due to the low expression of Shp2b in zebrafish embryos (Bonetti *et al*., 2014). We hypothesized that one or more of the remaining oxidized PTPs might also be required for regeneration. To test this hypothesis, we generated knock-out mutants using CRISPR-Cas9 of these 6 PTPs and 5 homologs.

Material and methods

Zebrafish husbandry

All procedures involving experimental animals were approved by the local animal experiments committee (AVD-8010020173786). All fish were housed and handled according to local guidelines and policies in compliance with national and European law. Zebrafish were raised and maintained under a 14 hours light / 10 hours dark cycle at 28.5˚C as described by (Westerfield, 2000). Fertilized eggs were harvested and incubated at 28.5˚C in E3 medium (5 mM NaCl, 0,17 mM KCl, 0.33 mM $CaCl_2$, 0.33mM $MgSO_4$).

CRISPR-Cas9 generation of knock-out mutants

The gRNAs were designed using the CHOPCHOP web tool for genome editing (https://chopchop.cbu.uib.no/) and produced according to the protocol of (Gagnon *et al*., 2014). using the published constant reverse oligo. The targeted regions were checked for SNPs by PCR and sequencing. The gene specific primers are specified in Table 1.

Table 1 Design of the gRNAs for the indicated genes.

Gene	Primer
ptpn1	taatacgactcactataggaagtttggcgatcttgcagttttagagctagaaatagcaag
ptpn2a	taatacgactcactataggtcccttgaagaacacttggttttagagctagaaatagcaag
ptpn2b	taatacgactcactatagggcttcttccattaccaccgttttagagctagaaatagcaag
ptpn4a	taatacgactcactataggatgaagaagaactcagacgttttagagctagaaatagcaag
ptpn4b	taatacgactcactataggccgtctccgcataatctggttttagagctagaaatagcaag
ptpn9a	taatacgactcactataggtttccggttttgctgggagttttagagctagaaatagcaag
ptpn9b	taatacgactcactataggcagttaaggggtcagcaggttttagagctagaaatagcaag
ptprɛa	taatacgactcactataggatacgctcagccgacgatgttttagagctagaaatagcaag
ptprɛb	taatacgactcactataggaagagtttcgcctccgcagttttagagctagaaatagcaag
ptprh (1&2)	taatacgactcactataggattatccagatggagttggttttagagctagaaatagcaag

Ribonucleoprotein complexes of N-terminal GFP-labeled Cas9 protein and gRNA were generated and injected into wild type Tüpfel long fin (TL) embryos at the one-cell stage. GFP positive embryos were selected at 6 hpi and raised to adulthood. F0 founders were screened for germline mutations by PCR genotyping of the offspring of an outcross with wild type TL fish for heterozygous mutations. Two founders presenting with different indel mutations, causing premature stop codons, were selected for every target gene.

These founders were crossed with WT AB to obtain a stable line, which was outcrossed again with WT TL to remove all likelihood of background mutations being present. Table 2 lists the mutations that were selected for further characterization.

Table 2. PTP mutations selected for further characterization

Gene	Mutation	Exon (location of mutation)
ptpn1	7 bp del	1 out of 6
ptpn1	13 bp del	1 out of 6
ptpn2a	6 bp del + 1 bp insert	4 out of 9
ptpn2a	11 bp del	4 out of 9
ptpn2b	17 bp insert	3 out of 10
ptpn2b	4 bp del	3 out of 10
ptpn4a	7 bp del + 3 bp insert	7 out of 27
ptpn4a	2 bp del + 13 bp insert	7 out of 27
ptpn4b	3 bp del + 7 bp insert	4 out of 26
ptpn4b	5 bp del	4 out of 26
ptpn9a	4 bp del	4 out of 13
ptpn9a	8 bp del	4 out of 13
ptpn9b	10 bp del	7 out of 13
ptpn9b	17 bp del	7 out of 13
ptpreа	32 bp del	3 out of 18
ptpreа	15 bp del + 2 bp insert	3 out of 18
ptpreb	4 bp del + 8 bp insert	4 out of 21
ptpreb	6 bp del + 1 bp insert	4 out of 21
ptprh1	28 bp del	2 out of 10
ptprh1	2 bp del + 28 bp insert	2 out of 10
ptprh2	4 bp del + 18 bp insert + 1 bp del + 10 bp insert	2 out of 12
ptprh2	5 bp del	2 out of 12

Genotyping

Genomic zebrafish DNA was extracted through lysis of embryos or fin clips in 100 ug/ml proteinase K (Sigma) diluted in SZL buffer (50 mM KCl, 2.5 mM MgCl, 10mM Tris pH 8.3, 0.005% NP40, 0.005% Tween-20 and 0.1% Gelatine). Samples were lysed at 60˚C for 1 hour, followed by inactivation for 15 min at 95˚C in a thermal cycler (BioRad T100). Mutations were analyzed by PCR targeting the mutation sites. PCR products were run on a 4% agarose gel (UltraPure agarose, Invitrogen) in TBE . Mutations were confirmed by sequencing.

Microscopy

For bright-field imaging, 5 dpf embryos were anesthetized using tricaine methanesulfonate and mounted in 2% methylcellulose (Sigma) on glass indented slides. They were imaged using a Leica M165FC connected to a DFC420C camera. Images were processed using ImageJ.

Caudal fin-fold amputation

Zebrafish embryos were amputated at the tail fin-fold as previously described (Hale & den Hertog, 2016). Amputations were performed at 2 dpf and regeneration was analyzed at 5 dpf. Regenerated tail fin-folds were imaged and whole embryos were lysed for genotyping. Regeneration was quantified by measuring the length from the tip of the notochord to the end of the fin-fold in ImageJ.

In situ hybridization and o-dianasidine staining

Zebrafish embryos were depigmented by adding 160 ul/L phenyl-2-thiourea to E3 medium at 24 hpf. For *in situ* hybridizations 5 dpf embryos were fixed in 4% paraformaldehyde at 4˚C overnight. *In situ* hybridizations were performed as previously described (Thisse & Thisse, 2008), using *rag1* digoxigenin-UTP-labelled anti-sense riboprobes.

For o-dianasidine staining dechorionated embryos were stained for 20 minutes in the dark at 28.5 ˚C in 2.86 mg/ml o-dianasidine staining solution (Sigma), 0.01 M sodium acetate and 0.65% hydrogenperoxide in 2 ml water. Embryos were fixed in 4% paraformaldehyde for 2h at room temperature in the dark. Fixed embryos were dehydrated using methanol and cleared overnight in benzyl benzoate/benzyl alcohol (2:1) in the dark.

Statistical analysis

Statistical tests were performed and data was visualized using Python (Pandas 1.0.5, MatPlotLib 3.2.2, SciPy 1.5.0, Seaborn 0.10.1).

Results

Early development and regeneration of zebrafish PTP knockout lines was not affected
We used CRISPR-Cas9 to generate knock-out lines (Figure 1). Cas9 protein was micro-injected into one-cell stage zebrafish embryos together with a PTP-specific guide RNA (Table 1). For every target gene, two knock-out lines were selected that were created using a gRNA oligo. Mutant founders were selected by PCR and sequencing, based on the presence of a frame-shift indel, resulting in a stop codon downstream of the mutation. All mutations and stop codons were located upstream of the active site of the PTPs (Figure 2, Table 2), effectively resulting in mutants lacking the function of the respective PTP. In total, 22 mutant knock-out lines were created. In order to remove any potential background mutations, the mutant lines were outcrossed with WT lines twice, before they were investigated.

Embryonic development of homozygous mutant lines lacking a functional PTP was investigated by analysis of the morphology from 0-5 dpf, followed by genotyping of the embryos by analysis of the size of the PCR product on 4% agarose gel. Specifically, we investigated the presence of oedemas, the development of the jaw, head and eye structures and length of the embryo. The morphology of the mutant embryos was indistinguishable from their WT siblings (Figure 3A). Early mortality was also not obvious in embryos from the mutant lines. The survival to adulthood of all mutant lines was studied, by raising homozygous mutants and WT siblings. For all lines, homozygous mutants were found to reach adulthood. However, the number of Ptpn4a homozygous mutant adults was significantly lower than expected (Figure 3B). The proportion of mutant fish was 8.9% (CI=4.4-16.8% Agresti and Coull), which differs significantly from the expected Mendelian proportion of 25% (Chi square test, p-value=0.0077).

Subsequently, the mutant lines lacking functional PTPs were tested for defects in their regenerative capability. The tip of their tail fin fold was amputated at 2dpf, and the length of the regenerated tail fin folds was measured at 5dpf. No difference was seen in regeneration between homozygous mutant embryos and their WT siblings (Figure 3C).

Figure 1. Schematic representation of the generation of knock-out zebrafish lines. Cas 9 protein was injected with guide RNAs targeting selected genes. Injected embryos were raised, which results in mosaic individuals carrying multiple different mutations (F0 generation). The F0 founders were crossed with a WT partner and their progeny was screened for heterozygous mutations in the target genes. These F1 mutant fish were crossed with a WT partner to create a heterozygous F2 family. Fish from the F2 family were crossed with a WT partner again to create an F3 family, which was used to generate homozygous mutant progeny for the experiments. ►

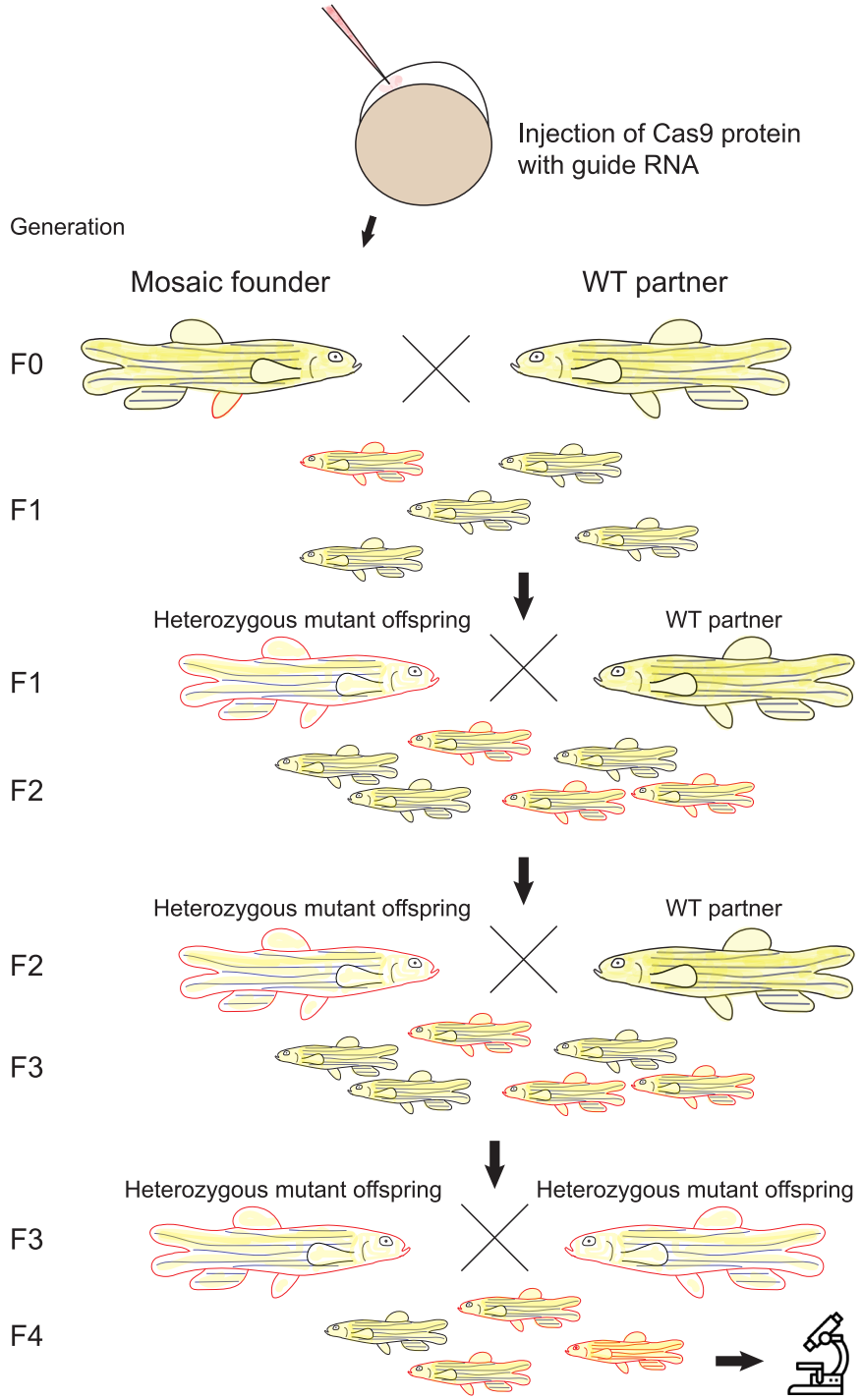

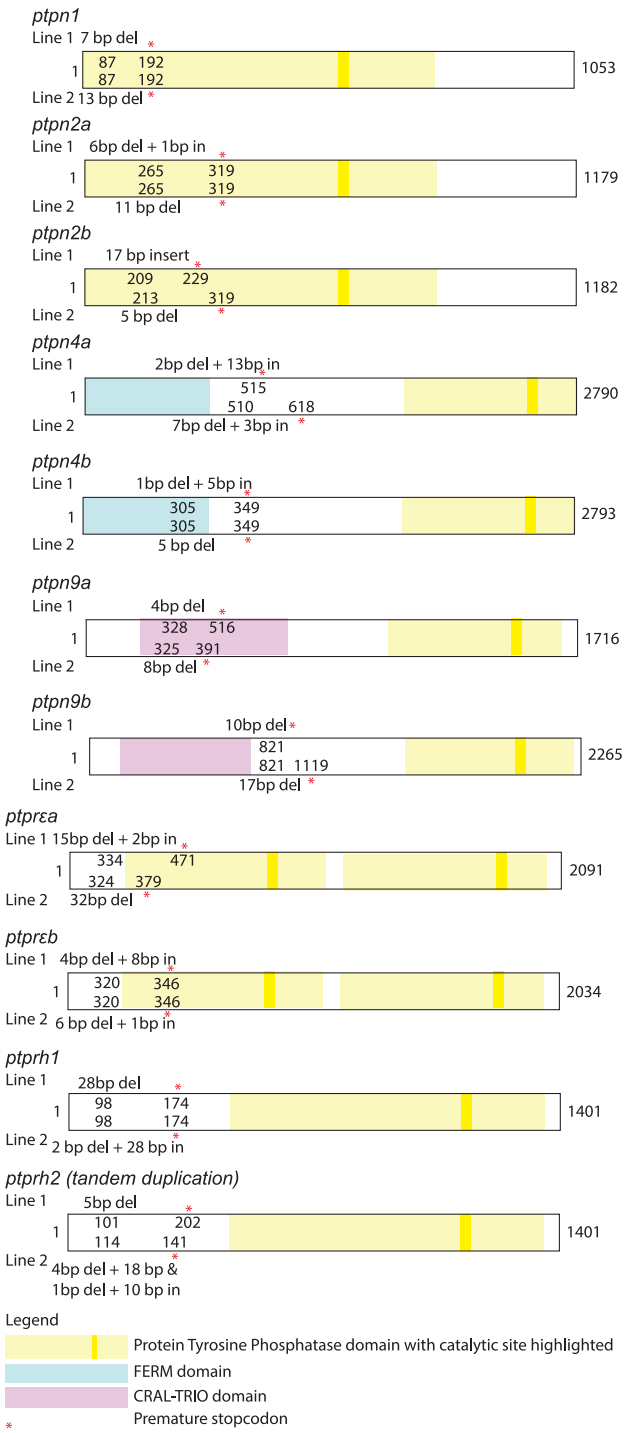

◂ Figure 2. Schematic overview of coding sequences of genes targeted with CRISPR-Cas9. For every target gene, two mutant lines were created. Location of the start of the mutations and the premature stopcodons are represented in number of basepairs in the coding sequence. Start and end of the coding sequences are indicated. Functional protein domains are presented in yellow, blue or pink.

We hypothesized that the presence of homologous genes was compensating for the loss of the target PTPs. Therefore we crossed the single mutant lines to create double mutant lines; *ptpn2a/ptpn2b*, *ptpn4a/ptpn4b*, *ptpn9a/ptpn9b*, *ptprεa/ptprεb* and the triple mutant line *ptpn1/ptpn2a/ptpn2b*. We then repeated the experiments to test the double and triple mutant lines for morphological defects, regenerative defects and reduced survival. We found no effect on regeneration or early development in the four double mutant lines or the triple mutant line (Figure 4A). Also no effect was detected on survival of the double or triple mutant lines, except for the *ptpn4a/ptpn4b* double mutant line, which showed a reduced survival to adulthood (Figure 4B).

Analysis of specific, expected phenotypes in mutant lines

In response to loss of some PTPs, specific defects were expected. For instance, mutations in *Ptpn2* are known to affect the differentiation of T-cells in mice (Pike *et al.*, 2017; Wiede *et al.*, 2012, 2014). Moreover, inhibition of *ptpn9* was previously found to affect the formation of red blood cells in zebrafish embryos and human red blood cells *in vitro* (Bu *et al.*, 2014; Xu *et al.*, 2003).

We investigated the formation and maturation of T-cells in the *ptpn2a/ptpn2b* knock-out line, by performing a *rag-1 in situ* hybridization, which stains lymphocytes in the thymus. We found no difference in the size of the thymus between *ptpn2a/ptpn2b* mutants and their WT siblings (Figure 5A).

We hypothesized that Tc-ptp affects only the later stages of T-cell maturation. Therefore, we crossed the *ptpn2a/ptpn2b* knock-out to a transgenic zebrafish line that expresses GFP under the control of the *lck* promoter, which is active during maturation of T-cells (Langenau *et al.*, 2004). No difference was detected in the size or intensity of the GFP-positive thymus in *Tg(lck*:GFP) transgenic *ptpn2a/ptpn2b* mutants compared to their WT siblings (Figure 5B&C). This shows that also the later stages of T-cell maturation were not affected in the *ptpn2a/ptpn2b* mutant line.

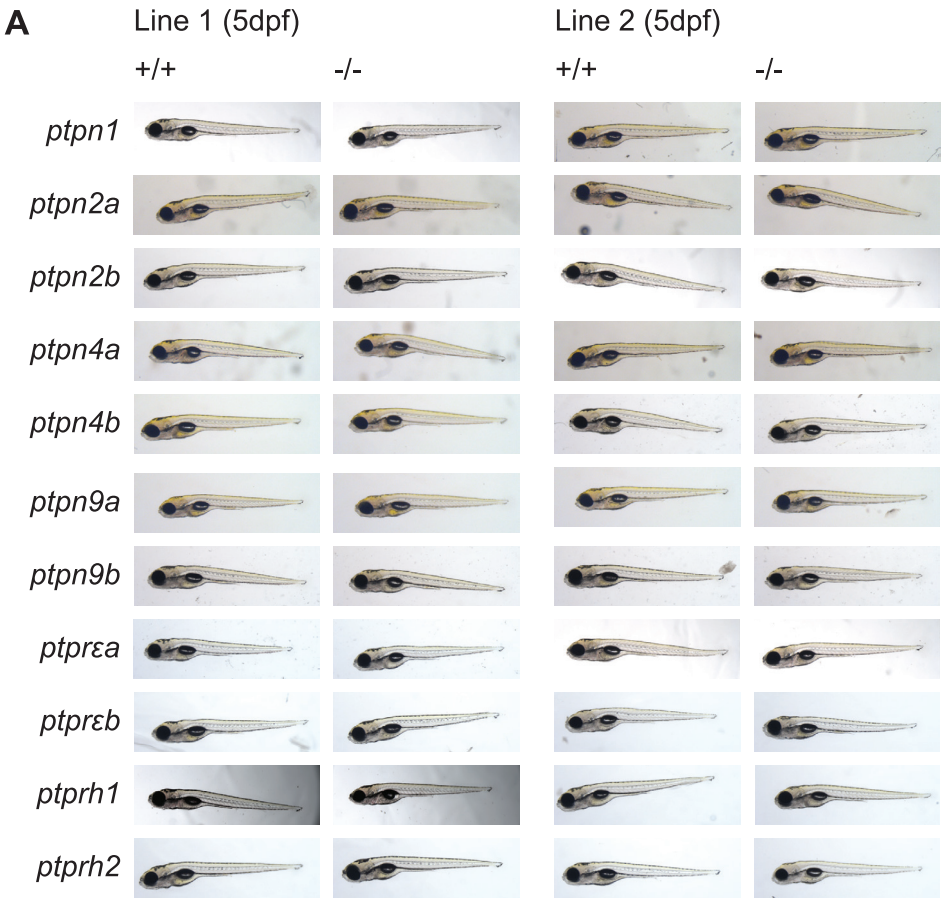

Figure 3. Effect of PTP knock-out mutations on zebrafish development and regeneration. A: Brightfield pictures of 5 dpf zebrafish embryos carrying a frameshift mutation in the indicated PTP gene were compared to their wild-type siblings. Representative pictures are shown. B: Schematic representation of the genotype division among adult (12 wpf) progeny of mutant zebrafish carrying a frameshift mutation. C: Tail fin folds were amputated at the tip of the notochord at 2 dpf. Embryos were allowed to recover and regenerated fins were imaged at 5 dpf. Length was measured from the tip of the notochord to the end of the tail fin. Fish were genotyped afterwards. T-tests were performed to compare the regeneration between embryos with a frameshift mutation and their wild-type siblings.

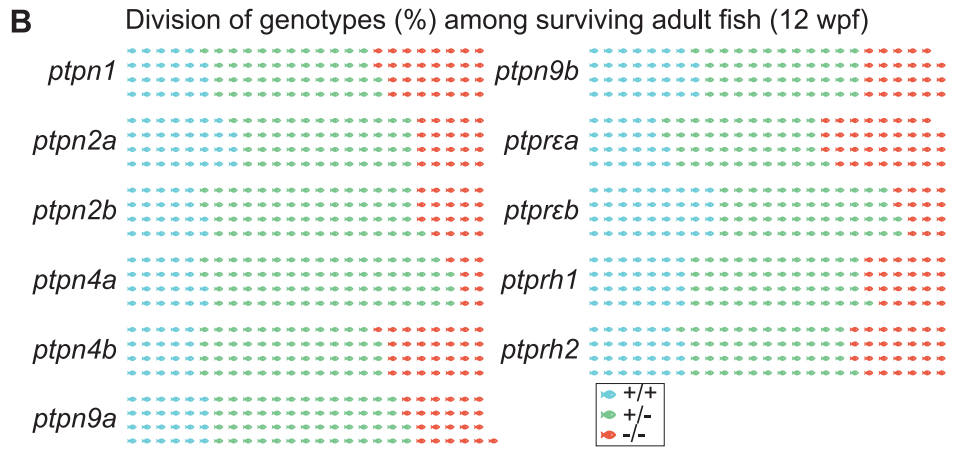

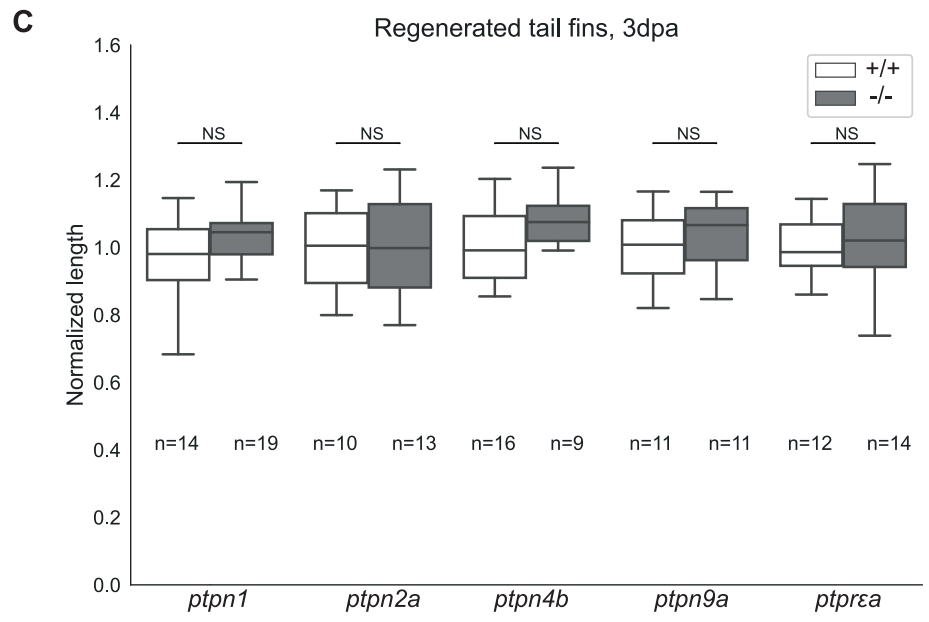

Figure 3. Continued.

To check the *ptpn9* mutant line for defects in red blood cell development, we stained fixed embryos with o-dianisidine and compared the amount of staining between mutant and WT siblings. No difference in the amount of o-dianisidine staining was detected (Figure 5D), indicating that red blood cell development was not affected in the *ptpn9* mutant line.

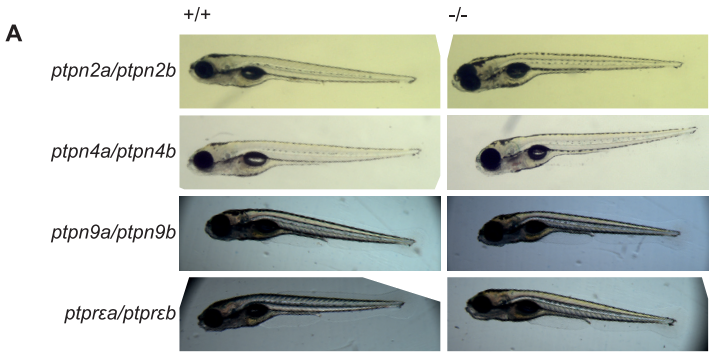

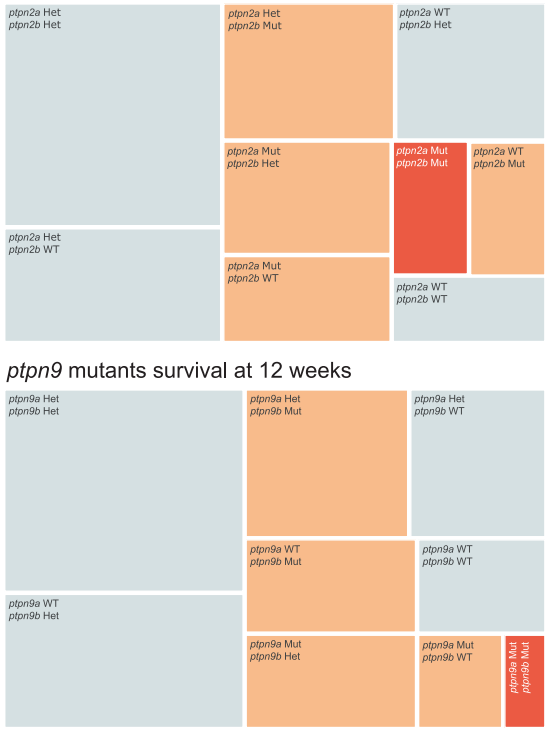

Figure 4. Effect of knock-out mutations in both paralogs of target genes on zebrafish development and regeneration. A: Brightfield pictures of 5dpf zebrafish embryos carrying frameshift mutations in both paralogs of PTP target genes as indicated were compared to their wildtype siblings. Representative pictures are shown, B: Schematic representation of the genotype division among adult (12 wpf) progeny of zebrafish carrying mutations in both paralogs of the indicated target genes. The size of the blocks represent the percentage of adult fish alive with that genotype. Double knock-out mutants are indicated in red. Single knock-out mutant fish are indicated in orange. C: Tail fin folds were cut at the tip of the notochord at 2dpf. Embryos were allowed to recover and regenerated fins were imaged at 5dpf. Length was measured from the tip of the notochord to the end of the fin. Fish were genotyped afterwards. T-tests were performed, including a Bonferroni correction, to compare the regeneration between mutants and their WT siblings. Shp2a mutant fish were used for the positive control.

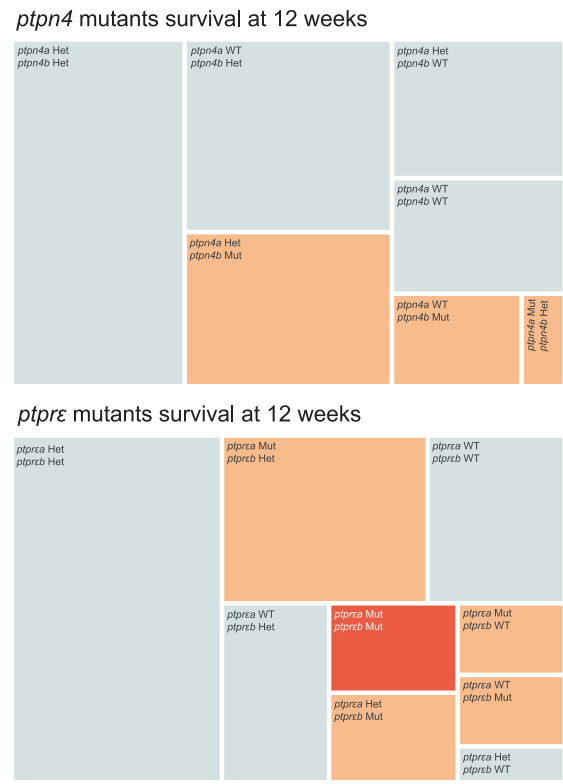

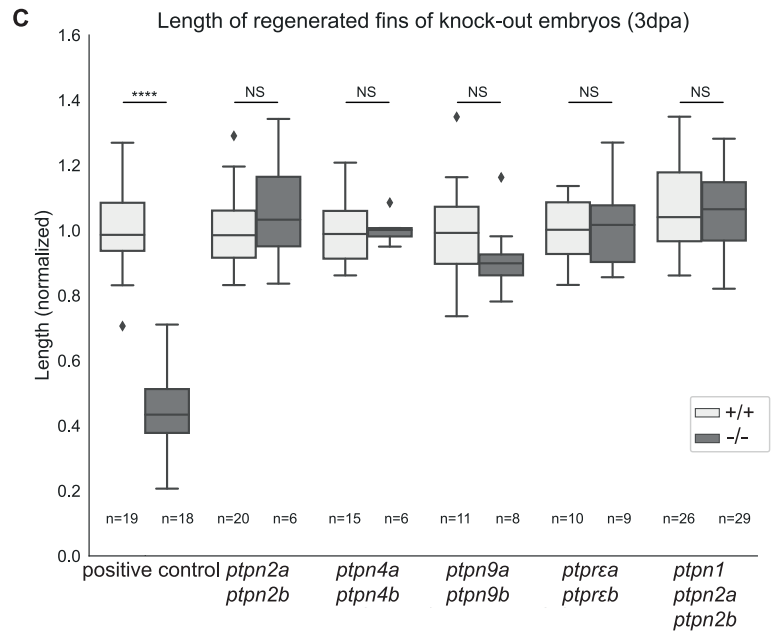

Figure 4. Continued.

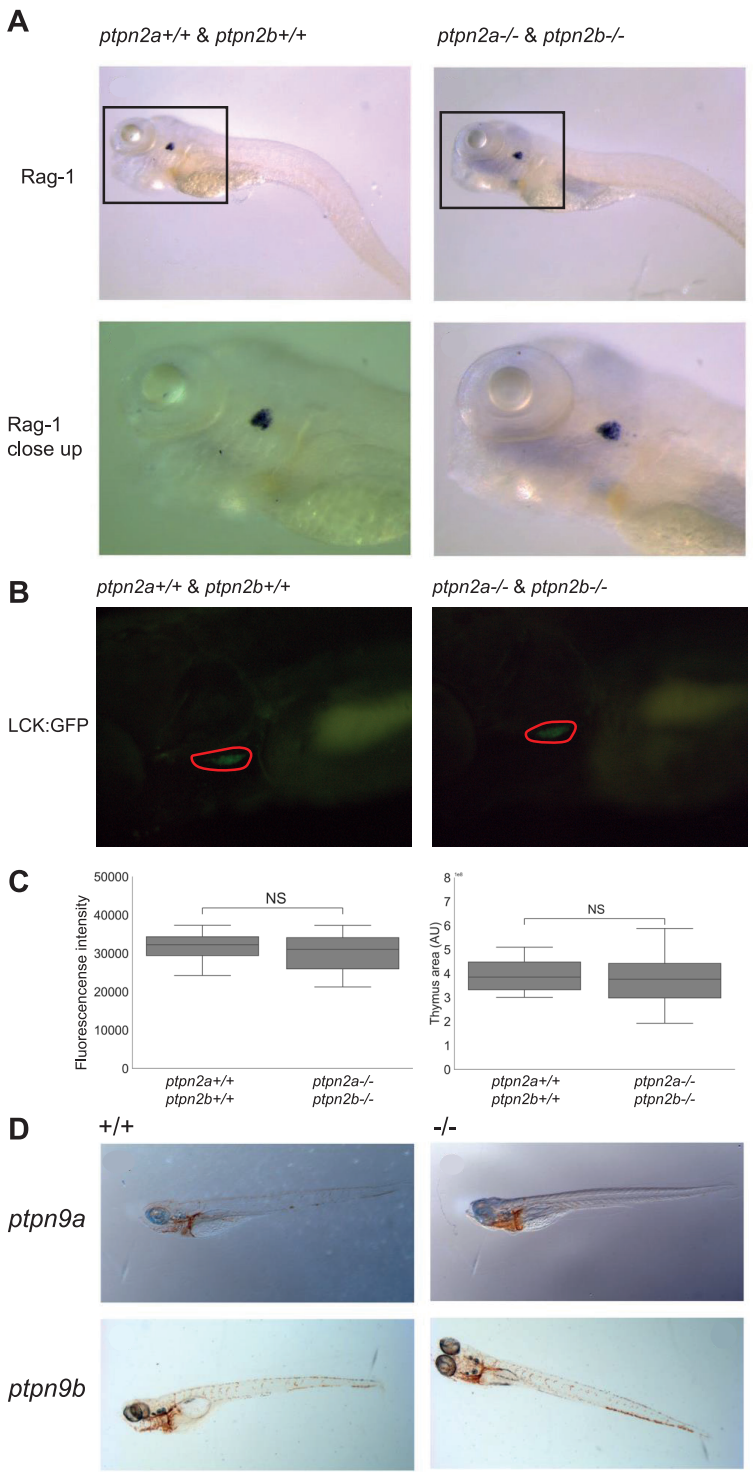

◂ Figure 5. No defects in T-cell and red blood cell development in 5dpf mutant zebrafish embryos. A: 5dpf embryos were fixed and stained by in situ hybridization using probes specific for *rag-1*. Homozygous *ptpn2a/ptpn2b* double mutants were analyzed as well as their WT siblings. Representative embryos are shown with a close-up in the bottom panels. B: Transgenic zebrafish embryos (WT sibling and *ptpn2a/ptpn2b* mutant) expressing GFP under the control of the thymus-specific *lck* promoter were imaged at 5dpf. C: Thymus area and intensity of GFP expression were quantified. No difference was seen between ptpn2a/ptpn2b mutants (n=13) and their WT siblings (n=4) (t-test, equal variance not assumed). D: 5dpf embryos were fixed and stained with o-dianisidine. Representative *ptpnga* (top) or *ptpngb* (bottom) mutant embryos and their WT siblings are shown.

No evidence for effects on expression or alternative splicing of mutant mRNAs

During the translation process, aberrant mRNA molecules with a premature stopcodon are normally destroyed by a process called nonsense-mediated decay. This is the way cells safeguard themselves against aberrant mRNA transcripts (Nickless *et al.*, 2017). We hypothesized that the mRNA transcripts of our mutant genes might be targeted by nonsense-mediated decay, as a result of the premature stopcodons. To investigate this, we collected mRNA from mutant and WT siblings at 5dpf and performed QPCRs to determine the relative mRNA expression of the respective genes. We noticed that several mutant knock-outs showed reduced mRNA expression compared to their WT siblings, especially *ptpn2a* line 2, *ptpn2b* line 1 and 2 and *ptpn9b* line 1 and 2 (Figure 6). However, the mRNA levels in these mutant fish were still between 25% and 50% of the levels of their WT siblings. On the other hand, there were also mutant fish that showed an upregulation of the mutant mRNA expression compared to their WT siblings, namely *ptpn4b* line 2 and *ptprh2* line 1. The levels of *ptprh1* were too low to detect. The other mutant fish showed mRNA levels closer to the levels of their WT siblings.

We then investigated the possibility that mutant zebrafish skipped the exon with the mutation to create a functional mRNA. To this end, we amplified the cDNAs of the target genes using primers at the 5'-end and 3'-end of the coding sequence and then sequenced the product. We found no evidence for alternative splicing or exon skipping. This indicates that the level of mRNA that we observed in the homozygous mutants was due to mRNA molecules that included the respective deletions. These deletions resulted in a frame-shift and thus did not give rise to functional proteins from these mRNAs. However, we were not able to confirm this at protein level due to a lack of functional antibodies.

***ptprh* has been tandem duplicated**

During our initial studies we noticed that *ptprh* was annotated twice in the Ensembl genome assembly, once in the forward direction and once in the reverse direction. We cloned *ptprh* from cDNA and confirmed that both genes were expressed. The

sequences differ sufficiently from each other to establish two distinct genes and both genes are expressed, though at low levels. At 5dpf we were able to detect *ptprh2*, the reversely ordered *ptprh*, by QPCR, but not *ptprh1*. The Sap1 protein that was detected in the oxidation MS experiment (Wu *et al*., 2017) correlates to the *ptprh1* gene. We conclude that *ptprh1* is expressed and translated, at least in adult zebrafish. However, we have no evidence yet that *ptprh2* is translated and gives rise to a protein product.

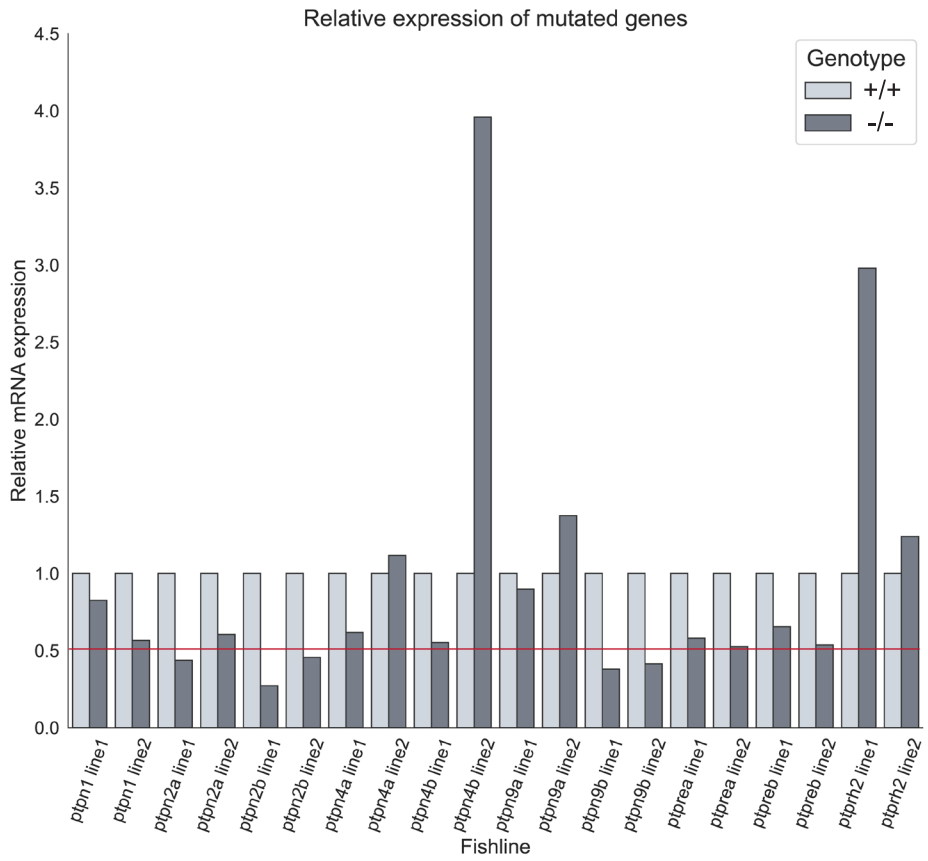

Figure 6. Relative mRNA expression of homozygous 5dpf mutant embryos compared to their WT siblings. mRNA was collected from 5dpf embryos after genotyping. Per genotype, 5 embryos were pooled, the mRNA was extracted and oligo-dT-primed cDNA was generated. QPCRs were performed on the cDNA using primers specific for the respective *ptp* gene. Expression of the target mRNA was compared to expression of *ppial*. The ratio of target gene expression in the mutant relative to wild type (WT), both normalized using *ppial* is depicted here. The red line indicates 50% of the WT expression.

Discussion

In this chapter we present the generation of 22 knock-out zebrafish lines, corresponding to 11 different PTPs, each containing a frameshift mutation that leads to a premature stopcodon. We showed that these knockout mutants do not have defects in caudal fin-fold regeneration, overthrowing the hypothesis that these PTPs have a role in the process, because they were oxidized upon amputation of the caudal fin in adult zebrafish. We also showed that all knockout mutants are viable and fertile, although *ptpn4a* mutants show partial mortality. We suspected that the absence of developmental defects could be due to compensation by the homologous gene, so we crossed mutant lines and generated double mutants. Surprisingly, these double and triple mutants (*ptpn2a/ptpn2b, ptpn4a/ptpn4b, ptpn9a/ptpn9b, ptpn1/ptpn2a/ptpn2b*) were viable and fertile too. Finally, several zebrafish knockout mutant lines did not recapitulate phenotypes we expected based on previous reports of mouse knock-outs of the corresponding PTPs.

We suspect that the reason for the absence of phenotypes in the majority of the mutant lines is genetic compensation. It has become clear that many mutant zebrafish, mouse and other model organism lines do not show the expected phenotypes. In some cases the expected phenotypes are present when the genes are targeted using temporary knockdown strategies, such as morpholino-mediated knockdowns (Rossi *et al*., 2015). Recently, it was shown that this effect is most likely due to transcriptional adaptation, a form of genetic compensation, that requires decay of the mutated mRNA that contains a premature stopcodon (El-Brolosy *et al*., 2019). Cells that displayed transcriptional adaptation upregulated the expression of several genes with sequence similarity to the mutated gene. The underlying mechanism may involve binding of fragments of the broken down mRNA to genes in the genome with sequence similarity, thus causing their upregulation. El-Brolosy *et al.* (2019) argue that support for this hypothesis comes from the observation that transcriptional adaptation correlates with lower levels of mutant mRNA. They show that their mutant lines that do not show transcriptional adaptation, also do not show lower levels of mutant mRNA. For some of our mutant lines, the mRNA expression data correspond to their observation. For the *ptpn2a* and *ptpn2b* lines for instance, we observed a lower level of mRNA expression of the mutated gene, which may lead to transcriptional adaptation. Eventually, we did not detect the expected phenotype in T-cell development, which may be due to transcriptional adaptation.

On the other hand, the *ptpn9a* mutants that we generated showed the same level of *ptpn9a* mRNA expression as their WT siblings, but they did not recapitulate the phenotype caused by morpholinos against *ptpn9a*. These data would argue against the hypothesis that transcriptional adaption correlates with lower mRNA levels. On the

other hand, it could also mean that the previously found phenotype was not due to the lack of *ptpn9a*, but a result of off-target effects. Off-target effects were one of the main reasons of the zebrafish field to become extra cautious about the use of morpholinos and instead turn to stable mutant lines created by CRISPR-Cas9 (Kok *et al*., 2015).

All in all, it is evident that more research is needed to determine the exact role that PTPs play in cell signaling, development and regeneration. Using CRISPR-Cas9 knock-out mutant lines eliminates the off-target effects caused by morpholinos. However, the use of CRISPR-Cas9 knock-out mutant lines causes its own challenges, including genetic compensation.

We hypothesize that the absence of clear phenotypes in our PTP knockout lines is due to genetic compensation of the mutants by upregulating genes that are similar to the inactivated genes. To test if this is indeed the case, expression of all PTPs and perhaps any other genes with a strong similarity to the gene with the premature stop codon, should be investigated. Detectable upregulation of one or more of these similar genes would be a strong indication for genetic compensation. If a knock-out or transient inhibition of the compensating genes then induces a phenotype or developmental defect, this would be a clear signal that transcriptional adaptation is indeed compensating for the loss of the targeted protein.

To circumvent the transcriptional adaptation, RNA-less mutants should be created, by removing either the promoter, several exons or the entire gene. Another approach is to investigate the CRISPR F0 generation, which is feasible if the CRISPR rate reaches close to 100%. The general idea is that these embryos have not yet adapted their transcription to compensate for the mutated gene. We initiated investigations along these lines by analysis of the CRISPR F0 generation for *ptpn2a* and *ptpn2b*, but we were unable to complete a thorough investigation of the embryos. Preliminary data suggests that injected embryos were viable till at least 5 dpf, with a minority of the embryos showing developmental defects. It would be very interesting to further investigate these F0 mutant embryos (crispants) for defects in T-cell development.

To summarize, we generated 22 knock-out zebrafish lines lacking functional PTPs, but we found no developmental defects in most knock-out lines, even though certain phenotypes were expected. We believe the lack of obvious phenotypes was due to genetic compensation in these mutants.

Literature list

Banu, S., Gaur, N., Nair, S., Ravikrishnan, T., Khan, S., Mani, S., Bharathi, S., Mandal, K., Kuram, N. A., Vuppaladadium, S., Ravi, R., Murthy, C. L. N., Quoseena, M., Babu, N. S., & Idris, M. M. (2022). Understanding the complexity of epimorphic regeneration in zebrafish caudal fin tissue: A transcriptomic and proteomic approach. *Genomics*, *114*(2), 110300. https://doi.org/10.1016/J.YGENO.2022.110300

Blum, N., & Begemann, G. (2012). Retinoic acid signaling controls the formation, proliferation and survival of the blastema during adult zebrafish fin regeneration. *Development (Cambridge, England)*, *139*(1), 107–116. https://doi.org/10.1242/DEV.065391

Bonetti, M., Rodriguez-Martinez, V., Paardekooper Overman, J., Overvoorde, J., van Eekelen, M., Jopling, C., & Hertog, J. den. (2014). Distinct and Overlapping Functions of ptpn11 Genes in Zebrafish Development. *PLoS ONE*, *9*(4), e94884. https://doi.org/10.1371/journal.pone.0094884

Bu, Y., Su, F., Wang, X., Gao, H., Lei, L., Chang, N., Wu, Q., Hu, K., Zhu, X., Chang, Z., Meng, K., & Xiong, J.-W. (2014). Protein tyrosine phosphatase PTPN9 regulates erythroid cell development through STAT3 dephosphorylation in zebrafish. *Journal of Cell Science*, *127*(Pt 12), 2761–2770. https://doi.org/10.1242/jcs.145367

Devarajan, P., Mishra, J., Supavekin, S., Patterson, L. T., & Potter, S. S. (2003). Gene expression in early ischemic renal injury: Clues towards pathogenesis, biomarker discovery, and novel therapeutics. *Molecular Genetics and Metabolism*, *80*(4), 365–376. https://doi.org/10.1016/j.ymgme.2003.09.012

El-Brolosy, M. A., Kontarakis, Z., Rossi, A., Kuenne, C., Günther, S., Fukuda, N., Kikhi, K., Boezio, G. L. M., Takacs, C. M., Lai, S. L., Fukuda, R., Gerri, C., Giraldez, A. J., & Stainier, D. Y. R. (2019). Genetic compensation triggered by mutant mRNA degradation. *Nature*, *568*(7751), 193–197. https://doi.org/10.1038/s41586-019-1064-z

Gagnon, J. A., Valen, E., Thyme, S. B., Huang, P., Ahkmetova, L., Pauli, A., Montague, T. G., Zimmerman, S., Richter, C., & Schier, A. F. (2014). Efficient Mutagenesis by Cas9 Protein-Mediated Oligonucleotide Insertion and Large-Scale Assessment of Single-Guide RNAs. *PLoS ONE*, *9*(5), e98186. https://doi.org/10.1371/journal.pone.0098186

Gauron, C., Rampon, C., Bouzaffour, M., Ipendey, E., Teillon, J., Volovitch, M., & Vriz, S. (2013). Sustained production of ROS triggers compensatory proliferation and is required for regeneration to proceed. *Scientific Reports*, *3*(1), 2084. https://doi.org/10.1038/srep02084

Hale, A. J., & den Hertog, J. (2016). Studying Protein-Tyrosine Phosphatases in Zebrafish. *Methods in Molecular Biology (Clifton, N.J.)*, *1447*, 351–372. https://doi.org/10.1007/978-1-4939-3746-2_19

Hale, A. J., & den Hertog, J. (2018). Shp2-Mitogen-Activated Protein Kinase Signaling Drives Proliferation during Zebrafish Embryo Caudal Fin Fold Regeneration. *Molecular and Cellular Biology*, *38*(4), e00515-17. https://doi.org/10.1128/MCB.00515-17

Hunter, M. V, Willoughby, P. M., Bruce, A. E. E., & Fernandez-Gonzalez, R. (2018). Oxidative Stress Orchestrates Cell Polarity to Promote Embryonic Wound Healing. *Developmental Cell*, *47*(3), 377-387.e4. https://doi.org/10.1016/j.devcel.2018.10.013

Jang, J. Y., Min, J. H., Chae, Y. H., Baek, J. Y., Wang, S. Bin, Park, S. J., Oh, G. T., Lee, S.-H., Ho, Y.-S., & Chang, T.-S. (2014). Reactive Oxygen Species Play a Critical Role in Collagen-Induced Platelet Activation *via* SHP-2 Oxidation. *Antioxidants & Redox Signaling*, *20*(16), 2528–2540. https://doi.org/10.1089/ars.2013.5337

Kok, F. O., Shin, M., Ni, C. W., Gupta, A., Grosse, A. S., vanImpel, A., Kirchmaier, B. C., Peterson-Maduro, J., Kourkoulis, G., Male, I., DeSantis, D. F., Sheppard-Tindell, S., Ebarasi, L., Betsholtz, C., Schulte-Merker, S., Wolfe, S. A., & Lawson, N. D. (2015). Reverse genetic screening reveals poor correlation between morpholino-induced and mutant phenotypes in zebrafish. *Developmental Cell*, *32*(1), 97–108. https://doi.org/10.1016/J.DEVCEL.2014.11.018

Langenau, D. M., Ferrando, A. A., Traver, D., Kutok, J. L., Hezel, J. P. D., Kanki, J. P., Zon, L. I., Thomas Look, A., & Trede, N. S. (2004). In vivo tracking of T cell development, ablation, and engraftment in transgenic zebrafish. *Proceedings of the National Academy of Sciences of the United States of America*, *101*(19), 7369. https://doi.org/10.1073/PNAS.0402248101

Lee, Y., Grill, S., Sanchez, A., Murphy-Ryan, M., & Poss, K. D. (2005). Fgf signaling instructs position-dependent growth rate during zebrafish fin regeneration. *Development (Cambridge, England)*, *132*(23), 5173–5183. https://doi.org/10.1242/DEV.02101

Li, L., Yan, B., Shi, Y. Q., Zhang, W. Q., & Wen, Z. L. (2012). Live imaging reveals differing roles of macrophages and neutrophils during zebrafish tail fin regeneration. *Journal of Biological Chemistry*, *287*(30), 25353–25360. https://doi.org/10.1074/JBC.M112.349126/ATTACHMENT/F834DDA9-9B59-43E0-ABB3-59B983EEF484/MMC1.ZIP

Mao, S. A., Glorioso, J. M., & Nyberg, S. L. (2014). Liver regeneration. *Translational Research : The Journal of Laboratory and Clinical Medicine*, *163*(4), 352–362. https://doi.org/10.1016/J.TRSL.2014.01.005

Meng, T.-C., Fukada, T., & Tonks, N. K. (2002). Reversible oxidation and inactivation of protein tyrosine phosphatases in vivo. *Molecular Cell*, *9*(2), 387–399. http://www.ncbi.nlm.nih.gov/pubmed/11864611

Meng, T. C., Buckley, D. A., Galic, S., Tiganis, T., & Tonks, N. K. (2004). Regulation of insulin signaling through reversible oxidation of the protein-tyrosine phosphatases TC45 and PTP1B. *The Journal of Biological Chemistry*, *279*(36), 37716–37725. https://doi.org/10.1074/JBC.M404606200

Nickless, A., Bailis, J. M., & You, Z. (2017). Control of gene expression through the nonsense-mediated RNA decay pathway. *Cell & Bioscience 2017 7:1*, *7*(1), 1–12. https://doi.org/10.1186/S13578-017-0153-7

Niethammer, P., Grabher, C., Look, A. T., & Mitchison, T. J. (2009). A tissue-scale gradient of hydrogen peroxide mediates rapid wound detection in zebrafish. *Nature*, *459*(7249), 996–999. https://doi.org/10.1038/nature08119

Owlarn, S., Klenner, F., Schmidt, D., Rabert, F., Tomasso, A., Reuter, H., Mulaw, M. A., Moritz, S., Gentile, L., Weidinger, G., & Bartscherer, K. (2017). Generic wound signals initiate regeneration in missing-tissue contexts. *Nature Communications*, *8*(1). https://doi.org/10.1038/s41467-017-02338-x

Pike, K. A., Hatzihristidis, T., Bussières-Marmen, S., Robert, F., Desai, N., Miranda-Saavedra, D., Pelletier, J., & Tremblay, M. L. (2017). TC-PTP regulates the IL-7 transcriptional response during murine early T cell development. *Scientific Reports*, *7*(1), 13275. https://doi.org/10.1038/s41598-017-13673-w

Pirotte, N., Stevens, A. S., Fraguas, S., Plusquin, M., Van Roten, A., Van Belleghem, F., Paesen, R., Ameloot, M., Cebrià, F., Artois, T., & Smeets, K. (2015). Reactive oxygen species in planarian regeneration: An upstream necessity for correct patterning and brain formation. *Oxidative Medicine and Cellular Longevity*. https://doi.org/10.1155/2015/392476

Poss, K. D., Shen, J., Nechiporuk, A., McMahon, G., Thisse, B., Thisse, C., & Keating, M. T. (2000). Roles for Fgf signaling during zebrafish fin regeneration. *Developmental Biology*, *222*(2), 347–358. https://doi.org/10.1006/DBIO.2000.9722

Rossi, A., Kontarakis, Z., Gerri, C., Nolte, H., Hölper, S., Krüger, M., & Stainier, D. Y. R. (2015). Genetic compensation induced by deleterious mutations but not gene knockdowns. *Nature*, *524*(7564), 230–233. https://doi.org/10.1038/nature14580

Roy, S., Khanna, S., Nallu, K., Hunt, T. K., & Sen, C. K. (2006). Dermal wound healing is subject to redox control. *Molecular Therapy*, *13*(1), 211–220. https://doi.org/10.1016/j.ymthe.2005.07.684

Salamonsen, L. A. (2003). Tissue injury and repair in the female human reproductive tract. *Reproduction*, *125*(3), 301–311. https://doi.org/10.1530/REP.0.1250301

Stoick-Cooper, C. L., Weidinger, G., Riehle, K. J., Hubbert, C., Major, M. B., Fausto, N., & Moon, R. T. (2007). Distinct Wnt signaling pathways have opposing roles in appendage regeneration. *Development (Cambridge, England)*, *134*(3), 479–489. https://doi.org/10.1242/DEV.001123

Tal, T. L., Franzosa, J. A., & Tanguay, R. L. (2010). Molecular Signaling Networks That Choreograph Epimorphic Fin Regeneration in Zebrafish – A Mini-Review. *Gerontology*, *56*(2), 231. https://doi.org/10.1159/000259327

Tauzin, S., Starnes, T. W., Becker, F. B., Lam, P., & Huttenlocher, A. (2014). Redox and Src family kinase signaling control leukocyte wound attraction and neutrophil reverse migration. *The Journal of Cell Biology*, *207*(5), 589–598. https://doi.org/10.1083/jcb.201408090

Thisse, C., & Thisse, B. (2008). High-resolution in situ hybridization to whole-mount zebrafish embryos. *Nature Protocols*, *3*(1), 59–69. https://doi.org/10.1038/nprot.2007.514

Weibrecht, I., Böhmer, S. A., Dagnell, M., Kappert, K., Östman, A., & Böhmer, F. D. (2007). Oxidation sensitivity of the catalytic cysteine of the protein-tyrosine phosphatases SHP-1 and SHP-2. *Free Radical Biology & Medicine*, *43*(1), 100–110. https://doi.org/10.1016/J.FREERADBIOMED.2007.03.021

Westerfield, M. (2000). *The Zebrafish Book: A Guide for the Laboratory Use of Zebrafish (Danio Rerio)* (4th ed.). Universitu of Oregon Press. https://books.google.nl/books/about/The_Zebrafish_Book.html?id=Iy8PngEACAAJ&redir_esc=y

Wiede, F., Chew, S. H., van Vliet, C., Poulton, I. J., Kyparissoudis, K., Sasmono, T., Loh, K., Tremblay, M. L., Godfrey, D. I., Sims, N. A., & Tiganis, T. (2012). Strain-Dependent Differences in Bone Development, Myeloid Hyperplasia, Morbidity and Mortality in Ptpn2-Deficient Mice. *PLoS ONE*, *7*(5), e36703. https://doi.org/10.1371/journal.pone.0036703

Wiede, F., La Gruta, N. L., & Tiganis, T. (2014). PTPN2 attenuates T-cell lymphopenia-induced proliferation. *Nature Communications*, *5*, 3073. https://doi.org/10.1038/ncomms4073

Wu, W., Hale, A. J., Lemeer, S., & den Hertog, J. (2017). Differential oxidation of protein-tyrosine phosphatases during zebrafish caudal fin regeneration. *Scientific Reports*, *7*(1), 8460. https://doi.org/10.1038/s41598-017-07109-8

Xu, M. -j., Sui, X., Zhao, R., Dai, C., Krantz, S. B., & Zhao, Z. J. (2003). PTP-MEG2 is activated in polycythemia vera erythroid progenitor cells and is required for growth and expansion of erythroid cells. *Blood*, *102*(13), 4354–4360. https://doi.org/10.1182/blood-2003-04-1308

Microscope icon Figure 1: Flaticon.com

Acknowledgements

The authors would like to thank the animal caretakers at the Hubrecht Institute for excellent care of the zebrafish.

Author contributions

Conceptualization: M.A., J.d.H.; Methodology: M.A, J.d.H.; Validation: M.A.; Formal analysis: M.A.; Investigation: M.A., D.W., F.D.; Resources: M.A., J.d.H.; Data curation: M.A.; Writing – original draft: M.A., J.d.H.; Writing - review & editing: M.A., J.d.H.; Visualization: M.A., D.W.; Supervision: J.d.H.; Project administration: J.d.H.; Funding acquisition: J.d.H.

Funding

This work was funded by a grant from the Dutch Research Council to J.d.H. (ALW OP.234).

Knock-out of Ptpn4a causes lethal neurological defects late during development in zebrafish

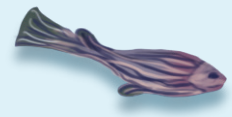

Maaike Allers[1], Fereshte Dadkhodai[1], Danielle T.J. Woutersen[1], Tieme Bijlsma[1], Jeroen Bakkers[1] and Jeroen den Hertog[1,2†]

1. Hubrecht Institute-KNAW and University Medical Center Utrecht, Utrecht, the Netherlands
2. Institute Biology Leiden, Leiden University, Leiden, the Netherlands

Abstract

Recently, mutations in *PTPN4* were discovered as the cause of intellectual disability in several unrelated human patients. The severity of the symptoms differs strongly between patients, which is probably due to differences in the nature and location of the mutations. The symptoms are strongly reminiscent of RETT syndrome, with a few notable differences. We decided to harness the strength of the zebrafish as a model system for neurological disorders and investigate whether mutations in *PTPN4* lead to neurodevelopmental defects. Here, we report the essential role of *PTPN4* in neurological development. Zebrafish with a mutation in *ptpn4a* showed strong mortality between 3 and 5 weeks of age. In the absence of any other cause of death, we concluded that the mutant fish most likely died as a result of a sudden epileptic seizure, which we observed several times. We also show that some survivors were able to compensate for the loss of Ptpn4a and passed along this capability to part of their progeny. To conclude, specific symptoms of human patients were recapitulated in zebrafish with a mutation in *ptpn4a*, which confirms the conservation of the essential neurodevelopmental function of *PTPN4* across species. We believe our *ptpn4a* mutant zebrafish line may be a valuable tool for future research into the exact molecular defect that affects patients with a mutation in *PTPN4*.

Introduction

Every year many children are diagnosed with intellectual disability (ID). Unfortunately, in the majority of the cases, the cause of the ID is not known. It can be caused by injury, genetics, the environment or a combination of the above. Recently, mutations in *PTPN4* were discovered as a cause for ID in several unrelated human patients (Chmielewska *et al*., 2021; Szczałuba *et al*., 2018; Williamson *et al*., 2015). Human patients with mutations in *PTPN4* suffer from a range of symptoms. The severity of the symptoms differs strongly between patients, which is probably due to differences in the nature and location of the mutations. As far as we can determine, all human patients show a normal prenatal development and birth. They are generally described as being quiet babies. Between 6 and 12 months, the patients are diagnosed with ID. In addition to ID, the patients show a variety of other symptoms, including epileptic seizures, macrocephaly, heart defects, skeletal anomalies, stereotypical hand movements, gradual loss of speech and growth deficiency or excess. The symptoms are strongly reminiscent of RETT syndrome, with a few differences, notably the lack of scoliosis, breathing disturbances and loss of fine motor skills in patients with *PTPN4* mutations. The notion that *PTPN4* is a target of MECP2, the primary affected protein in patients with Rett syndrome, may explain the similarities between the patients (Williamson *et al*., 2015).

The *Drosophila* homolog of *PTPN4*, called *ptpmeg*, has previously been shown to have a neurodevelopmental function, in that *ptpmeg* functions to regulate the maintenance of the mushroom body axon branches (Whited *et al*., 2007). Mutation of *ptpmeg* in *Drosophila* does not cause mortality or obvious motor defects, but it does cause flies to become trapped alive in their food under normal culturing conditions.

In recent years, the zebrafish has emerged as a research model for neurological disorders. Break-through discoveries using zebrafish have been done investigating neurologically active small-molecules, as well as neurological disorders like anxiety disorders and epilepsy (Fontana *et al*., 2018; Pitchai *et al*., 2019). Even though there are considerable anatomical differences between the brain structures of zebrafish and mammals, all important characteristics of mammalian brains are present in zebrafish brains. For example, regions homologous to the hippocampus and the amygdala have been located (Fontana *et al*., 2018).

We decided to harness the strength of the zebrafish as a model system for neurological disorders and investigate whether mutations in *Ptpn4a* lead to neurodevelopmental defects. Here, we report data that support the notion that

mutations in *PTPN4* cause ID in humans. Specific symptoms of human patients were recapitulated in zebrafish with a mutation in *ptpn4a*, which confirms the conservation of the essential neurodevelopmental function of *PTPN4* across species.

Material and methods

Zebrafish husbandry

All procedures involving experimental animals were approved by the local animal experiments committee (AVD-8010020173786). All fish were housed and handled according to local guidelines and policies in compliance with national and European law. Zebrafish were raised and maintained under a 14 hours light / 10 hours dark cycle at 28.5˚C as described by (Westerfield, 2000). Fertilized eggs were harvested and incubated at 28.5˚C in E3 medium (5 mM NaCl, 0,17 mM KCl, 0.33 mM $CaCl_2$, 0.33mM $MgSO_4$).

Genotyping

Genomic zebrafish DNA was extracted through lysis of embryos or fin clips in 100 µg/ml proteinase K (Sigma) diluted in SZL buffer (50 mM KCl, 2.5 mM MgCl, 10mM Tris pH 8.3, 0.005% NP40, 0.005% Tween-20 and 0.1% Gelatine). Samples were lysed at 60˚C for 1 hour, followed by inactivation for 15 min at 95˚C in a thermal cycler (BioRad T100). Mutations were analyzed by PCRs targeted to the mutation sites. PCR products were run on a 4% agarose gel (UltraPure agarose, Invitrogen) in TBE . The following primers were used to amplify the mutation sites:

ptpn4a forward	TCGTGAGTCATGCCTGTTATTC
ptpn4a reverse	CTGCCAGAGTGAGTTTAGAGCA
ptpn4b forward	AGAAAACAGCTCAAAAGTAGGC
ptpn4b reverse	ACGTACCTTGTGTACTCTTCCTG

Survival experiments

Embryos were finclipped at 2dpf and the isolated fin material was lysed and genotyped. Embryos were kept in 48 well plates overnight, before being sorted based on genotyping. They were raised to adulthood in families of 10-20 siblings. Tanks were checked for dead zebrafish twice per day. Dead zebrafish were collected for genotyping. Length of fish was measured by sedating the fish using tricaine methane sulfonate and imaging them positioned next to a ruler once a week.

Statistical analysis

Statistical tests for the survival curves were performed and data was visualized using GraphPad PRISM. Statistical tests for the other data were performed and data was visualized using Python (Pandas 1.0.5, MatPlotLib 3.2.2, SciPy 1.5.0, Seaborn 0.10.1).

Microscopy
For bright-field and fluorescence imaging, 5 dpf embryos were anesthetized using tricaine methane sulfonate and mounted in 2% methylcellulose (Sigma) on glass indented slides. They were imaged using a Leica M165FC connected to a DFC420C camera. Images were processed using ImageJ.

Live imaging
Zebrafish of 0 to 5 weeks of age were transferred to 24 or 6 wells plates with fish water from their tank. They were live imaged in a ZebraBox (ViewPoint Behavior Technology) with the light intensity setting to 10% and temperature constant at 28.5˚C. Zebrafish were imaged for several hours.

QPCR
Total RNA was extracted from genotyped larvae in Trizol (Invitrogen). Snapfrozen samples were crushed with an Eppendorf tube pestle and further homogenized using a syringe. cDNA was synthesized using superscriptIII first strand synthesis kit (Invitrogen). qRT-PCR was performed using SYBR green and a CFX-96 Connect Real-Time system (Bio-Rad). All samples were measured in duplicate and averaged. Data was analyzed by applying the $2^{-\Delta\Delta Ct}$ method (Livak and Schmittgen, 2001) . Expression of Ppial or Ef1a was used as a baseline to compensate for differences in concentration. Individual fold changes were calculated compared to the average WT dCT value. The individual fold changes were tested for a statistically significant difference between WT and mutant individuals using T-test assuming unequal variance and Bonferroni correction.

Histology
Zebrafish that were found dead, but not yet disintegrated, were fixed in 4% paraformaldehyde overnight 4˚C. Samples were washed with increasing amounts of EtOH for 30 min each and dehydrated in 100% EtOH 3 times. Subsequently, samples were washed thrice with butanol and thrice with paraffin at 58˚C, before being embedded in paraffin. The samples were sliced, stained with hematoxylin and eosin stain and imaged at 20x magnification.

Results

Specific mutation in *ptpn4a* causes growth defect and mortality at 4 weeks post fertilization
As described previously in this thesis, we used CRISPR-Cas9 to create knockout lines of genes encoding protein tyrosine phosphatases (PTPs), including Ptpn4a and Ptpn4b. Two different founders were chosen for every line. For *ptpn4a* we selected a 13 bp insertion with a 2 bp deletion (line 1) and a 7 bp deletion with a 3 bp insertion (line 2) (Figure 1A&B). For *ptpn4b* we selected a 5 bp deletion (line 2) (Figure 1C). These lines were outcrossed twice with wild-type (WT) zebrafish, to mitigate the possibility of background mutations causing a phenotype. The fish were incrossed and development of the progeny was investigated. Morphologically, the homozygous *ptpn4a* mutant embryos showed normal development at 5 days post fertilization (dpf) (Figure 1D). The homozygous *ptpn4b* fish also showed no developmental defects. We selected the *ptpn4a* line 1 and *ptpn4b* line 2 to generate double mutants. Double homozygous *ptpn4a – ptpn4b* mutants showed normal morphological development at 5 dpf (Figure 1D).

We monitored the offspring of incrosses over time. At 3 weeks post fertilization (wpf) the homozygous mutants of line 1 (13 bp insertion and 2 bp deletion) showed strong mortality (Figure 2A). 75% of the mutant zebrafish died, usually between 3 and 5 wpf. The survival rate was consistent over multiple experiments with parents from multiple generations through the course of 1 year. The WT and heterozygous siblings, which were raised in the same tanks, showed no strong mortality until they neared 50 wpf. The *ptpn4b* loss of function mutation did not affect viability of the fish. Moreover, combining the mutations in *ptpn4a* line 1 and *ptpn4b* by incrossing, resulted in double mutants with similar mortality rates as the *ptpn4a* line 1 by itself (Figure 2B).

However, mutant fish from *ptpn4a* line 2 did not show significant mortality or any other phenotype (Figure 2C). This was unexpected, because even though the stop codons caused by the mutations differ between *ptpn4a* mutant lines 1 and 2, both mutations are predicted to generate non-functional Ptpn4a.

The *ptpn4a* mutant fish from line 1 are smaller than their WT siblings at 4 wpf, although this difference was not statistically significant (Figure 3A&B). However, the fish that survived to adulthood, caught up with their siblings with regards to their length at 7 wpf (Figure 3B). It is noteworthy that the average length of mutant fish caught up with the average length of their WT and heterozygous siblings, because the fish that remain smaller, die between 4 and 7 wpf and surviving *ptpn4a* mutant fish had normal size. Homozygous survivors showed no other defects and reached the end of their life similarly to their siblings.

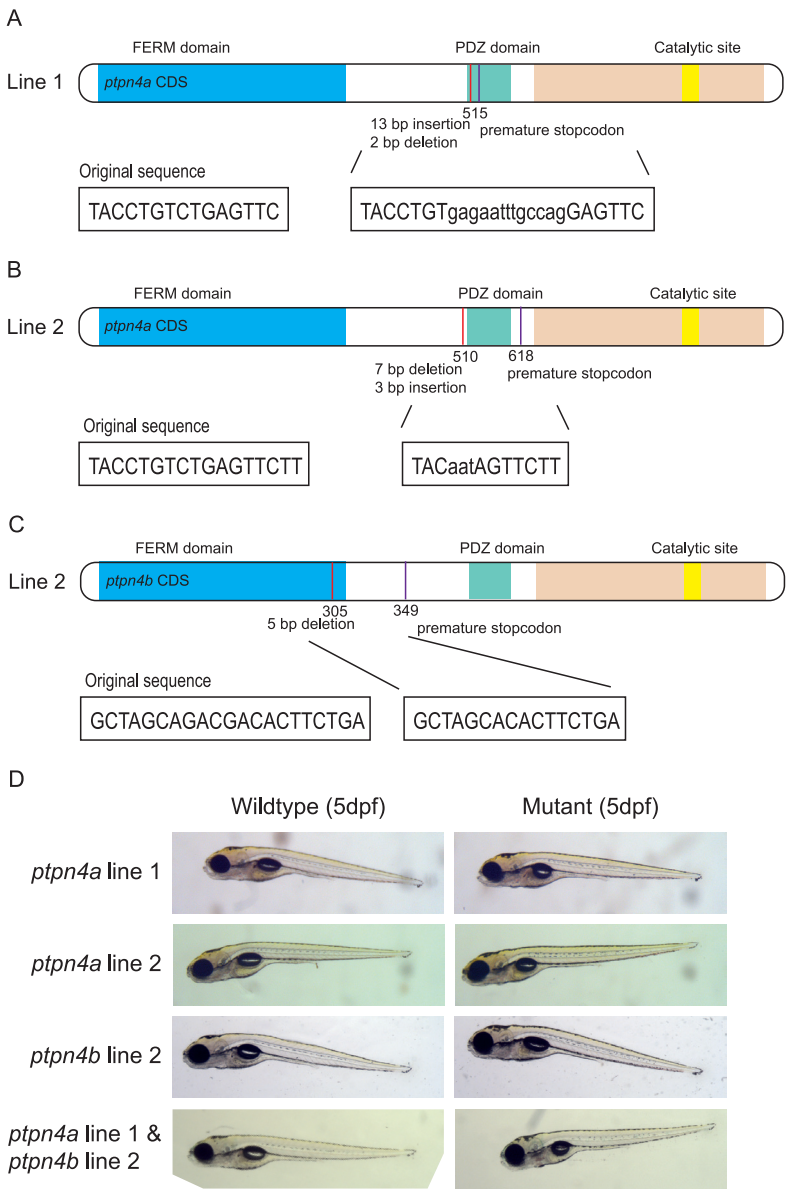

Figure 1: Generation of the *ptpn4a* and *ptpn4b* knockout lines. A-C: Schematic representation of the coding sequences of *ptpn4a* and *ptpn4b*. The location of the mutations are indicated with a red stripe and the location of the premature stopcodons are indicated with a purple stripe. The exact number of the locations in basepairs of the CDS are written below the schematics. The FERM (blue), PDZ (aqua) and catalytic (orange) domains are indicated in the schematic. The original sequence of the mutation location and the new sequence including the insertions and deletions are written below the schematics, with insertions in small letters. D: Representative pictures of mutants and WT siblings at 5 dpf are shown.

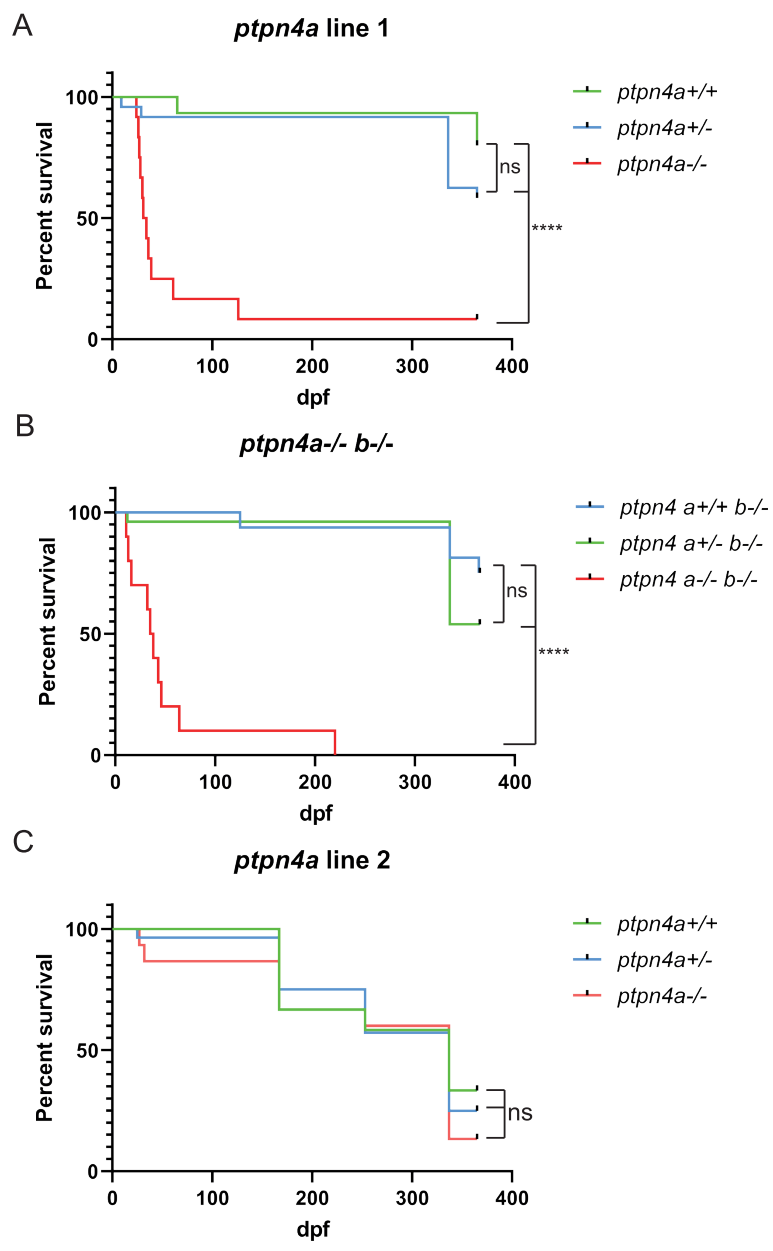

Figure 2: Survival of the *ptpn4a* and *ptpn4b* mutant lines. The survival rate over one year is shown. Mutants of the first generation are indicated in red, WT siblings in green and heterozygous siblings in blue. In panel D and E, mutants generated by incrossing the surviving mutants from the first generation are indicated in orange. The offspring that was generated by incrossing survivors of second generation mutants (offspring's offspring) are indicated in purple. Statistical tests were performed by GraphPad PRISM (Kaplan-Meier method).

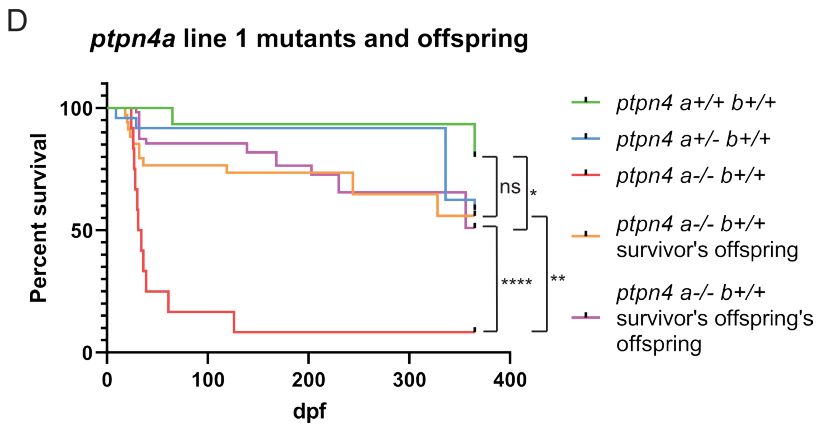

Figure 2: Continued.

The homozygous *ptpn4a* mutant fish that survived were also fertile. The progeny of the survivors showed strongly decreased mortality compared to the original mutant fish. However, the age of the fish that died was similar to the first generation (Figure 2D). Around 60% of the progeny survived to adulthood. This indicates that the survival capability is partially hereditary, but does not segregate in a mendelian fashion. This observation is supported by the notion that the mortality in the next generation was also decreased (Figure 2D). Similarly, decreased mortality was visible in the *ptpn4a -/- ptpn4b -/-* double mutant offspring, which shows that there was no additional effect on the mortality of the survivor's offspring caused by the *ptpn4b* knock-out (Figure 2E).

There may be a small additional effect of the mutation in *ptpn4b* on the growth defect of *ptpn4a* mutant fish, in that double mutant fish showed a bigger difference in length compared to their WT siblings than single mutant fish without functional *ptpn4a* (Figure 3C).

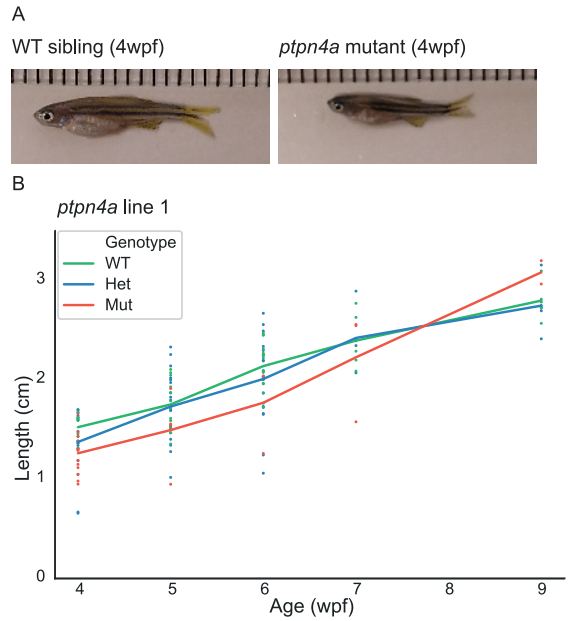

Figure 3: *ptpn4a-/-* fish are smaller than their WT sibling at 4-6 weeks post fertilization. A: Representative pictures are shown of a *ptpn4a-/-* fish at 4 weeks post fertilization and a WT sibling. Fish were sedated and imaged next to a ruler. B, C: Length of the same zebrafish was followed over time from 4 till 9 weeks post fertilization, by imaging the fish next to a ruler every week. Average length of the fish is presented as solid line, with the individual measurements as points (green for WT siblings, blue for heterozygous siblings and red for mutant siblings). B: WT n =7, Heterozygous n=18, Mutant n=14. ANOVA tests indicated no statistically significant differences between the lengths of the fish from different genotypes in *ptpn4a* line 1. C: WT n =11, Heterozygous n=19, Mutant n=8. ANOVA tests indicated statistically significant differences between the fish from the different genotypes in the double mutant line at 4, 5 and 6 weeks old (p-values were 7.5e-5, 4.5e-6 and 0.001).

The cause of death is most likely a sudden seizure

Previous literature gave little indication of the potential cause of death of these *ptpn4a* mutant fish. The fish were investigated by a veterinarian for symptoms of bacterial or parasitic infection after fixation in PFA. None were found. Also, the maturation of T-cells in mutant fish was investigated by assessment of the size of the thymus in transgenic *lck-GFP* zebrafish embryos. No difference was seen between the mutant fish and their WT siblings (Figure 4).

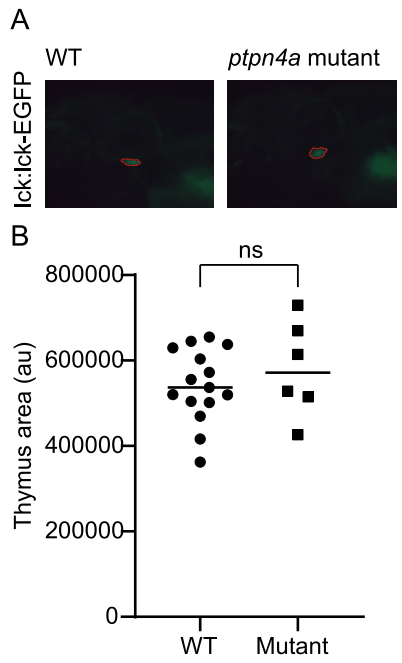

Figure 4: The maturation of T-cells is not affected in *ptpn4a* mutants. A: Representative pictures are shown of transgenic 3dpf *lck-GFP* zebrafish for *ptpn4a* mutants and their WT siblings. The thymus area is visible in green and outlined in red. B: The thymus areas were measured in transgenic *lck-GFP* zebrafish embryos. Subsequently, the embryos were genotyped by sequencing and the thymus area was compared using Student's T-test. All data points are plotted and the averages are indicated with a stripe.

Next, we switched to overnight live imaging of the fish when they were 3-5 weeks old. In this way we were able to image the death of two fish, and we observed a third death in person. All three fish were seen to undergo an episode that was most likely a sudden epileptic seizure. The speed and movements of the dying fish were strongly different from the movements of their healthy siblings. Bursts of contraction alternated with loss of balance (Figure 5 and movie 1). This corresponds with reports about human patients suffering from epileptic seizures.

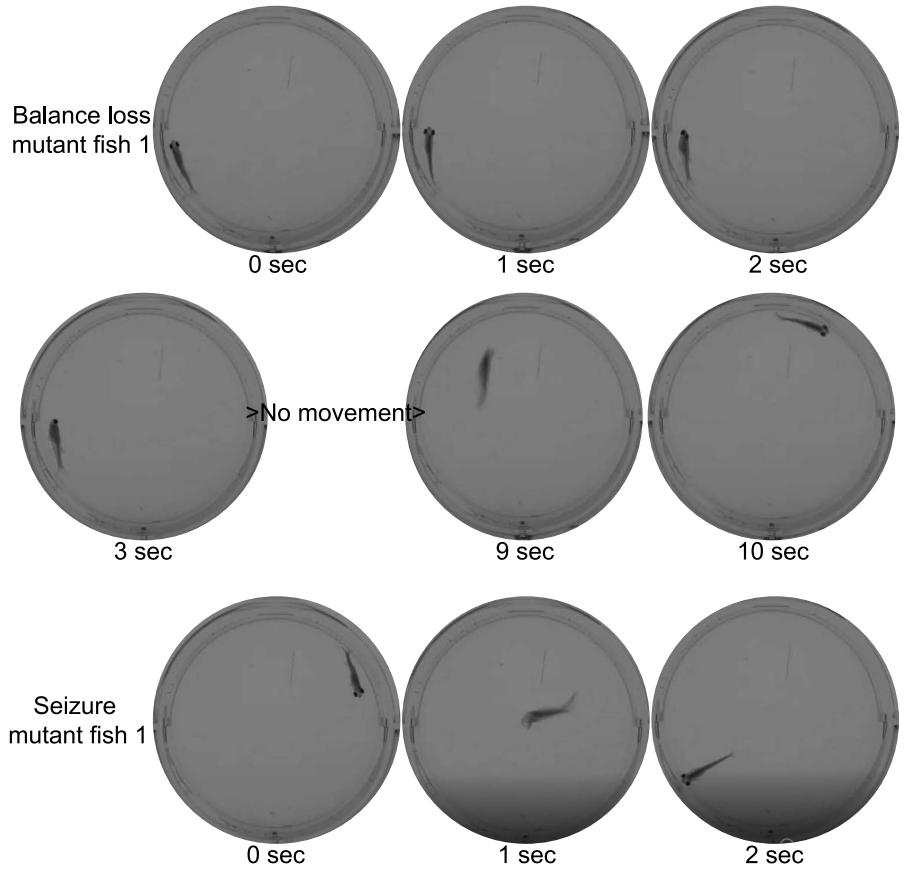

Figure 5: *ptpn4a* mutant zebrafish of 4 wpf suffered from epileptic seizures. Screenshots from movie 1 are shown in this figure. The 4 wpf *ptpn4a* mutant zebrafish was seen showing very fast movements and periods of inactivity, both not seen in WT siblings, resembling an epileptic seizure. The zebrafish subsequently stopped showing any activity and was found dead.

No evidence was found for the zebrafish suffering from epileptic seizures prior to the one that caused their death. No zebrafish was observed undergoing and surviving the seizure, which led us to conclude that the most likely cause of death for the majority of the *ptpn4a* mutant fish was a sudden, deadly epileptic seizure.

We were interested to see if we noticed any gross effect on the brain morphology of the *ptpn4a* mutant zebrafish. Therefore, we fixed several zebrafish mutants right after they were found dead and their WT siblings. Sections from these fish were generated and imaged. We observed no difference between the *ptpn4a* mutant fish and their WT sibling (Figure 6).

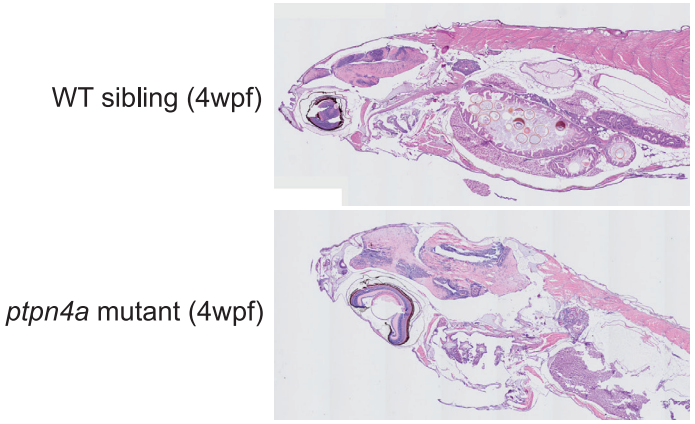

Figure 6: No obvious defects are visible in the brain morphology of *ptpn4a* mutants. Dead *ptpn4a* mutant zebrafish and their WT siblings of 4 wpf were fixed in PFA, embedded in paraffin and stained with eosin/hematoxylin. Their morphology was checked for gross defects. None were found. Representative pictures of a *ptpn4a* mutant and a WT sibling are shown (n=3).

ptpn4a mutant line 2 developed mortality over time

Surprisingly, the *ptpn4a* mutant line 2 did not show high mortality rates around 4 wpf, unlike the *ptpn4a* mutant line 1, even though both lines have mutations that result in lack of expression of functional Ptpn4a. We hypothesized that the zebrafish from *ptpn4a* line 2 had up- or downregulated the expression of other genes to compensate for the loss of *ptpn4a*. The decreased mortality seen in next generations of survivors from *ptpn4a* line 1 support the hypothesis that (expression of) other genes may affect mortality in response to loss of functional Ptpn4a. To investigate if line 2 was compensating by up- or downregulating another PTP we tested the expression of several PTPs at 4 wpf. We compared the expression in both line 1 and line 2 with their WT siblings. We displayed only the PTPs that showed a difference in expression, although no effects were found to be statistically significant (Figure 7). Line 1 and 2 showed the same effect for many PTPs, for instance *ptpn4a*, *ptpn21* and *ptpn23a* were downregulated in both lines, compared to their WT siblings. However, for three genes there was an opposing effect visible in the expression levels between the two lines. *Ptpn2a* was downregulated in line 1 and upregulated in line 2, whereas *ptpn9a* was upregulated in line 1 and downregulated in line 2. *Ptpn4b* was upregulated in line 1 and downregulated in line 2. The mortality rates in *ptpn4a-/-* line 1 fish were not affected by loss of functional *ptpn4b* (Figure 2B), suggesting that the upregulation of *ptpn4b* in *ptpn4a-/-* line 1 fish was not involved in the enhanced mortality of *ptpn4a-/-* fish. We hypothesized that line 2 could be compensating for the loss of *ptpn4a* by upregulating *ptpn2a* or downregulating *ptpn9a*.

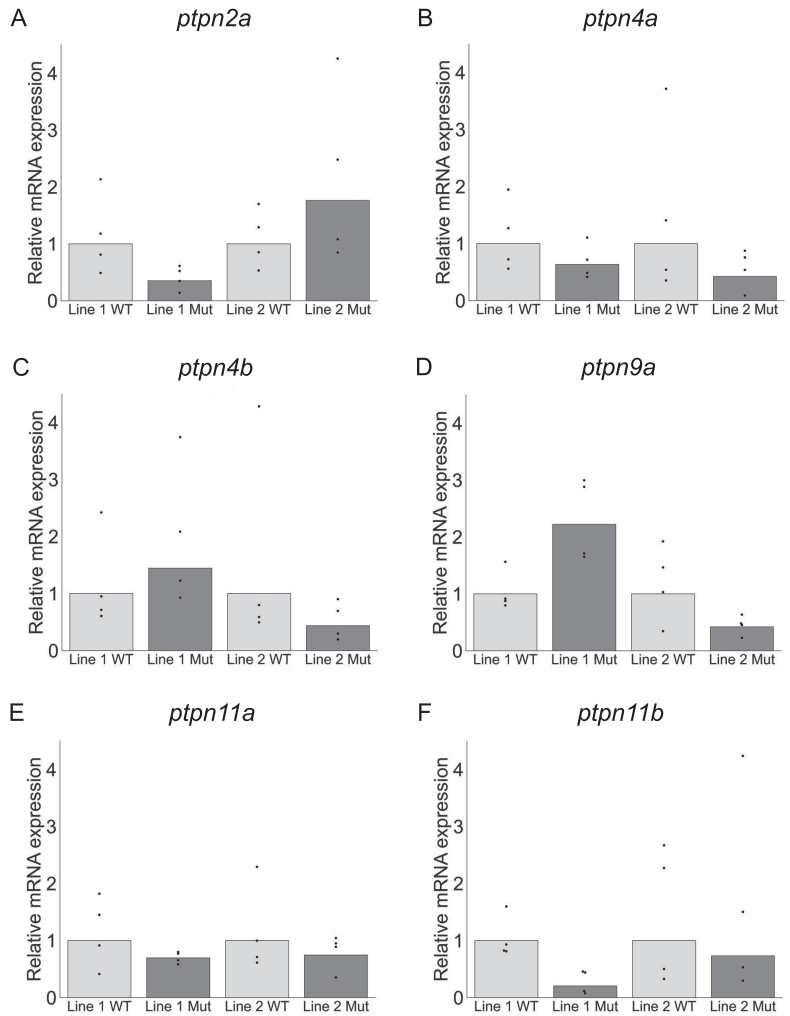

Figure 7: Expression of several PTPs is affected in *ptpn4a* mutants at 4 wpf. We tested the expression of a panel of PTPs in *ptpn4a* mutants (n=4) and their WT siblings (n=4) at 5dpf and 4 wpf for both *ptpn4a* line 1 and 2. Here we show the expression levels of the PTPs that were found to differ between *ptpn4a* mutants (dark grey) and their WT siblings (light grey) at 4wpf. All samples were measured in duplicate and averaged. The fold changes (shown in bar graphs) were calculated using the average dCt of the 4 WT and 4 mutant values and normalized compared to the average WT dCt value. Expression of Ppial or Ef1a was used as a baseline to compensate for differences in concentration of the mRNA. Individual fold changes were calculated compared to the average WT dCT value and plotted as black points. The individual fold changes were tested for a statistically significant difference between WT and mutant individuals using T-test assuming unequal variance and Bonferroni correction. No statistically significant differences were found.

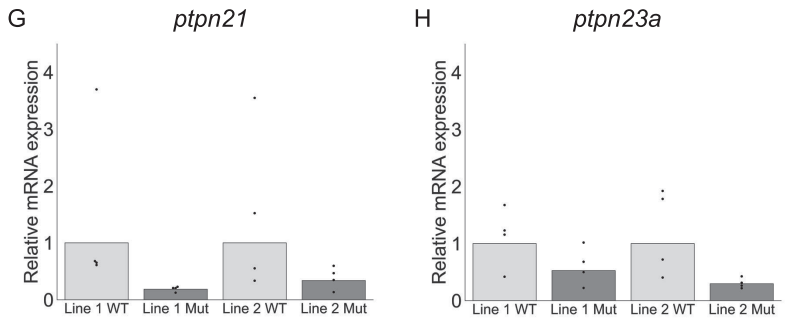

Figure 7: Continued.

To test the hypothesis that upregulation of ptpn2a was involved in compensating for the loss of ptpn4a in line 2, we created a double knock-out of *ptpn2a* and *ptpn4a* line 2. To our surprise, independent of the *ptpn2a* mutation, the zebrafish mutant for *ptpn4a* showed strong mortality in the juvenile stage (Figure 8A), unlike in earlier experiments, using earlier generations of *ptpn4a* mutant fish line 2 (Figure 2C). The mortality seemed to range between 50% and 90%, depending on which family was used for the experiment, and was significantly different from the survival rate of the WT siblings. We saw no additional effect of a knockout of *ptpn2a*, but since the *ptpn4a* line 2 mutants no longer showed a strong survival rate, we cannot conclude whether or not Ptpn2a was contributing to the compensation for the loss of Ptpn4a (Figure 8B). Apparently, *ptpn4a* mutant fish line 2 lost the capacity to compensate for the loss of Ptpn4a over time/ generations.

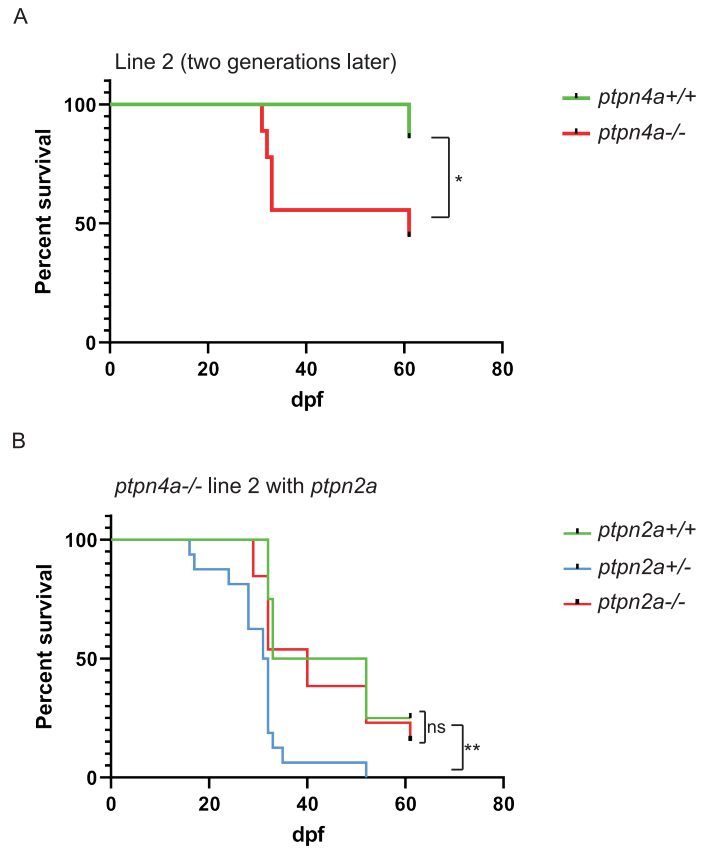

Figure 8: Mortality in *ptpn4a* line 2 two generations after the original survival experiments. A: The survival rate of *ptpn4a* line 2, two generations later than the generation that was used to test the survival rate initially (Figure 2B) in red, compared to WT siblings in green. B: The *ptpn4a* line 2 was crossed with a knockout line for *ptpn2a*, to test the compounding effect of *ptpn2a* loss on the *ptpn4a* mutants. No difference was found in the survival rate. All zebrafish were mutant for ptpn4a. Mutants for *ptpn2a* are indicated in red, WT siblings in green and heterozygous siblings in blue. Statistical tests were performed by GraphPad PRISM (Kaplan-Meier method).

Discussion

In this chapter we showed that a loss of function mutation in *ptpn4a* leads to mortality in juvenile zebrafish. In addition, we showed that the mutant zebrafish were shorter than their WT siblings at 4 wpf and we observed several fish that underwent a sudden epileptic seizure.

We have investigated several possible reasons for the death of the juvenile zebrafish and we concluded that they most likely all died from undergoing a seizure. A minority of the mutant fish escaped death during their juvenile stage. These survivors caught up with their WT siblings in length and showed no problems during their adult life. Their progeny showed a higher survival rate than the original generation, which indicates a hereditary survival capability. However, this capability did not segregate in mendelian fashion. In addition we showed that *ptpn4a* mutant line 2, while originally not lethal, apparently lost their capacity to compensate for the lack of Ptpn4a over the years and showed the same mortality as *ptpn4a* mutant line 1 showed a few years earlier. It appears based on *ptpn4a* mutant line 2 and the survivors of mutant line 1, that loss of functional Ptpn4a is not always lethal. Some individuals are capable of compensating for the loss of functional Ptpn4a. This compensation is hereditary, but not stagnant. By maintaining the *ptpn4a* mutant line 2 as heterozygous fish, these fish lost the necessity to compensate for the loss of *ptpn4a.* Over the course of a few years, the progeny did not show the same survival as their ancestors.

Human patients with a mutation in *PTPN4* show a variety of symptoms in addition to ID. The essential role of *PTPN4* is supported by the observation that *PTPN4* has a high LoF intolerance, as there are less LoF mutations present in the normal population than you would expect (Lek *et al*., 2016). The human patients may be separated into two groups: the first group has a Loss-of-Function (LoF) or severely damaging missense variant, and the second group has moderately damaging missense variants (hypomorphs) in *PTPN4.* The human patients in group 1 with a severe variant of *PTPN4* segregate to the 1st or 2nd percentile for height and undergo epileptic seizures (Chmielewska *et al*., 2021). This corresponds to our data where we have shown that zebrafish with a LoF mutation in *ptpn4a* are smaller than their WT siblings and we have seen them undergoing epileptic seizures. These similarities support the notion that the function of *PTPN4* in development is essential and conserved over species.

To confirm the notion that the symptoms we see in our zebrafish model are due to a lack of Ptpn4a, we should perform a rescue experiment, in which we express WT Ptpn4a in mutant zebrafish and check if this omits the developmental defects. Standard procedure

for embryonic lethal mutations is to microinject mRNA encoding the target gene at the one-cell stage. However, because lethality is late (around 4 wpf), mRNA injection, which results in protein production for several days, cannot be applied to *ptpn4a*. In this case, an expression vector for *ptpn4a* or a bacterial artificial chromosome (BAC) containing the entire *ptpn4a* gene should be microinjected to rescue loss of Ptpn4a expression in the mutant. Nevertheless, since the symptoms between human patients and our zebrafish model are similar, we feel confident in stating that we believe the symptoms we see are due to the lack of functional Ptpn4a.

Two patients present with a missense variant in *PTPN4* in the FERM domain (L72S and G239A). These mutations prevent the correct localization of PTPN4 to the dendritic spines of neuronal cells *in vitro* (Chmielewska *et al*., 2021; Szczałuba *et al*., 2018). These patients suffered from ID and autistic features, but did not show growth deficiency or undergo seizures. Apparently, correct localization of PTPN4 to the synapses of neurons is essential for correct neurological development. This is further corroborated by the observation that the dendritic spines are also affected in RETT syndrome, where *PTPN4* is a target of MECP2 (Chapleau *et al*., 2009, 2012; Landi *et al*., 2011).

However, Ptpn4a most likely also has other functions, independent of its correct localization to the dendritic spines, that affect growth and prevent epileptic seizures. In mice, it is well accepted that PTPN4 functions by dephosphorylation of the NDMAR subunits GluN2A and GluN2B at the synapses (Espinoza *et al*., 2020). However, its targets or the pathways in which Ptpn4 functions at other locations are still unclear. In human cell lines, Ptpn4 has been implicated in affecting cell growth and motility by interacting with CrkI (Zhou *et al*., 2013). In addition, PTPN4 has been shown in mouse cell lines to interact with TRAM and TCR ζ in immune cells (Huai *et al*., 2015; Young *et al*., 2008). However, as both our data and data of others have shown, there is no effect of *Ptpn4* deletion on the development of T-cells (Young *et al*., 2008).

To summarize, our research has shown that *ptpn4a* is essential for correct neurological development, and the lack of Ptpn4a leads to deadly epileptic seizures and growth deficiencies in juvenile zebrafish. The exact target and/or pathway in which Ptpn4a functions to affect these processes is still unknown and it would be highly interesting to investigate this further. While the target of Ptpn4a at the synapses is probably known, it is likely that the growth deficiency, and possibly also the seizures, are due to the role of Ptpn4a in another, yet unknown pathway. Since the role of PTPN4 in development seems to be highly conserved between humans and zebrafish, our zebrafish model would be well suited to investigate this recently discovered syndrome further.

Literature list

Chapleau, C. A., Boggio, E. M., Calfa, G., Percy, A. K., Giustetto, M., & Pozzo-Miller, L. (2012). Hippocampal CA1 Pyramidal Neurons of Mecp2 Mutant Mice Show a Dendritic Spine Phenotype Only in the Presymptomatic Stage. *Neural Plasticity*, *2012*. https://doi.org/10.1155/2012/976164

Chapleau, C. A., Calfa, G. D., Lane, M. C., Albertson, A. J., Larimore, J. L., Kudo, S., Armstrong, D. L., Percy, A. K., & Pozzo-Miller, L. (2009). Dendritic spine pathologies in hippocampal pyramidal neurons from Rett syndrome brain and after expression of Rett-associated MECP2 mutations. *Neurobiology of Disease*, *35*(2), 219–233. https://doi.org/10.1016/J.NBD.2009.05.001

Chmielewska, J. J., Burkardt, D., Granadillo, J. L., Slaugh, R., Morgan, S., Rotenberg, J., Keren, B., Mignot, C., Escobar, L., Turnpenny, P., Zuteck, M., Seaver, L. H., Ploski, R., Dziembowska, M., Wynshaw-Boris, A., & Adegbola, A. (2021). PTPN4 germline variants result in aberrant neurodevelopment and growth. *Human Genetics and Genomics Advances*, *2*(3), 100033. https://doi.org/10.1016/J.XHGG.2021.100033

Espinoza, S., Arredondo, S. B., Barake, F., Carvajal, F., Guerrero, F. G., Segovia-Miranda, F., Valenzuela, D. M., Wyneken, U., Rojas-Fernández, A., Cerpa, W., Massardo, L., Varela-Nallar, L., & González, A. (2020). Neuronal surface P antigen (NSPA) modulates postsynaptic NMDAR stability through ubiquitination of tyrosine phosphatase PTPMEG. *BMC Biology*, *18*(1). https://doi.org/10.1186/s12915-020-00877-2

Fontana, B. D., Mezzomo, N. J., Kalueff, A. V., & Rosemberg, D. B. (2018). The developing utility of zebrafish models of neurological and neuropsychiatric disorders: A critical review. In *Experimental Neurology* (Vol. 299, pp. 157–171). Academic Press Inc. https://doi.org/10.1016/j.expneurol.2017.10.004

Huai, W., Song, H., Wang, L., Li, B., Zhao, J., Han, L., Gao, C., Jiang, G., Zhang, L., & Zhao, W. (2015). Phosphatase PTPN4 Preferentially Inhibits TRIF-Dependent TLR4 Pathway by Dephosphorylating TRAM. *The Journal of Immunology*, *194*(9), 4458–4465. https://doi.org/10.4049/jimmunol.1402183

Landi, S., Putignano, E., Boggio, E. M., Giustetto, M., Pizzorusso, T., & Ratto, G. M. (2011). The short-time structural plasticity of dendritic spines is altered in a model of Rett syndrome. *Scientific Reports*, *1*(1), 1–7. https://doi.org/10.1038/srep00045

Lek, M., Karczewski, K. J., Minikel, E. V., Samocha, K. E., Banks, E., Fennell, T., O'Donnell-Luria, A. H., Ware, J. S., Hill, A. J., Cummings, B. B., Tukiainen, T., Birnbaum, D. P., Kosmicki, J. A., Duncan, L. E., Estrada, K., Zhao, F., Zou, J., Pierce-Hoffman, E., Berghout, J., … Williams, A. L. (2016). Analysis of protein-coding genetic variation in 60,706 humans. *Nature*, *536*(7616), 285–291. https://doi.org/10.1038/NATURE19057

Pitchai, A., Rajaretinam, R. K., & Freeman, J. L. (2019). Zebrafish as an Emerging Model for Bioassay-Guided Natural Product Drug Discovery for Neurological Disorders. *Medicines*, *6*(2), 61. https://doi.org/10.3390/medicines6020061

Szczałuba, K., Chmielewska, J. J., Sokolowska, O., Rydzanicz, M., Szymańska, K., Feleszko, W., Włodarski, P., Biernacka, A., Murcia Pienkowski, V., Walczak, A., Bargeł, E., Królewczyk, K., Nowacka, A., Stawiński, P., Nowis, D., Dziembowska, M., & Płoski, R. (2018). Neurodevelopmental phenotype caused by a de novo PTPN4 single nucleotide variant disrupting protein localization in neuronal dendritic spines. *Clinical Genetics*, *94*(6), 581–585. https://doi.org/10.1111/cge.13450

Westerfield, M. (2000). *The zebrafish book. A guide for the laboratory use of zebrafish (Danio rerio).* (4th ed.). Univ. of Oregon Press.

Whited, J. L., Robichaux, M. B., Yang, J. C., & Garrity, P. A. (2007). Ptpmeg is required for the proper establishment and maintenance of axon projections in the central brain of Drosophila. *Development*, *134*(1), 43–53. https://doi.org/10.1242/dev.02718

Williamson, S. L., Ellaway, C. J., Peters, G. B., Pelka, G. J., Tam, P. P., & Christodoulou, J. (2015). Deletion of protein tyrosine phosphatase, non-receptor type 4 (PTPN4) in twins with a Rett syndrome-like phenotype. *European Journal of Human Genetics*, *23*(9), 1171–1175. https://doi.org/10.1038/ejhg.2014.249

Young, J. A., Becker, A. M., Medeiros, J. J., Shapiro, V. S., Wang, A., Farrar, J. D., Quill, T. A., van Huijsduijnen, R. H., & van Oers, N. S. C. (2008). The protein tyrosine phosphatase PTPN4/PTP-MEG1, an enzyme capable of dephosphorylating the TCR ITAMs and regulating NF-κB, is dispensable for T cell development and/or T cell effector functions. *Molecular Immunology*, *45*(14), 3756–3766. https://doi.org/10.1016/j.molimm.2008.05.023

Zhou, J., Wan, B., Shan, J., Shi, H., Li, Y., & Huo, K. (2013). PTPN4 negatively regulates CrkI in human cell lines. *Cellular & Molecular Biology Letters*, *18*(2), 297–314. https://doi.org/10.2478/s11658-013-0090-3

Acknowledgements

The authors would like to thank the animal caretakers at the Hubrecht Institute for excellent care of the zebrafish.

Author contributions

Conceptualization: M.A., J.d.H.; Methodology: M.A, J.d.H.; Validation: M.A.; Formal analysis: M.A.; Investigation: M.A., D.W., F.D., T.B.; Resources: M.A., J.d.H.; Data curation: M.A.; Writing – original draft: M.A., J.d.H.; Writing - review & editing: M.A., J.B., J.d.H.; Visualization: M.A.; Supervision: J.d.H.; Project administration: J.d.H.; Funding acquisition: J.d.H.

Funding

This work was funded by a grant from the Dutch Research Council to J.d.H. (ALW OP.234).

Loss of Shp1 impairs myeloid cell function and causes lethal inflammation in zebrafish larvae

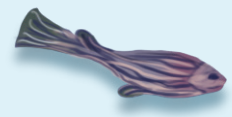

Maaike Allers[1*], Petra A. Bakker[1,2*], Jelmer Hoeksma[1], Herman P. Spaink[2] and Jeroen den Hertog[1,2‡]

1. Hubrecht Institute-KNAW and University Medical Center Utrecht, Utrecht, the Netherlands
2. Institute Biology Leiden, Leiden University, Leiden, the Netherlands

* these authors contributed equally to this work
‡ Author for correspondence (j.denhertog@hubrecht.eu)

Adapted from Disease Models and Mechanisms 16(2): dmm049715 (2023)

Abstract

PTPN6 encodes SHP1, a protein tyrosine phosphatase with an essential role in immune cell function. SHP1 mutations are associated with neutrophilic dermatoses and emphysema in humans, which resembles the phenotype seen in *motheaten* mice that lack functional SHP1. We investigated the function of Shp1 in developing zebrafish embryos. We generated a *ptpn6* knockout zebrafish line lacking functional Shp1. Shp1 knockout caused severe inflammation and lethality around 17 days post fertilization (dpf). During early development the myeloid lineage was affected, resulting in a decrease in the number of neutrophils, and a concomitant increase in the number of macrophages. The number of emerging hematopoietic stem and progenitor cells (HSPCs) was decreased, but due to hyperproliferation, the number of HSPCs was higher in *ptpn6* mutants than in siblings at 5 dpf. Finally, directional migration of neutrophils and macrophages was decreased in response to wounding and less macrophages were recruited to the wound site. Yet, regeneration of the caudal fin fold was normal. We conclude that loss of Shp1 impaired neutrophil and macrophage function and caused severe inflammation and lethality at the larval stage.

Introduction

The non-receptor protein tyrosine phosphatase SHP1 encoded by the *PTPN6* gene is a key regulator of immune cell function. SHP1 consists of two N-terminal Src-homology 2 (SH2) domains, a catalytic domain and a C-terminal regulatory tail, and is mainly expressed in hematopoietic cells (Neel, Gu and Pao, 2003). Because of its important role in regulating immune cell function, SHP1 has become an interesting target for treatment of auto-immune diseases and cancer in recent years (Watson *et al.*, 2016).

SHP1 function has been studied extensively in the context of the *motheaten* (*me/me*) mouse that has a spontaneous recessive mutation in *Ptpn6*. This mutation creates a cryptic splice site, which results in the loss of functional SHP1 (Tsui *et al.*, 1993). The homozygous mutation leads to immune deficiency, widespread inflammation, skin lesions and death within 2-6 weeks due to lethal pneumonitis characterized by infiltration of myeloid cells (Green and Shultz, 1975). In the decades following the initial identification of the *me/me* mouse, multiple alternative less lethal mutations in *Ptpn6* have been described. *Motheaten viable* has a mutation in a splice consensus site of *Ptpn6*, which results in alternative splicing. SHP1 from *motheaten viable* mice exhibits 80% reduction in phosphatase activity and *motheaten viable* mice are lethal at 9-12 weeks (Shultz *et al.*, 1984). *Spin* has a Y208N mutation in the C-terminal SH2 domain of SHP1, resulting in 50% residual catalytic activity and *spin* mice die after more than one year (Croker *et al.*, 2008). The symptoms of *motheaten viable* are highly similar to the symptoms of *motheaten,* although they develop lethal pneumonitis approximately 8 weeks later. *Spin* mutants do not show lethal pneumonitis or immunodeficiency. This is likely due to the higher residual phosphatase activity of mutant SHP1 in *spin* mice. Heterozygous missense and splice variant mutations in *PTPN6* have also been found in human patients. These mutations are associated with emphysema and neutrophilic dermatoses (Nesterovitch *et al.*, 2011; Bossé *et al.*, 2019).

Compound mouse knock out lines and conditional knock out strains were generated to study the function of depletion of SHP1 in specific cell types. Mouse double-knockouts lacking RAG1 and SHP1 still show the *motheaten* phenotype, which indicates that the acquired immune system is not essential for the symptoms caused by loss of SHP1 (Yu *et al.*, 1996). Conditional neutrophil-specific knockout of SHP1 does not recapitulate the lethal pneumonitis phenotype nor autoimmunity that was observed in the complete SHP1 knockout. Yet, knockout of SHP1 in the neutrophil specific lineage causes dermal inflammation. Knockout of SHP1 in the dendritic cell lineage does not cause inflammation, but it does cause lymphadenopathy and autoimmunity (Abram *et al.*, 2013; Abram and Lowell, 2017), indicating that depletion of SHP1 in different cell types results in distinct hematologic defects.

Zebrafish do not have a functional acquired immune system until the larvae are 4-6 weeks old (Lam *et al.*, 2004). During early development, zebrafish only have innate immunity. In addition, zebrafish provide the opportunity to investigate embryonic development from the start, due to their translucent eggs and embryos. Therefore, zebrafish is the ideal model system to investigate the function of Shp1 in the innate immune system in a whole organism.

Previous morpholino-mediated knockdown studies in zebrafish embryos showed that Shp1 knockdown reduced the ability of embryos to combat infection with *Salmonella typhimurium* and *Mycobacterium marinum*. The innate immune system was hyperactivated to a contra-productive level. Experiments suggest that Shp1 functions as a negative regulator that imposes a tight control over the level of innate immune response activation (Kanwal *et al*., 2013).

Here, we developed a genetic zebrafish model lacking functional Shp1 to study the hematopoietic system during early development in the absence of Shp1. Zebrafish mutant for Shp1 recapitulated the lethality and inflammation seen in *motheaten* mice. In addition, we investigated the development of HSPCs and all major blood lineages. We found that macrophage numbers were increased, whereas neutrophil numbers were decreased during early development. Emergence of HSPCs was reduced, but their subsequent proliferation was strongly increased. Finally we show that recruitment of macrophages and neutrophils to wound sites is disturbed in Shp1 mutants. Our results indicate that Shp1 has a role in hematopoietic development from the start until the development of specific cell types of the myeloid lineage, and Shp1 has an essential role in myeloid behavior after development as well.

Materials and methods

Zebrafish Husbandry

All fish were housed and handled according to local guidelines and policies in compliance with national and European law. All procedures involving experimental animals were approved by the local animal experiments committee (AVD8010020173786). Larvae raised in survival experiments were fed shrimp larval diet with a diameter of 5-50µM (Caviar, Bernaqua) to control for the possible inability of small larvae to eat the normal feed.

Generation of the *ptpn6* mutant

The gRNA was designed using the CHOPCHOP web tool for genome editing (https://chopchop.cbu.uib.no/) and produced according to the protocol of (Gagnon *et al.*, 2014)) using the published constant reverse oligo and the following gene-specific forward primer: 5'taatacgactcactataggaaccctacaggataaagagttttagagctagaaatagcaag3'. Ribonucleoprotein complexes of n-terminal GFP labeled Cas9 protein and the gRNA were generated by mixing Cas9 protein and 75 ng gRNA in 4 µl buffer. The complex was injected into wild type TL embryos at the one-cell stage. GFP positive embryos were selected at 6hpi and raised to adulthood. F0 was screened for germline mutations by PCR genotyping of the offspring for heterozygous mutations. A 7bp mutation was identified and the founder was outcrossed twice to TL to obtain a stable line. PCR products of the offspring were sub-cloned in pBluescript sk^- for sanger sequencing of the mutation. mRNA was isolated from individual embryos of a heterozygous incross at 5 dpf. Reverse transcription and PCR using a forward primer targeting the translation start site at the junction of exon 2 and 3, 5' ATGGTTCGGTGGTTTCACAGAG 3' and a reverse primer targeting junction exon 6 and 7, 5' CGTCGAGTAATAGGGCTGTT 3' allowed sequencing of the 7 bp deletion in *ptpn6* transcripts.

Genotyping

Ptpn6 mutations were analyzed by PCR of lysed embryos or fin clips using the following primers targeted to the mutation site: fw 5'ggattcaaaacacaggggatta3' and rev 5'tttaacttggcaaacacacctg3'. PCR products were run on a 4% agarose gel for analysis.

Polyclonal zebrafish Shp1 antibody

GST-Shp1 fusion protein was produced by expression of pGex-GST-Shp1 in *E. coli* B12 followed by glutathione-agarose affinity purification (Sigma). Purified protein was shipped for antibody production (custom polyclonal antibodies, Eurogentec). Rabbit polyclonal anti-Shp1 was purified in house by affinity purification. Briefly, serum was precleared using immobilized GST and GST-fusion protein of highly homologous zebrafish Shp2, to

remove antibodies binding GST and antibodies cross reacting with Shp2. Subsequently, Shp1-specific antibodies were affinity purified using immobilized GST-Shp1 fusion protein. Before use, zfShp1-specific antibody (1:500 in 5% milk) was incubated with purified zfShp2 protein for 1 h to prevent residual cross reaction with Shp2.

Immunoblotting

Prior to snap freezing, fin clips of 5dpf embryos were collected for genotyping. 3 embryos/genotype were pooled and lysed in cold lysis buffer (25mM HEPES pH 7.4, 150mM NaCl, 0.25% deoxycholate, 1% triton X-100, 10mM $MgCl_2$, 1mM EDTA, 10% glycerol + 1:10 cOmplete mini protease inhibitor cocktail (Roche)) by incubation on ice followed by sonication (Bioruptor, 15 min, 30 sec on/off). Lysate of HEK2933T cells expressing zebrafish Shp1 was used as a control. Samples were resolved on a 10% acrylamide gel and transferred to a PVDF membrane. Immunoblotting was performed using Akt-specific (1:500, 9272S Cell Signaling) and Shp1-specific (1:500) antibodies.

Confocal, fluorescence, bright field microscopy

Confocal microscopy was performed on a Leica SP5. Embryos were anesthetized in tricaine and mounted in 0.8% low melting agarose in E3 medium in a glass cover dish. For live imaging mounted embryos were covered in E3 medium containing tricaine. Stereo-fluorescence imaging and bright field imaging of stained embryos and *in situ* hybridizations was performed on a Leica M165FC connected to a DFC420C camera. Images were processed using imageJ or Imaris.

Quantitative real-time PCR

Larvae were monitored during raising and were sacrificed at a defined end point (curved, skinny body, not able to swim upright and/or severe skin alterations). The genotype was established by fin clipping, PCR and sequencing. If 2 or more mutant larvae of the same age were available, healthy siblings in the same tank were picked, genotyped by finclipping and sacrificed to serve as control samples. Total RNA was extracted from genotyped larvae in Trizol (Invitrogen). Snapfrozen samples were crushed with an Eppendorf tube pestle and further homogenized using a syringe. cDNA was synthesized using superscriptIII first strand synthesis kit (Invitrogen). qRT-PCR was performed using SYBR green and a CFX-96 Connect Real-Time system (Bio-Rad). Data was analyzed by applying the $2^{-\Delta\Delta Ct}$ method (Livak and Schmittgen, 2001). Primers are listed in Table S1.

Sudan Black, O-dianasidine & Acridine Orange staining

3 and 5dpf embryos were fixed and stained using Sudan Black (Sigma-Aldrich) (le Guyader *et al.*, 2008) and counted as published (Choorapoikayil *et al.*, 2014). O-dianisidine (Sigma-Aldrich) stainings were performed as described (Iuchi and Yamamoto, 1983),

but embryos were fixed afterwards (4% PFA) and cleared in 2:1 benzylbenzoate/benzylalcohol. Acridine Orange staining was carried out as described by Choorapoikayil (Choorapoikayil *et al.*, 2014).

***In situ* hybridization**

Embryos were fixed in 4% PFA in PBS. *In situ* hybridizations were performed as previously described (Thisse and Thisse, 2008). Published Digoxigenin-UTP-labeled riboprobes were used (Choorapoikayil *et al.*, 2014).

Whole mount immunohistochemistry

Embryos were fixed overnight in 2% PFA. Samples were washed 2x in PBS + 0,1% Tween-20 (PBS-T) followed by 15 min permeabilization in 1- µg/ml proteinase K (Roche) and 3 washes in PBS-T. Samples were blocked for at least 2 h with 10% goat serum + 0.3% triton X-100 in PBS and incubated overnight with chicken anti-GFP (1:500, Aves Labs Inc) or rabbit anti-pHis3 (1:250, Merck Millipore). Embryos were washed 10x 10min in PBS + 0.3% Triton X-100 (PBS-X), followed by 1 h blocking and overnight incubation in either anti-chicken Alexa 488 (1:500, Invitrogen) or Cy5 anti-rabbit (1:500, Jackson Immuno Research). The next day samples were repeatedly washed in PBS-X for 3-4 hrs and imaged.

Plasmid construction, RNA synthesis and micro – injections

The coding sequence of zebrafish Shp1 was obtained by PCR (fw 5'accctgtttacgtgtcgaga 3', rev 5'agccttggctcagttttctt3') from a mix of cDNA of 3 and 5dpf TL embryos and cloned into pCS^{2+}eGFP-p2a using infusion (Takarabio). The R462M point mutation in the PTP domain was introduced by Q5 site-directed mutagenesis (NEB). pCS^{2+} constructs were linearized using NotI and transcribed *in vitro* (mMessage machine SP6, ambion). mRNA was injected in 1 cell stage embryos at a concentration of 5 ng/µl.

Tailwound assays

4 dpf *Tg(mpx:GFP/mpeg:mCherry)* embryos were anesthesized with tricaine and tails were transsected distal to the notochord by scalpel blade. Embryos were immediately mounted for confocal imaging and imaged from ~30 min post wounding, for 7 h, every minute. Particles were detected and tracks were analyzed using the Trackmate plugin from Fiji (Tinevez *et al.*, 2017). The linear motion algorithm was used with a maximum allowed gap of 4 time frames and a maximum allowed radius of 50 µm. Wound area was defined as 200 µm and closer from the edge of the tail in the first timeframe. Mean speed of tracks outside the wound area was determined by dividing the total distance/the total time of the track. Meandering index of tracks outside the wound area was determined by dividing the net distance (distance between first and last point of track)/

the total distance of the track. Wound persistence was determined for each track that entered the wound area by dividing the number of time frames spent inside the wound area/ number of time frames left till the end of the movie.

Statistical analysis

Analytical statistics were performed in GraphPad Prism 7 (version 7.04). For the tailwounding descriptive statistics were determined using Python (matplotlib 3.3.2, numpy 1.18.5, scipy 1.50, statmodels 0.11.1). For all experiments, samples were genotyped after analysis and split in different experimental groups based on their genotype. Hence, researchers were blinded to the genotype during analysis. All successful images and movies were taken along for analysis, none were excluded. Sample size was specified to be the maximum number of samples available, since the effect size was unknown prior to the experiment. Statistical tests used in this paper include ANOVA, Tukey's multiple comparisons test, SIDAK's multiple comparisons test, Benjamini-Hochberg procedure, log-rank test, ordinary least squared regression, unequeal variance T-test and two sided 95% confidence intervals. Data used for the statistical tests meets the assumptions of the specific test. Specifics of the statistical analyses are indicated in the figure legends.

Regeneration assay

Zebrafish embryos were amputated at the tail as previously described (Hale *et al.*, 2017). Amputations were performed at 2 dpf and regeneration was analyzed at 5 dpf. Regenerated tails were imaged and whole embryos were lysed for genotyping. Regeneration was quantified by measuring the length from the tip of the notochord to the end of the fin-fold in ImageJ.

Supplemental material

Table S1. Sequences of QPCR primers

mmp9 FW	CATTAAAGATGCCCTGATGTATCCC
mmp9 Rev	AGTGGTGGTCCGTGGTTGAG
il1b Fw	GAACAGAATGAAGCACATCAAACC
il1b Rev	ACGGCACTGAATCCACCAC
tnfa FW	AGACCTTAGACTGGAGAGATGAC
tnfa Rev	CAAAGACACCTGGCTGTAGAC
fkbp5 FW	TCTGCCAGCACAAGATTCGTGAGC
fkbp5 Rev	GACCCTGCTTATTCTGATCGGAAA
irg1/acod1 FWD	CATCTCAGCTCGCTCTTT
irg1/acod1 REV	GAGGGACGTAATCTGGATAG
b-actin1 FW	CGAGCAGGAGATGGGAACC
b-actin1 Rev	CAACGGAAACGCTCATTGC

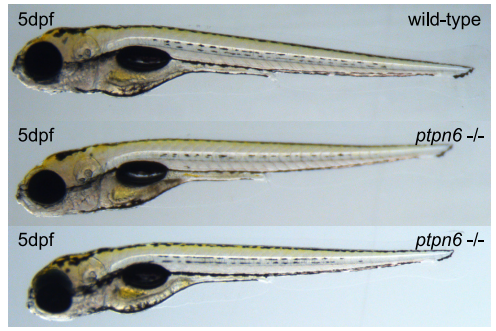

Fig. S1. No morphological defects in 5 dpf embryos lacking functional Shp1. Wild type and *ptpn6*$^{-/-}$ embryos were imaged using a stereomicroscope at 5 dpf. Representative images are shown.

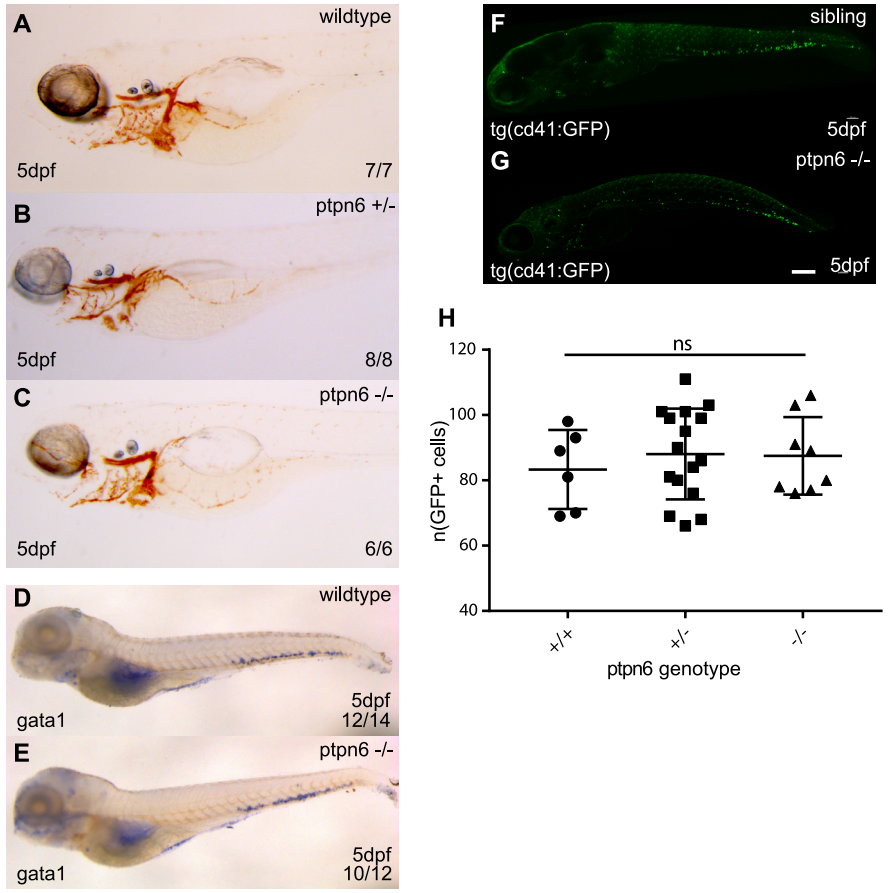

Fig. S2. The erythroid and megakaryocyte lineages are not affected by *ptpn6* knock out. (A-C) Representative stereo images of O-dianasidine stainings of 5dpf embryos and (D,E) *gata1* whole mount in situ hybridization.The number of embryos showing the depicted pattern / total number of embryos is shown in the bottom right corner. (F,G) Representative confocal images of fixed 5dpf *tg(cd41:GFP)* embryos showing thromobyctes, 20x objective. Scale bar represents 200µm. (H) Quantification of thrombocytes. The fluorescence threshold was set at a level that only GFP^{high} cells were detected and subsequently, the number of GFP-positive cells was determined using IMARIS software Statistical comparisons were performed by ANOVA.

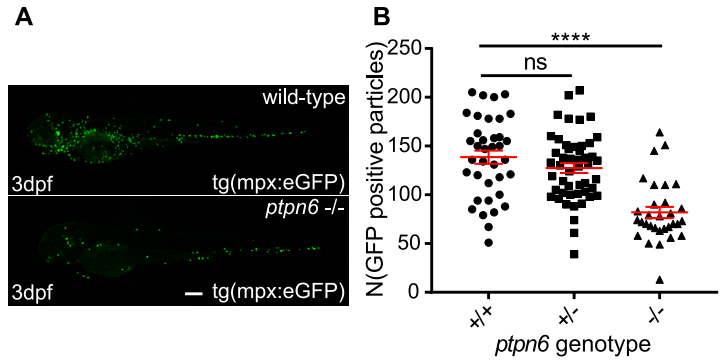

Fig. S3. Reduced numbers of neutrophils in *ptpn6*$^{-/-}$ embryos at 3 dpf. (A) Representative images of wild type and *ptpn6*$^{-/-}$ embryos in *tg(mpx:eGFP)* background, showing reduced number of GFP-positive neutrophils in mutant embryos, lacking functional Shp1. Scale bar represents 200µm. (B) Quantification of the number of GFP-positive neutrophils in wild-type, heterozygous and homozygous *ptpn6* mutant embryos at 3 dpf. Quantification was performed in ImageJ by particle analysis. ANOVA and multiple comparisons (Tukey) were applied for statistical comparisons. ****p<0.0001, error bars = SEM

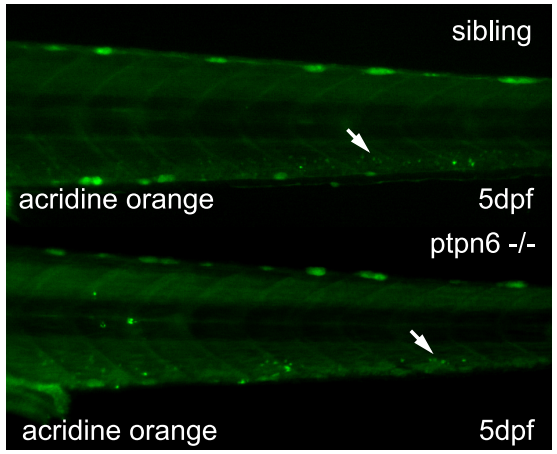

Fig. S4. The reduction of neutrophil number in the CHT of embryos lacking functional Shp1 is not caused by increased apoptosis. Stereo fluorescent images of the CHT of 5dpf embryos stained with acridine orange. Arrows indicate the bright spots representing apoptotic cells. 20x objective, Pinhole 2AU, step size 2.52µm

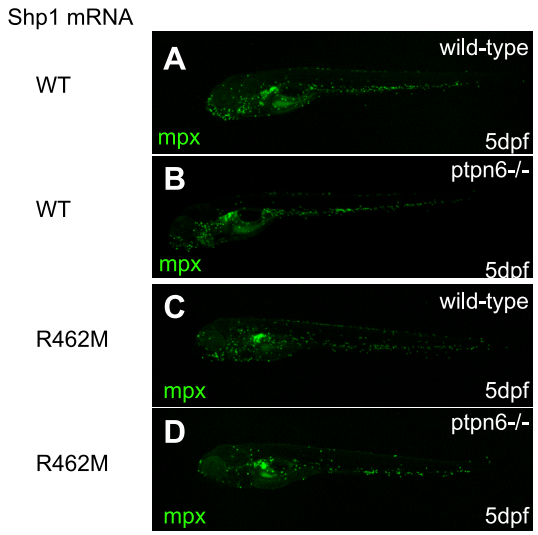

Fig. S5. Reduced number of neutrophils in *ptpn6*$^{-/-}$ embryos is rescued by expression of Shp1, but not catalytically inactive Shp1-R462M. At 5 dpf, images were obtained of wild type or *ptpn6*$^{-/-}$ embryos in the *Tg(mpx:eGFP)* transgenic background that had been injected at the one-cell stage with synthetic mRNA encoding Shp1 or catalytically inactive Shp1-R462M. GFP-positive neutrophils were quantified and the quantification is depicted in Fig. 4I. Representative images of embryos are depicted here.

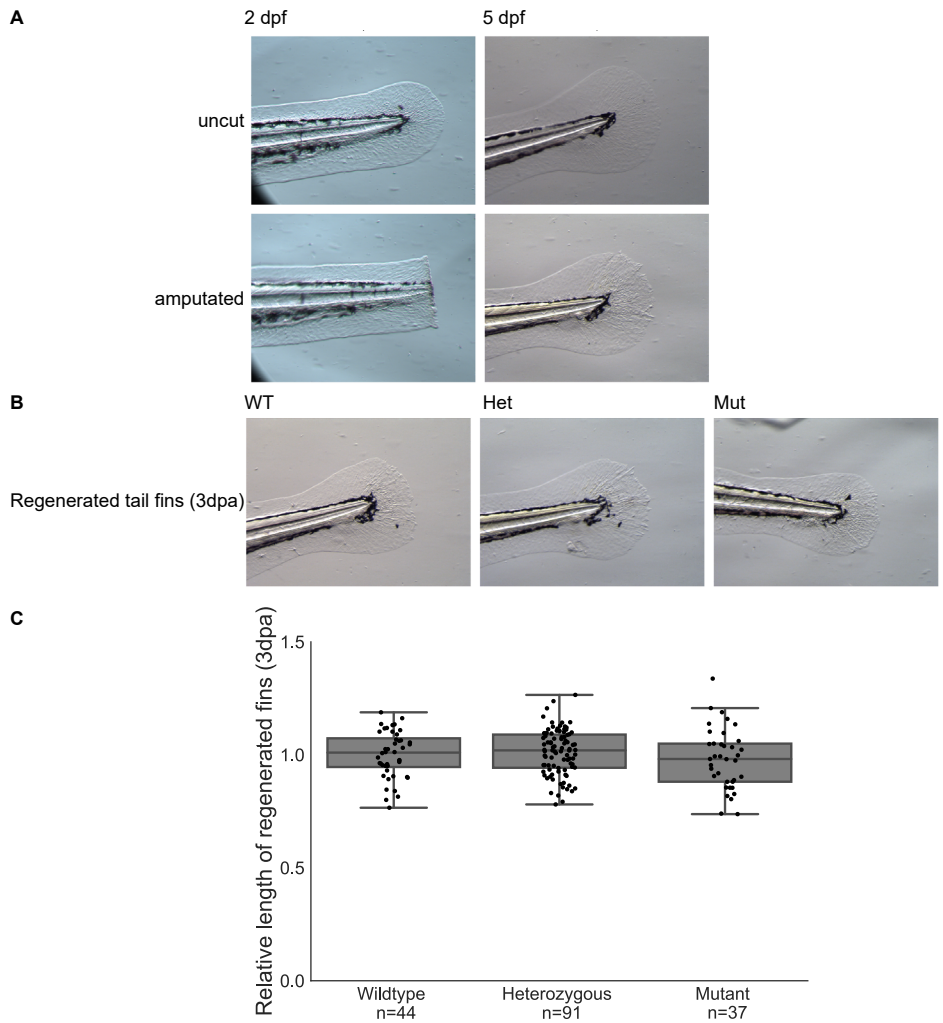

Fig. S6. Tail fin fold regeneration is not affected in Shp1 mutant zebrafish embryos. A. Tail fin folds were cut at the tip of the notochord at 2 dpf. Three days after amputation the tail fin fold regenerated and was indistinguishable from the tail fin fold of uncut controls. Representative pictures are shown. B. There is no difference between WT, heterozygous and mutant Shp1 siblings in tail fin fold regeneration. Representative pictures are shown. C. Length from the tip of the notochord to the end of the fin fold was measured at 3 dpa. Results were normalized to the results of WT siblings. One way Anova resulted in p-value=0.38 (statmodels). Boxplots represent quartiles. All observations are added as single dots.

Results

Shp1 knock-out leads to inflammation and is lethal at late larval stage

We generated mutations in the zebrafish *ptpn6* gene using CRISPR-Cas9 technology at the 1 cell stage, followed by screening of the F0 generation for germline mutations. We identified a 7bp deletion in exon 4 resulting in a frameshift and a premature stop codon 10 amino acids downstream of the mutation site. Exon 4 encodes the C-terminal part of the N-terminal SH2 domain positioning the mutation well up-stream of the catalytic PTP domain and predicts production of a severely truncated protein of 96 amino acids (Fig 1A). Reverse transcription PCR and sequencing indicated that mRNA species with the 7 bp deletion were produced in the mutant. To confirm the absence of Shp1 protein we detected total Shp1 protein levels in 5dpf zebrafish embryo lysates with a zebrafish Shp1 specific antibody, which we generated (Fig 1B). At 5dpf *ptpn6* mutants show no obvious phenotype (Fig. S1), in contrast to previous morpholino studies, which showed pleiotropic defects from 2 dpf onwards (Kanwal *et al.*, 2013).

During later larval stages the *ptpn6* mutants appear smaller and skinnier than siblings, and develop a curved phenotype. Moreover, as described for the *motheaten* mouse, the mutants show abnormalities in their skin epithelium (ruffled epithelial edges and bumps) (Fig 2A-D) (Green and Shultz, 1975). To look at infiltration of the skin with immune cells we used the *Tg(mpxeGFP)* line marking myeloid-specific peroxidase producing neutrophils. We followed the developing larvae, mutants and siblings, over time and imaged them either at the moment of sacrifice or at the end point of the experiment (either 12 or 19dpf). Surprisingly, we did not only observe neutrophil infiltration of the skin, but the most prominent accumulation of neutrophils was found in the gill area (Fig 2C,D). *Motheaten* mice succumb to pneumonitis which is characterized by neutrophil and macrophage accumulation in the lungs. We semi-quantified the neutrophil accumulation phenotype by scoring the number of neutrophils in the gill and mandibular area in three categories: normal (WT), elevated, and high, at 7-12 dpf or 13-19 dpf (Fig 2E,F). It is evident that neutrophil numbers in the scored area are greatly increased in mutants.

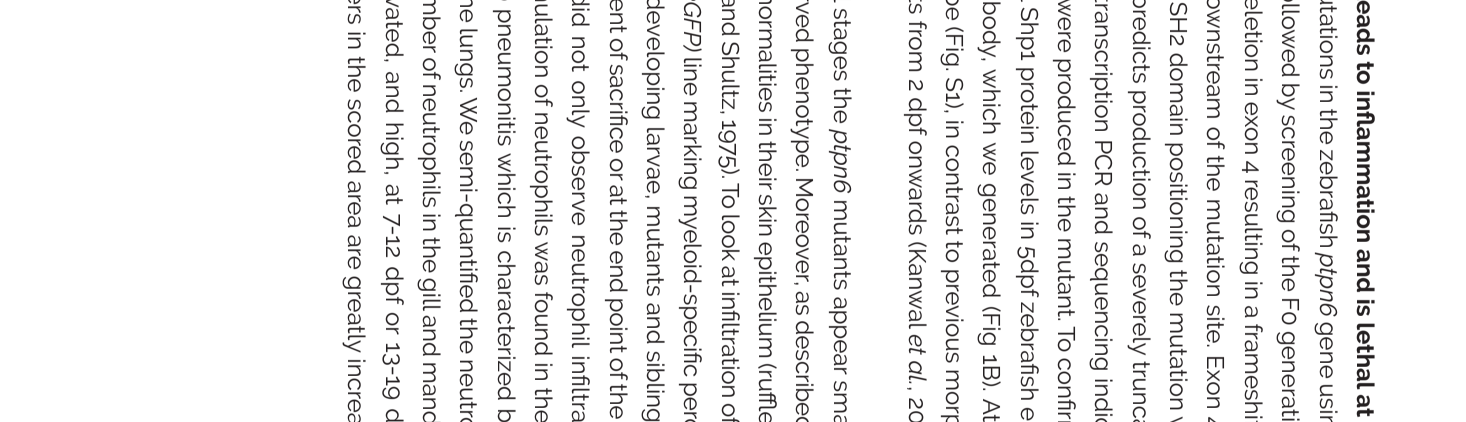

Figure 1. Zebrafish *ptpn6* mutant generated using CRISPR/Cas9 is a strong null allele. (A) Schematic overview of Shp1. gRNA was targeted to the C-terminal end of the N-terminal SH2 domain, inducing a 7 bp deletion in exon 4, indicated by the red box in the wild type sequence. Mutation was confirmed by sanger sequencing after sub-cloning of F1 DNA. The 7 bp deletion leads to a frameshift and a stop codon in exon 4, 10 amino acids downstream of the mutation site. (B) Immunoblot detecting endogenous Shp1 in WT and heterozygous embryos, but not homozygous *ptpn6* mutant embryos. Lysate of transfected Hek293T cells expressing zebrafish Shp1 was used as a control for detection of zebrafish Shp1. Akt-specific antibody was used to monitor equal loading.

In accordance with the *Ptpn6*$^{me/me}$ and *Ptpn6*$^{me\text{-}v/me\text{-}v}$ mice, *ptpn6* mutant zebrafish do not survive to adulthood (Green and Shultz, 1975; Shultz *et al.*, 1984) . The absence of Shp1 is lethal at late larval stages with a median survival of 17 days (Fig 2G). To investigate whether affected larvae present with inflammation, we collected mRNA from mutants (n=12) and age matched siblings (n=9) at the end points of the mutant larvae at 10, 14 and 18 dpf. We performed qPCR for several pro-inflammatory genes and genes which are upregulated during inflammation (*mmp9, il1B, tnfa*, *fkbp5* and *irg1/acod1*), of which the first two were previously found to be upregulated in the *ptpn6* morpholino studies in zebrafish embryos (Kanwal *et al.*, 2013). All five genes were significantly upregulated compared to siblings (Fig. 2H), indicating that loss of functional Shp1 evokes an inflammatory response, although we cannot exclude the possibility that this response is caused by non-specific inflammation or necrosis.

The development of erythroid and thrombocyte lineages are unaffected in ptpn6 mutants.

To assess erythropoiesis we performed an O-dianisidine staining and *gata1 in situ* hybridization on 5dpf embryos. O-dianisidine detects heme in hemoglobin and *gata1* marks early erythrocytes (Iuchi and Yamamoto, 1983; Ransom *et al.*, 1996). We found no difference in erythrocyte numbers or distribution between *ptpn6* mutants and siblings (Fig. S2A-E). To investigate the thrombocyte lineage, the nucleated equivalents of mammalian megakaryocytes/platelets, we quantified the GFP^{high} cells in *Tg(cd41:GFP)* embryos at 5dpf by confocal microscopy. In these transgenic embryos, thrombocytes express a high level of GFP and HSPCs a low level of GFP (Kissa *et al.*, 2008). After fixation only GFP^{high} cells are visible (Fig. S2F,G). Counting of GFP^{high} cells revealed no difference in thrombocyte numbers between siblings and *ptpn6* mutants (Fig. S2H). Hence, the erythroid and thrombocyte lineages in zebrafish embryos lacking functional Shp1 appear to be unaffected at 5 dpf.

Development of the myeloid cell lineage but not early lymphocyte development is affected in ptpn6 mutants

To investigate the development of leukocytes in *ptpn6* mutants we first determined *l-plastin* expression, a pan-leukocyte marker, by whole mount *in situ* hybridization. *L-plastin* expression was higher in the Caudal Hematopoietic Tissue (CHT, the equivalent of mammalian embryonic liver, where HSPCs migrate to mature before they migrate to the location where they produce blood of all lineages for the rest of their life, i.e. head kidney for fish and bone marrow for mammals) of *ptpn6* mutants, indicating an increase in total leukocyte numbers (Fig 3A,B). To determine which cell type was responsible for this increase we performed *in situ* hybridizations and stainings, and used transgenic lines to quantify cell numbers. First, we investigated the expression of *ikaros* and

rag1 by *in situ* hybridization, to determine whether the development of the lymphoid lineage was affected. *Ikaros* is an early lymphocyte marker and *rag1* is essential for V(D)J recombination in maturing B and T cells (Willett *et al.*, 1997, 2001). As expected, *ikaros* expression was detectable in the CHT and the thymus of 5dpf embryos and no differences in expression level or location were observed between *ptpn6* mutants and siblings (Fig 3C-F). Quantification of the *rag1-positive* area in mutants, heterozygous embryos and wild type siblings revealed no difference in thymus size, a direct read-out for developing B- and T-cell numbers in the thymus (Fig 3G-I). We conclude that early development of the lymphocyte system is not affected in *ptpn6* mutants.

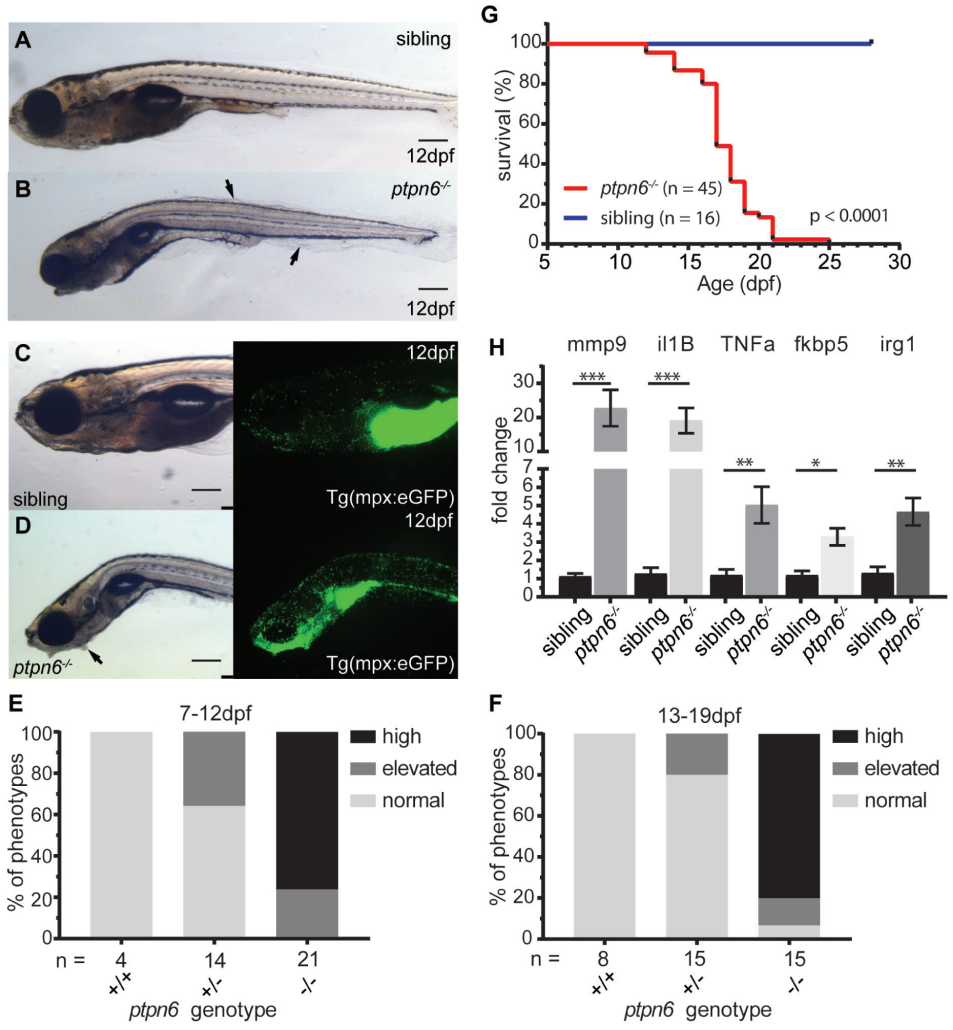

◂ Figure 2. Zebrafish *ptpn6* mutants show an inflammatory response with neutrophil accumulation and do not survive to adulthood. (A-D) Stereo microscope representative pictures of embryos at 12 dpf. The larvae were genotyped by PCR and sequencing following imaging. (A,C) siblings and (B,D) *ptpn6*$^{-/-}$ mutant displaying the "motheaten" like phenotype. Arrows indicate the affected epithelium. (C,D) GFP-positive neutrophils in *tg(mpx:eGFP)* transgenic line localize to the gill and mandibular area in *ptpn6*$^{-/-}$ embryos. (E,F) Scoring of phenotypes in age cohorts of larvae. Larvae with an affected phenotype were selected along with age-matched controls and the number of neutrophils was scored by eye. Subsequently, the larvae were genotyped by PCR and sequencing. Larvae were classified as normal (distribution and number of neutrophils as in WT larvae), elevated (mildly increased number of neutrophils in gill and mandibular area) or high (massive increase of neutrophil numbers in the gill and mandibular area). (G) Survival curve of *ptpn6* mutants. Larvae were monitored during raising, sacrificed at a defined end point (curved, skinny body, not able to swim upright and/or severe skin alterations) and genotyped by PCR and sequencing. Curve comparison by log-rank (Mantel-Cox) test. (H) Increased expression of pro-inflammatory genes in mutants. RNA was extracted from larvae sacrificed upon observation of a severe phenotype (n=12) and their age-matched siblings (n=9). Gene expression was determined by qPCR and fold changes were calculated per time point (10, 14 & 18dpf) and pooled afterwards. Statistical comparisons were performed by non parametric ANOVA (Kruskal-Wallis) followed by multiple comparisons (original FDR method Benjamini Hochberg). *p<0.05, **p<0.01, ***p<0.001, error bars = SEM

Next, we investigated the two main cell types in the myeloid lineage, the monocytes/macrophages and the neutrophils. Expression of *csf1r* , a marker for macrophages, was upregulated in the CHT of *ptpn6* mutants at 5 dpf (Fig 3J,K). Sudan Black (SB) stains the granules of immature and mature neutrophils and was used to quantify these in 3 and 5dpf embryos. SB-positive cells in the head are mainly derived from the primitive wave at early time points in development, whereas SB-positive cells in the CHT are derived from the definitive wave (le Guyader *et al.*, 2008). SB-positive cells were counted in these two areas of the embryos, indicated by a black box (the head, including the heart), and by brackets (the CHT)(Fig 3L-O). Surprisingly, given the late larval phenotype with increased neutrophil numbers (Fig. 2C,D), at 3dpf neutrophil numbers in the head area of *ptpn6* mutants were reduced by approximately 80% compared to WT siblings, and by 65% in the CHT (Fig 3P). At 5dpf these numbers were reduced to approximately 50% and 35% respectively (Fig 3Q). In addition to the SB staining we quantified neutrophils in 3dpf *Tg(mpx:GFP)* embryos, which facilitated counting of neutrophils in intact embryos. Mpx is a neutrophil marker which is expressed already early in neutrophil differentiation, from the promyelocyte phase onwards (Bainton, Ullyot and Farquhar, 1971; Borregaard and Cowland, 1997; Kumar *et al.*, 2010). Total *mpx*-positive neutrophil numbers were reduced by 41% in *ptpn6* mutants, compared to wild type siblings. Because *mpx* is expressed from early neutrophil precursors onwards, this indicated that the whole neutrophil lineage was affected, and not just later steps in neutrophil maturation (Fig. S3A,B).

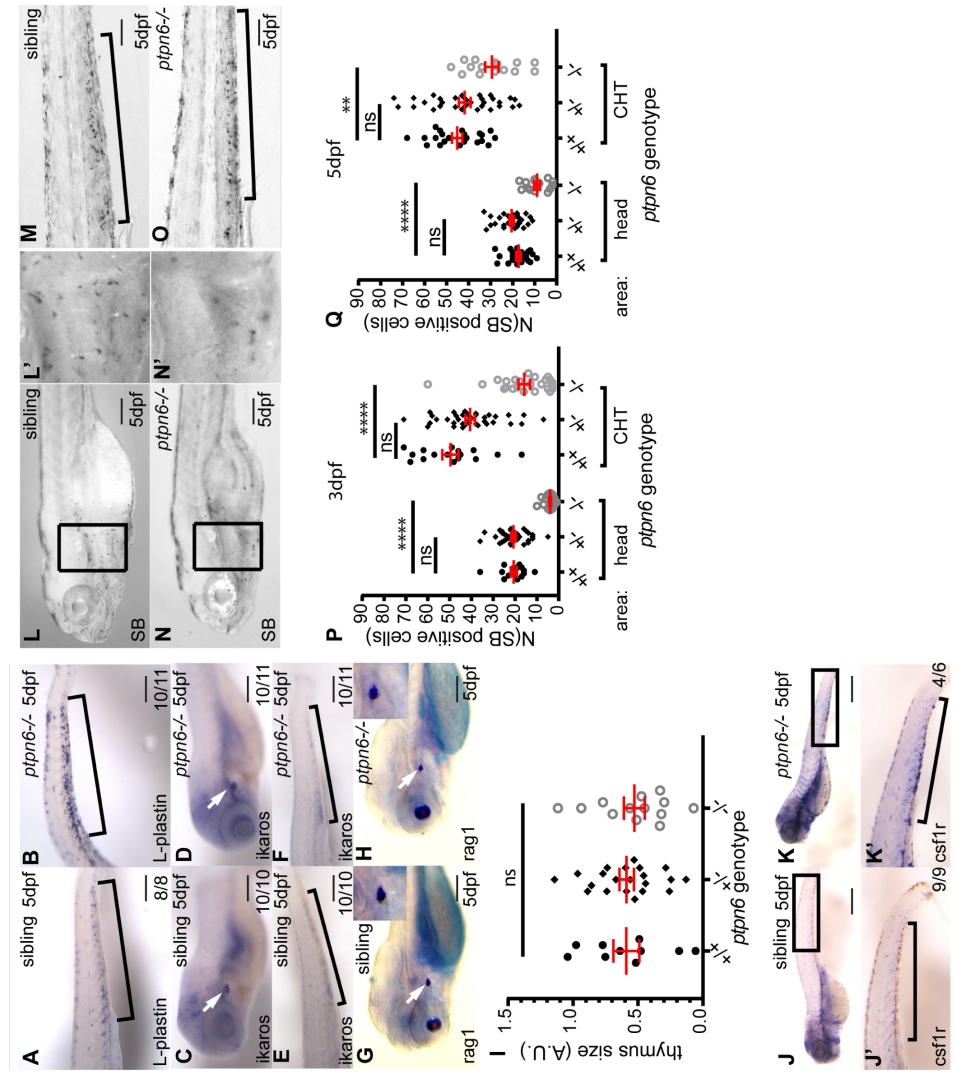

◄ Figure 3. Development of the leukocyte lineages in *ptpn6* mutants. (A-J) A panel of *in situ* hybridization markers for leukocyte lineages was used on 5dpf wild-type and *ptpn6*$^{-/-}$ embryos. CHT is indicated by bracket and thymus by white arrow. The number of embryos showing the depicted pattern/ total number of embryos is shown in the bottom right corner. (A,B) L-plastin, pan-leukocyte marker; (C-F) ikaros, lymphoid progenitors, and (G,H) rag1, lymphocytes. Representative lateral views of the thymus are shown, with close ups of the thymus in the inset. (I) quantification of rag1-positive area (n.s., ANOVA). (J,K) csf1r, macrophage marker with (J',K') close ups of the CHT. The number of neutrophils in two parts of the embryo was quantified by SB staining at 3 and 5 dpf (L-O). (L', N') Show magnifications of the boxed areas in L and N. (P, Q) SB-positive cells were counted in the head (mainly primitive wave) and CHT (mainly definitive wave) at 3 and 5 dpf. All embryos were genotyped after *in situ* hybridization or SB staining and imaging by PCR and sequencing. Statistical comparisons were performed by ANOVA followed by multiple comparisons (Tukey) for both areas per time point separately. **p<0.01, ****p<0.0001, error bars = SEM

To further investigate the development of the granulocyte-monocyte lineage we used *Tg(mpx:GFP/mpeg1:mCherry)* transgenic fish to simultaneously quantify neutrophil and macrophage numbers. *Mpeg* expression is restricted to the monocyte/macrophage lineage during early development (Ellett *et al.*, 2011). By confocal imaging we acquired images of the rostral part and the CHT of 3 and 5dpf *ptpn6* mutant and sibling embryos (Fig 4A-D, 3dpf not shown). Macrophage (Fig 4E) and neutrophil (Fig 4F) numbers in both areas and at both time points were determined using ImageJ. Macrophage numbers were increased in both areas and at both time points during development, whereas neutrophil numbers were reduced. The increase in *mpeg* signal was very pronounced in the area of the pro-nephros, the site of late-larval and adult hematopoiesis in zebrafish (Al-Adhami and Kunz, 1977; Willett *et al.*, 1999), where macrophage numbers were up by ~55%. Similarly, whereas peripheral neutrophils were scarcely found in the head, the pro-nephros was well populated with *mpx*-positive cells.

To exclude apoptosis as the cause of the reduction in neutrophils in *ptpn6* mutant embryos, we performed acridine orange staining. No increase in apoptosis was observed in the CHT of 5dpf *ptpn6* mutant embryos (Fig. S4). These results suggest that *ptpn6* mutant fish suffer from an altered lineage balance within the myeloid cell lineage and early onset increased proliferation in the macrophage lineage.

The early developmental phenotype of the myeloid lineage is dependent on catalytic activity of Shp1

Next, we questioned whether restoring Shp1 expression rescued the phenotype observed in *ptpn6* mutant embryos. We micro-injected *Tg(mpx:GFP)* embryos at the 1-cell stage with wild type *ptpn6* mRNA and allowed them to develop until 5dpf. The

mRNA also encoded GFP, linked with a P2a autocatalytic cleavage sequence. Upon expression, GFP was visible until approximately 3dpf, which allowed us to successfully select injected embryos at 1dpf. Non-injected controls are depicted in figure 4G and H. Expression of wild type Shp1 restored neutrophil numbers in *ptpn6* mutant embryos to those found in non-injected wild type controls at 5 dpf (Fig 4I, Fig. S5). Although catalytic activity is important for Shp1 function, other domains may exert alternative functions, e.g. scaffolding by SH2 domains (Timms *et al.*, 1998; An *et al.*, 2008; Abram and Lowell, 2017). To investigate whether catalytic activity of Shp1 is essential for the development of neutrophils we injected the catalytically inactive mutant Shp1-R462M. We used the R462M mutant and not the classic catalytic cysteine mutant C456S to avoid inadvertent substrate-trapping effects (Hale and den Hertog, 2018). Upon micro-injection of mRNA encoding GFP-P2a-Shp1-R462M, no increase in total neutrophil numbers was observed in *ptpn6* mutant embryos (Fig 4I, Fig. S5). Expression of Shp1 or inactive Shp1-R462M did not affect the number of neutrophils in wild type or heterozygous siblings (Fig. 4I). Therefore, we conclude that catalytic activity of the PTP domain of Shp1 is essential for its function in the development of the myeloid lineage.

Figure 4. Zebrafish *ptpn6* mutants have an increased number of macrophages and a reduced number of neutrophils, and this phenotype is dependent on phosphatase activity of Shp1. (A,B) Representative pictures of the head area and (C,D) of the anterior part of the CHT of 5dpf *tg(mpx:GFP/mpeg:mCherry) ptpn6* mutant and sibling embryos showing neutrophils and macrophages. 20x objective, pinhole 2AU, step size 1,83µM. (E,F) Scatterplot of macrophage (E) and neutrophil (F) numbers per embryo in the head and CHT of 3 and 5 dpf embryos. Quantification was performed in ImageJ by particle analysis. Statistical comparisons by ANOVA and Sidak's multiple comparison test for preselected columns. (G,H) Stereo images of 5dpf *tg(mpx:GFP)* wild-type and *ptpn6*$^{-/-}$ non injected embryos. Images of WT Shp1 and Shp1-R462M injected embryos are shown in Fig S4. (I) Quantification of total number of neutrophils in *tg(mpx:eGFP)* embryos injected with mRNA encoding WT Shp1 or Shp1-R462M. Scatterplot of total neutrophil numbers at 5dpi per embryo. Quantification was performed in ImageJ by particle analysis. Following imaging, the embryos were genotyped by PCR and sequencing. Statistical comparisons by ANOVA and Tukey multiple comparisons test. Scale bar represents (A-D) 100µm and (G-H) 200µm. *p<0.05, **p<0.01, ***p<0.001, ****p<0.0001, error bars = SEM ►

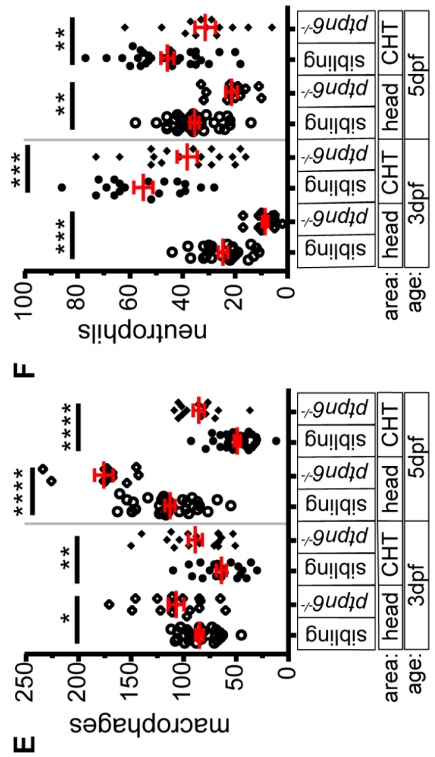

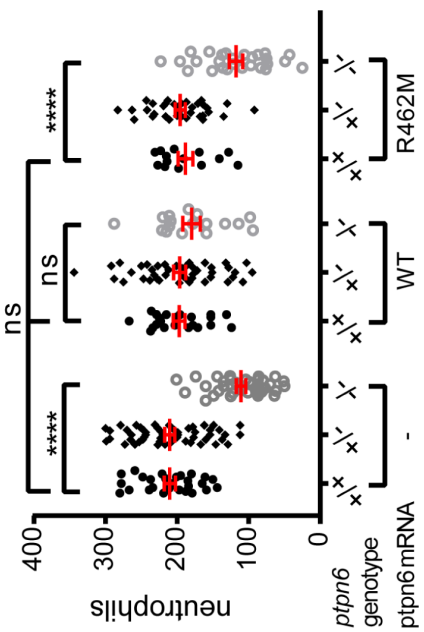

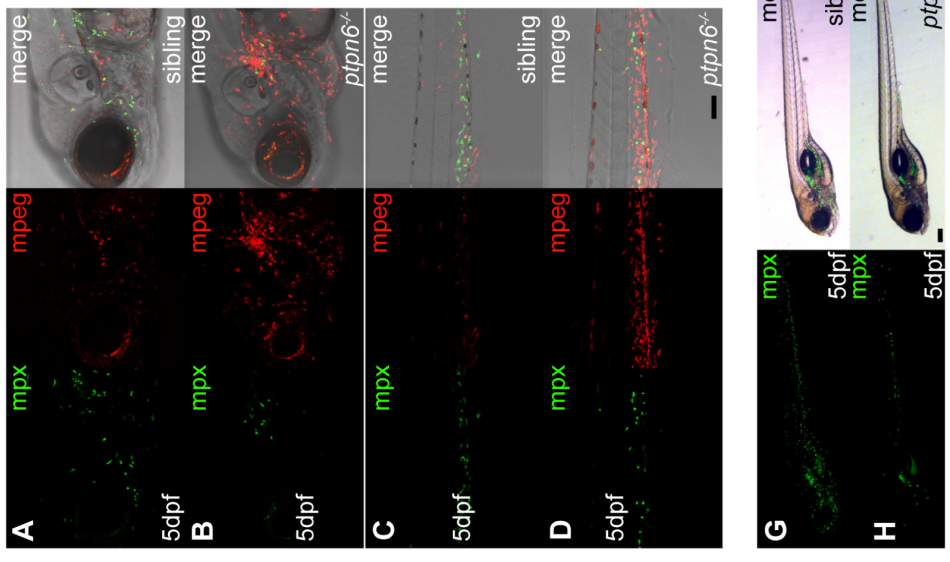

Early hematopoiesis is affected in ptpn6 mutants

Earlier reports indicated that hematopoietic stem cells (HSCs) in *motheaten* mice are not affected by SHP1 deficiency (Shultz, Bailey and Coman, 1987). However, recently, SHP1 was found to be involved in HSC quiescence in *Scl-CreER/Shp1*$^{fl/fl}$ mice (Jiang *et al.*, 2018). Therefore we investigated whether HSPC emergence, homing and proliferation was affected in *ptpn6* mutant zebrafish. First, the emergence and early homing of HSPCs at ~36hpf was investigated by *in situ* hybridization of *c-myb* mRNA in *ptpn6* mutants and siblings (Fig 5A,B). A minor decrease in signal was observed in *ptpn6* mutants. Subsequently *Tg(cd41:eGFP/kdrl:mCherry)* fish were used to quantify GFP^{low} HSPCs in the CHT after arrival (Kissa *et al.*, 2008; Choorapoikayil *et al.*, 2014). *Kdrl:mCherry*-positive embryos with red fluorescent endothelial cells were selected at 46hpf, and subjected to immunohistochemistry with a GFP specific antibody. Confocal imaging was used to capture the complete CHT, based on the *kdrl:mCherry* signal staining all endothelial cells of the CHT (Fig 5C,D). Note that HSPCs that arrive at the CHT expressed *kdrl:mCherry* themselves as well, because these cells were endothelial cells in the floor of the dorsal aorta that have undergone epithelial to hematopoietic transition (Kissa *et al.*, 2008). The mCherry signal in HSPCs was hardly detectable in fixed embryos and the signal from the *cd41:eGFP* transgene was used to quantify the number of HSPCs. GFP-positive cells in the CHT were quantified and at 46 hpf, a significant reduction in HSPCs in the CHT was observed in *ptpn6* mutant embryos, compared to heterozygous embryos ($P<0.05$) and a 17% reduction compared to wild type siblings ($p<0.01$) (Fig 5I). Next, live imaging was performed of the CHT of 5dpf *Tg(cd41:eGFP/kdrl:mCherry) ptpn6* mutant and sibling embryos (Fig 5E,F). The number of GFP^{low} HSPCs was quantified, showing expansion of HSPCs in the CHT over time from 46hpf to 5dpf. The number of HSPCs was 58% higher in mutant embryos at 5 dpf than in heterozygous and wild type embryos ($p<0.0001$) (Fig 5J). To investigate the cause of the increase in HSPC number, proliferation of HSPCs was assessed in the CHT of *ptpn6* mutant embryos by immunostaining using pHis3- and GFP-specific antibodies of 5dpf *Tg(cd41:eGFP/kdrl:mCherry)* embryos (Fig 5G,H). The *kdrl*-mCherry signal was used to determine which cells were located in the CHT and the pHis3-positive cells were counted. A 34% increase in proliferating cells was detected in the CHT of *ptpn6* mutant embryos compared to sibling cell numbers ($p<0.01$) (Fig 5K). Taken together, these results suggest that early HSPC emergence and/or arrival in the CHT is reduced or delayed in *ptpn6* mutant embryos and that the proliferation of these definitive blood cell progenitors is enhanced once they seed the CHT.

Directional migration of neutrophils and macrophages in response to tailwounding is affected in ptpn6 mutants

Neutrophils and macrophages play an essential role during injury response. They are among the first cells to be recruited to an injury site, where they remove debris and release molecules that promote inflammation and vasodilation. We investigated whether

the behavior of neutrophils and macrophages in *ptpn6* mutant embryos differed from siblings by live-imaging of 4dpf embryo tails following amputation of the tip of the tail fin fold (Fig 6A; representative movies are presented in Supplemental Material, SM1 and SM2). The number of neutrophils that migrated into the wound area (closer than 200 µm to the cut site) in mutant embryos was not significantly different from their siblings (Fig 6B). However, the meandering index (net distance travelled/ total distance travelled) of neutrophils outside the wound area was lower for mutant embryos than their siblings ($p<0.0001$). Speed and wound persistence of neutrophils were not different in mutants lacking functional Shp1 (Fig. 6C).

The total number of macrophages in embryos lacking Shp1 is increased at 3 dpf and 5 dpf (Fig. 4E). In contrast, the number of macrophages in the wound area is significantly decreased in mutant embryos compared to their siblings ($p<0.0001$) (Fig 6A,B, Supplemental Material SM1 and SM2). This is supported by the notion that wound persistence of macrophages is decreased in mutants compared to siblings ($p=0.007$) (Fig 6C). The meandering index of macrophages distant from the wound was significantly reduced in mutant embryos ($p=0.001$), while the speed was not affected (Fig 6C). In contrast to the total number of neutrophils and macrophages (Fig. 4E,F), the number of macrophages and neutrophils that were detected in the tail was not significantly different between mutants and siblings, although the number of neutrophils in mutant embryo tails trends towards a reduction (Fig 6C). Despite the lower number of macrophages in the wound area, there was no difference in regeneration between *ptpn6* mutant embryos and their siblings (Fig S6). Taken together, embryos lacking functional Shp1 exhibited differences in behavior of neutrophils and macrophages, which however did not affect caudal fin fold regeneration.

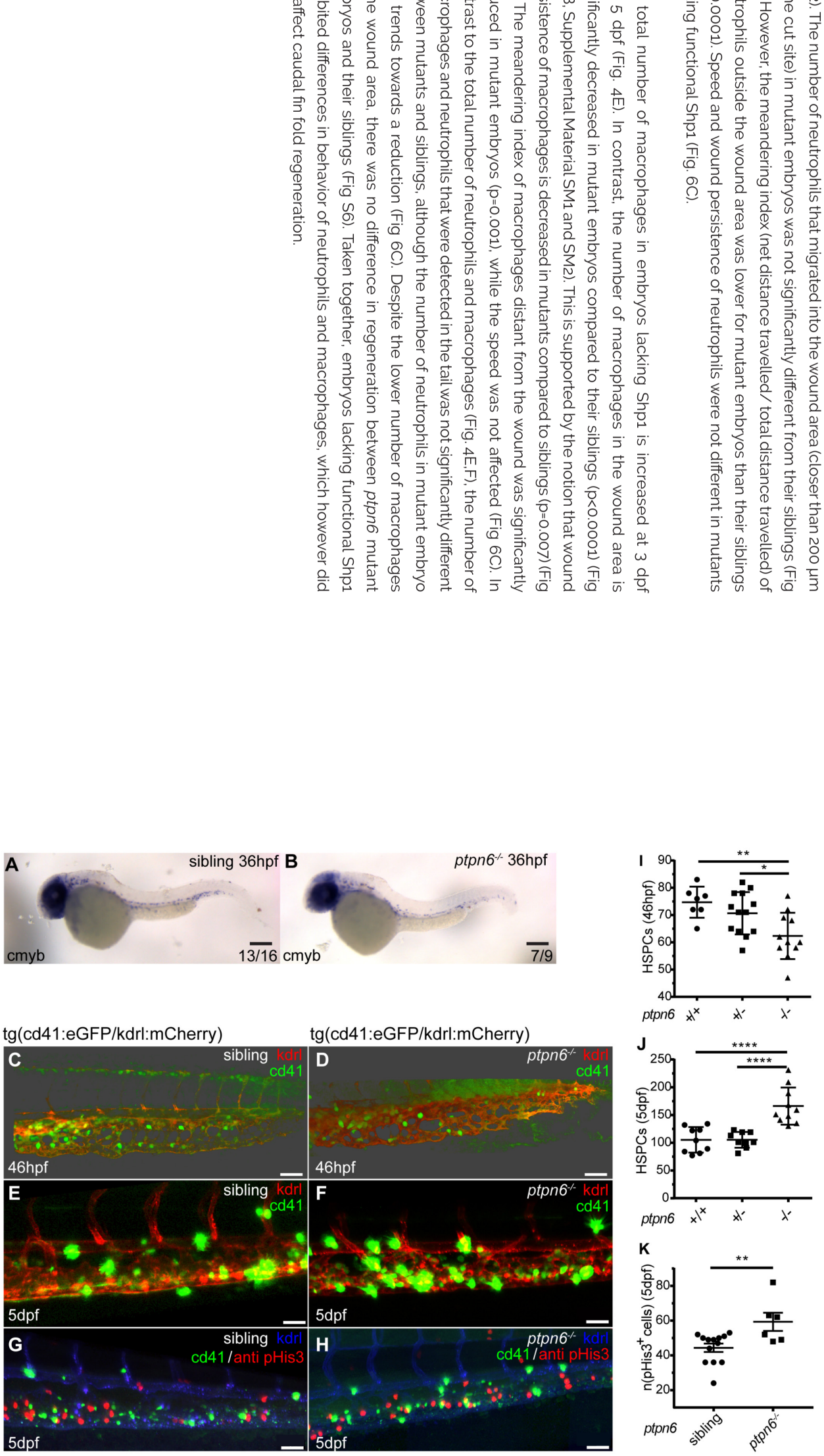

◀ Figure 5. HSPCs in *ptpn6* mutant embryos. (A,B) Stereo images of cmyb *in situ* staining, a HSPC marker, at 36hpf. The number of embryos showing the depicted pattern/ total number of embryos is shown in the bottom right corner. (C-H) confocal images of the CHT of *tg(cd41eGFP/kdrl:mCherry)* zebrafish, 40x objective, pinhole 2AU. The *cd41eGFP* transgene marks thrombocytes at later stages (GFP^{high}) and HSPCs (GFP^{low}); the *kdrl:mCherry* transgene marks endothelial cells, including HSPCs that derive from endothelial cells. (C,D) Embryos were selected and fixed at ~46hpf, when no GFP^{high} cells marking thrombocytes were present yet, only GFP^{low}-positive HSPCs. Whole-mount immunohistochemistry was performed using a GFP specific antibody. Representative 3D blended rendering images of the CHT of 46hpf embryos. Step size 1.5µm (E,F) Live imaging of 5dpf embryos. Representative 3D maximum intensity projection rendered images of part of the imaged region of the CHT are shown. Step size 2µm. (G,H) 5dpf embryos were fixed and whole-mount immunohistochemistry was performed using a pHis3 (proliferation) and GFP specific antibody (GFP^{low}: HSPCs). Representative 3D maximum intensity projection images of part of the imaged CHT are depicted. Step size 2µm. (I-J) Scatterplots of quantification of cells in confocal images using IMARIS. (I) GFP positive HSPCs in the CHT of 46hpf embryos and (J) GFP^{low} HSPCs in the CHT of 5dpf embryos. Statistical comparisons were performed by ANOVA followed by a Tukey's multiple comparisons test. (K) quantification of pHis3-positive cells in the CHT of 5dpf embryos. All embryos were genotyped following *in situ* hybridization, immunohistochemistry and imaging by PCR and sequencing. Means were compared using a 2-sided student's t-test. *p<0.05, **p<0.01, ***p<0.001, ****p<0.0001, error bars = SEM

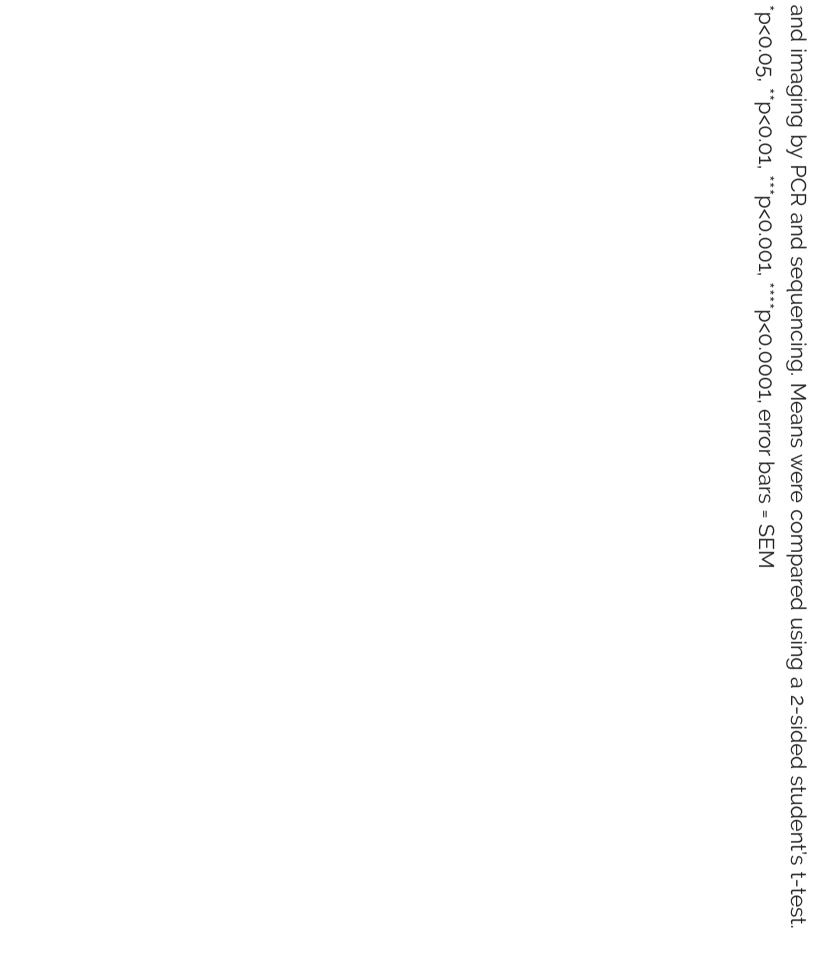

◂ Figure 6. Neutrophil and macrophage migration is affected upon tail fin fold amputation in Shp1 mutants. Embryos were genotyped by PCR and sequencing following imaging. (A) Stills from live imaging of mutant and sibling 4dpf embryos in *tg(mpx:GFP/mpeg:mCherry)* background show neutrophils in green and macrophages in red. Embryos were imaged every minute for 7 h, see Supplementary Material, SM1 and SM2. The outline of the amputated fin-fold at the start of imaging is indicated with a solid orange line. The border of the wound area is indicated with a dashed orange line. (B) Cells were detected using Trackmate. Cells within 200 µm of the wound were counted in every frame from 30 min after amputation till 410 min after amputation. Shaded area represents results of bootstrapping. Results of 6 mutants and 11 siblings were analyzed and compared by ordinary least squares regression (statmodels). For neutrophils, p-value=0.78 & 95% CI coefficient = [-2.10 - -1.54]; for macrophages, p-value<0.0001 & 95% CI coefficient = [-0.24 - 0.02]. (C) Meandering index and mean speed were determined for the distant cells (further than 200 µm from the wound edge) of 6 siblings and 4 mutant embryos. Meandering index was defined as the net distance travelled/ total distance travelled of a track. All results of the measurements in (C) were compared using unequal variance T-test (SciPy) and two sided 95% confidence intervals (statmodels). Meandering index was significantly reduced for neutrophils, p-value<0.0001, 95% CI[0.48- 0.52] vs [0.36-0.42] and macrophages, p-value=0.0014, 95% CI[0.39-0.44] vs [0.45-0.49]. Mean speed was not significantly different for neutrophils, p-value=0.5, 95% CI[7.3- 8.1] vs [7.4-8.5] and macrophages, p-value=0.48, 95% CI[4.82-5.35] vs [4.89-5.61]. The number of tracks was not significantly different for the entire tail of 6 siblings and 4 mutant embryos: neutrophils, p-value=0.092; macrophages, p-value=0.37. Wound persistence was determined for all cells that entered the wound area of 11 siblings and 6 mutants. For neutrophils, p-value=0.78, 95% CI[0.35- 0.41] vs [0.35-0.42]; macrophages, p-value=0.014, 95% CI[0.33- 0.38] vs [0.28-0.34]. NS, not significant; * p<0.05, ** p<0.01, *** p<0.001, **** p<0.0001. Boxplots show quartiles of data. Outliers were determined as datapoints outside 1.5 interquartile range. Number of cells and number of embryos are mentioned as n= cells/ embryos.

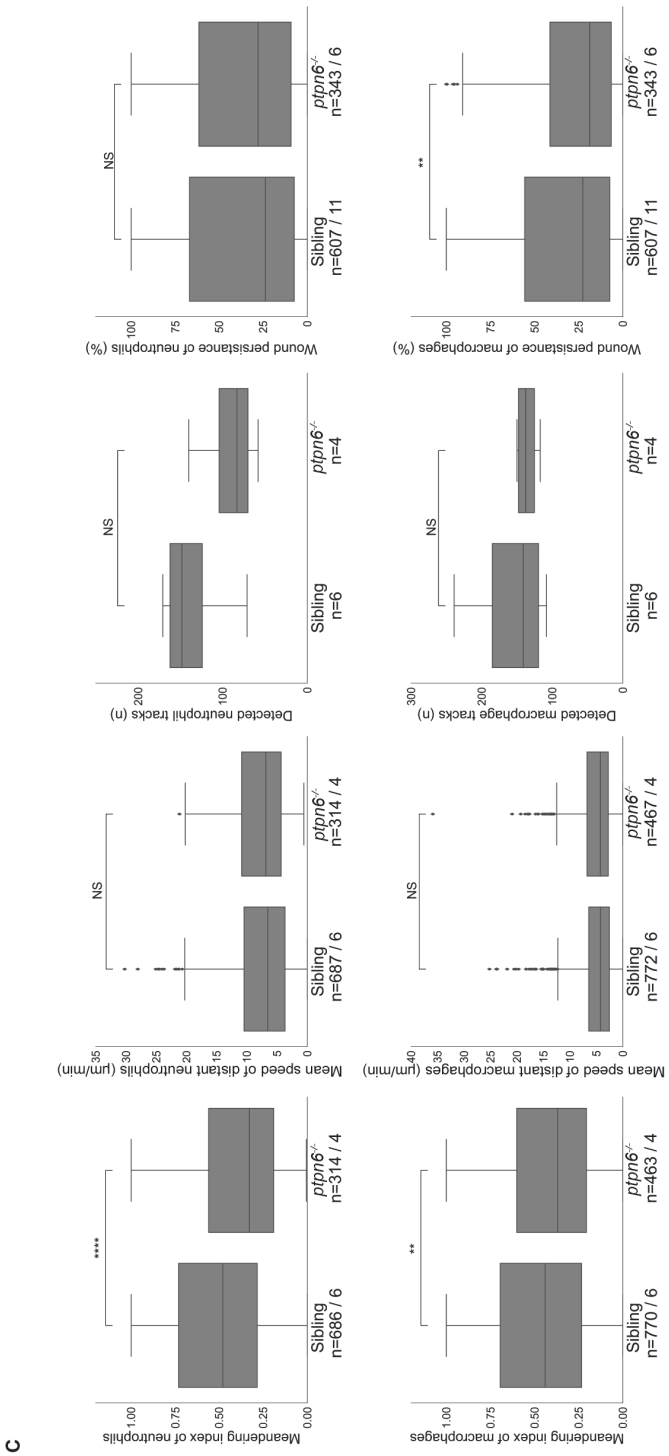

Figure 6. Continued.

Discussion

SHP1 *null* mutations have long been studied in the context of auto-immunity and inflammation in the *motheaten* mouse. Because mice develop in utero, and *motheaten* mice are already severely affected at birth (Green and Shultz, 1975) it has been difficult to study the early development of the hematopoietic system and inflammatory phenotype. In this study we developed a zebrafish model to study hematopoiesis during embryonic development in the absence of Shp1. In the mouse embryo, HSCs emerge from the dorsal aorta and colonize the liver before populating the adult organs of hematopoiesis (Sánchez *et al.*, 1996; de Bruijn *et al.*, 2000; Kumaravelu *et al.*, 2002; Boisset *et al.*, 2010). An equivalent process takes place in zebrafish embryos, where HSPCs emerge from the ventral wall of the dorsal aorta, temporarily colonize the CHT, which is homologous to the mouse fetal liver, before migrating to the head kidney, the adult site of hematopoiesis in zebrafish (Kissa and Herbomel, 2010; Murayama *et al.*, 2006). Furthermore, the zebrafish adaptive immune system is not functionally mature until 4-6 weeks post fertilization, allowing analysis of the function of Shp1 in innate immunity during embryonic development.

Shp1 knock-out in zebrafish is lethal at late larval stages, but did not induce obvious morphological defects in embryos. Morpholino-mediated knockdown of Shp1 induced pleiotropic defects from 3 dpf onwards (Kanwal *et al.*, 2013). The pleiotropic defects in response to morpholino-mediated knockdown may be due to off-target effects, causing non-specific inflammation. Alternatively, the difference between the morpholino-mediated knockdown and the knockouts we generated may be caused by intrinsic differences between morpholino-mediated knockdown and genetic knockouts. Morpholinos block translation or splicing from the moment the morpholino is administered, i.e. the one-cell stage, whereas in the genetic knockdown, maternally contributed Shp1 may persist, which may result in a later onset of the phenotype. It is interesting to note that the Shp1 morpholino elicited skin lesions similar to the lesions observed in the genetic mutant (Fig. 2A-D). The inflammatory response was also common between the morpholino-mediated knockdown and the genetic knock-out, suggesting that the response to loss of functional Shp1 was similar, but that the timing was different.

Mutant zebrafish larvae present with hyperinflammation, characterized by strong upregulation of several inflammatory genes. The phenotype includes skin lesions and infiltration of gills and mandibular area with neutrophils. The hyperinflammation, the skin lesions and the gill infiltration by neutrophils are very similar to the *motheaten* appearance and lethal pneumonitis found in *motheaten* mice (Green and Shultz,

1975; Jiao *et al.*, 1997). It also supports the sporadic cases of humans that present with mutations in *ptpn6,* which have been associated with neutrophilic dermatoses, and emphysema (Nesterovitch *et al.*, 2011; Bossé *et al.*, 2019). The neutrophil specific Shp1 knock-out mouse line suggests that the skin lesions and inflammation are caused by mutant neutrophils. However, the lethal pneumonitis is not recapitulated by neutrophil-specific mouse knock-out lines, which indicates that other cell types are involved in causing this phenotype. It is interesting to note that the sites of hyperinflammation are the sites of contact with the outside world, suggesting that external factors may have an important role in the process. The strong occurrence of gill and mandibular infiltration in Shp1 mutant zebrafish composes an ideal model to investigate the development of lethal pneumonitis/gill infiltration due to Shp1 knock-out.

Shp1 deficiency led to multiple hematopoietic defects during embryonic development, affecting the HSPCs and myeloid cell lineages. The number of emerging HSPCs was reduced in mutants compared to siblings. However, this reduction was compensated by enhanced proliferation of HSPCs later during development. These results are in contrast with a previous report that showed no effect on HSPCs in *motheaten* mice (Shultz, Bailey and Coman, 1983). However, our results support the finding that knock-out of Shp1 in HSPCs causes enhanced proliferation in mouse embryos (Jiang *et al.*, 2018). A possible explanation for this apparent discrepancy is that the earlier report missed an effect on HSPCs due to the use of a spleen assay to determine the number of HSPCs. Enhanced proliferation of HSPCs may have compensated for the lower number of early HSPCs. The zebrafish model facilitated continuous analysis of hematopoiesis from the moment HSPCs emerged from the dorsal aorta, thus revealing reduced numbers of HSPCs at the start, which showed enhanced proliferation later during development (Fig. 5). What drives hyperproliferation of HSPCs remains to be determined definitively. It has been reported in the mouse that loss of SHP1 may lead to enhanced STAT5 phosphorylation, which in turn leads to enhanced proliferation of HSCs (Xiao *et al.*, 2010). It will be interesting to investigate whether STAT5 phosphorylation is enhanced in *ptpn6* mutant zebrafish as well.

The number of macrophages was increased in *ptpn6* mutant zebrafish embryos (Fig. 4), which may simply be due to enhanced numbers of HSPCs in *ptpn6* mutant embryos. The enhanced number of macrophages in *ptpn6* mutant embryos is consistent with earlier findings in *motheaten* and *motheaten viable* mice. Macrophages from the spleen of *motheaten* mice showed increased proliferation and faster maturation than wild-type macrophages *in vitro* (McCoy *et al.*, 1982, 1983). Tissue sections from *motheaten viable* mice also show a significant increase in macrophage numbers in

spleen, bone marrow and peripheral tissues (Nakayama *et al.*, 1997). Finally, ES cells expressing dominant negative Shp1 differentiate into a strongly increased number of myeloid cell colonies in a hematopoietic colony forming assay (Paling and Welham, 2005). However, the observation that the increase in macrophage number occurred at the expense of the number of neutrophils (Fig. 4) has not been noticed in mice. It would be interesting to investigate the early numbers of neutrophils in mice lacking functional Shp1 to verify if the phenomenon we noticed in zebrafish is similar in mice.

Directional migration of neutrophils and macrophages after tail fin fold wounding was reduced (Fig. 6, Supplemental Material SM1 and SM2). Furthermore, the number of macrophages that were attracted to the wound site was reduced. This shows that Shp1 has a role in the attraction-migration process that occurs directly after wounding. It is likely that Shp1 has a role in sensing the attraction signal, rather than in sending the signal, given the predominant expression of Shp1 in hematopoietic cells and given the role of Shp1 in intracellular signalling (Plutzky, Neel and Rosenberg, 1992; Abram and Lowell, 2017). It is interesting to note that, even though the meandering index of neutrophils is reduced, this did not lead to a reduction in the number of neutrophils that reached the wound site. Apparently, there is still a strong attraction of neutrophils to the wound site. However, the cells struggled to migrate efficiently towards their target. This is consistent with a previous report that neutrophil adhesion is increased in motheaten mice, lacking functional SHP1 (Stadtmann *et al*., 2015). The lower number of macrophages that were present at the wound site indicated that less macrophages were attracted to the wound site, which was surprising because the number of macrophages in embryos lacking functional Shp1 was enhanced (Fig. 4, 6). Macrophages were primarily located in the anterior of the embryos, instead of the tail region, which may be due to enhanced adhesion of macrophages in the anterior region of the embryo. The molecular mechanism underlying reduced directional migration of neutrophils and macrophages may involve phosphatidylinositol phosphate levels, which may affect adhesion. SHP1 has a role in PIPKIγ regulation in neutrophils and in modulation of PI3K in macrophages (Stadtmann *et al*., 2015; Roach *et al*., 1998). However, further research is needed to definitively establish the effect of Shp1 on neutrophil and macrophage migration.

Regeneration was unaffected in *ptpn6* mutant zebrafish embryos (Fig. S6), despite the lower number of macrophages that reached the wound site. This is surprising, given a previous report that showed that ablation of macrophages severely impaired regeneration (Li *et al.*, 2012). Possibly the low number of macrophages that reached the wound site was still sufficient for normal regeneration. Another possibility is that Shp1 knock-out has affected signalling in macrophages in such a way that fewer

macrophages were required for the regeneration response. Taken together, whereas Shp1 is dispensable for regeneration of the caudal fin fold, Shp1 is required for normal behaviour of neutrophils and macrophages. More research is needed to determine the exact role of Shp1 in neutrophil and macrophage function. The *ptpn6* mutant we generated will be instrumental for further research into the function of Shp1 in neutrophils and macrophages.

Literature list

Abram, C. L. and Lowell, C. A. (2017). Shp1 function in myeloid cells. *J Leukoc Biol* 102, 657–675.

Abram, C. L., Roberge, G. L., Pao, L. I., Neel, B. G. and Lowell, C. A. (2013). Distinct Roles for Neutrophils and Dendritic Cells in Inflammation and Autoimmunity in motheaten Mice. *Immunity* 38, 489–501.

Al-Adhami, M. A. and Kunz, Y. W. (1977). ONTOGENESIS OF HAEMATOPOIETIC SITES IN BRACHYDANIO RERIO (HAMILTON-BUCHANAN) (TELEOSTEI)*. *Development, Growth and Differentiation* 19, 171–179.

An, H., Hou, J., Zhou, J., Zhao, W., Xu, H., Zheng, Y., Yu, Y., Liu, S. and Cao, X. (2008). Phosphatase SHP-1 promotes TLR- and RIG-I-activated production of type I interferon by inhibiting the kinase IRAK1. *Nat Immunol* 9, 542–550.

Bainton, D. F., Ullyot, J. L. and Farquhar, M. G. (1971). The development of neutrophilic polymorphonuclear leukocytes in human bone marrow. *J Exp Med* 134, 907–34.

Boisset, J.-C., van Cappellen, W., Andrieu-Soler, C., Galjart, N., Dzierzak, E. and Robin, C. (2010). In vivo imaging of haematopoietic cells emerging from the mouse aortic endothelium. *Nature* 464, 116–20.

Borregaard, N. and Cowland, J. B. (1997). Granules of the Human Neutrophilic Polymorphonuclear Leukocyte. *Blood* 89, 3503–3521.

Bossé, Y., Lamontagne, M., Gaudreault, N., Racine, C., Levesque, M. H., Smith, B. M., Auger, D., Clemenceau, A., Paré, M. È., Laviolette, L., *et al*. (2019). Early-onset emphysema in a large French-Canadian family: a genetic investigation. *Lancet Respir Med* 7, 427–436.

Choorapoikayil, S., Kers, R., Herbomel, P., Kissa, K. and den Hertog, J. (2014). Pivotal role of Pten in the balance between proliferation and differentiation of hematopoietic stem cells in zebrafish. *Blood2* 123, 184–190.

Croker, B. A., Lawson, B. R., Rutschmann, S., Berger, M., Eidenschenk, C., Blasius, A. L., Moresco, E. M. Y., Sovath, S., Cengia, L., Shultz, L. D., *et al*. (2008). Inflammation and autoimmunity caused by a SHP1 mutation depend on IL-1, MyD88, and a microbial trigger. *Proc Natl Acad Sci U S A* 105, 15028–33.

de Bruijn, M. F. T. R., Speck, N. A., Peeters, M. C. and Dzierzak, E. (2000). Definitive hematopoietic stem cells first develop within the major arterial regions of the mouse embryo. *The EMBO Journal* 19, 2465–2474.

Ellett, F., Pase, L., Hayman, J. W., Andrianopoulos, A. and Lieschke, G. J. (2011). mpeg1 promoter transgenes direct macrophage-lineage expression in zebrafish. *Blood* 117, e49-56.

Gagnon, J. A., Valen, E., Thyme, S. B., Huang, P., Ahkmetova, L., Pauli, A., Montague, T. G., Zimmerman, S., Richter, C. and Schier, A. F. (2014). Efficient Mutagenesis by Cas9 Protein-Mediated Oligonucleotide Insertion and Large-Scale Assessment of Single-Guide RNAs. *PLoS ONE* 9, e98186.

Green, M. C. and Shultz, L. D. (1975). Motheaten, an Immunodeficient Mutant of the Mouse: I. Genetics and pathology. *Journal of Heredity* 66, 250–258.

Hale, A. J. and den Hertog, J. (2018). Shp2-Mitogen-Activated Protein Kinase Signaling Drives Proliferation during Zebrafish Embryo Caudal Fin Fold Regeneration. *Mol Cell Biol* 38, e00515-17.

Hale, A. J., Kiai, A., Sikkens, J. and den Hertog, J. (2017). Impaired caudal fin-fold regeneration in zebrafish deficient for the tumor suppressor Pten. *Regeneration* 4, 217–226.

Iuchi, I. and Yamamoto, M. (1983). Erythropoiesis in the Developing Rainbow Trout, Salmo gairdneri irideus: Histochemical and Immunochemical Detection of Erythropoietic Organs. *THE JOURNAL OF EXPERIMENTAL ZOOLOGY* 226, 409–417.

Jiang, L., Han, X., Wang, J., Wang, C., Sun, X., Xie, J., Wu, G., Phan, H., Liu, Z., Zhang, C., *et al*. (2018). SHP-1 regulates hematopoietic stem cell quiescence by coordinating TGF-β signaling. *J Exp Med* jem.20171477.

Jiao, H., Yang, W., Berrada, K., Tabrizi, M., Shultz, L. and Yi, T. (1997). Macrophages from motheaten and viable motheaten mutant mice show increased proliferative responses to GM-CSF: detection of potential HCP substrates in GM-CSF signal transduction. *Exp Hematol* 25, 592–600.

Kanwal, Z., Zakrzewska, A., den Hertog, J., Spaink, H. P., Schaaf, M. J. M. and Meijer, A. H. (2013). Deficiency in hematopoietic phosphatase ptpn6/Shp1 hyperactivates the innate immune system and impairs control of bacterial infections in zebrafish embryos. *Journal of immunology* 190, 1631–45.

Kissa, K. and Herbomel, P. (2010). Blood stem cells emerge from aortic endothelium by a novel type of cell transition. *Nature* 464, 112–115.

Kissa, K., Murayama, E., Zapata, A., Cortés, A., Perret, E., Machu, C. and Herbomel, P. (2008). Live imaging of emerging hematopoietic stem cells and early thymus colonization. *Blood* 111, 1147–56.

Kumar, S., Jyoti, A., Keshari, R. shankar, Singh, M., Barthwal, M. K. and Dikshit, M. (2010). Functional and molecular characterization of NOS isoforms in rat neutrophil precursor cells. *Cytometry Part A* 9999A, NA-NA.

Kumaravelu, P., Hook, L., Morrison, A. M., Ure, J., Zhao, S., Zuyev, S., Ansell, J. and Medvinsky, A. (2002). Quantitative developmental anatomy of definitive haematopoietic stem cells/long-term repopulating units (HSC/RUs): role of the aorta-gonad-mesonephros (AGM) region and the yolk sac in colonisation of the mouse embryonic liver. *Development* 129, 4891–9.

Lam, S. H., Chua, H. L., Gong, Z., Lam, T. J. and Sin, Y. M. (2004). Development and maturation of the immune system in zebrafish, Danio rerio: a gene expression profiling, in situ hybridization and immunological study. *Developmental & Comparative Immunology* 28, 9–28.

le Guyader, D., Redd, M. J., Colucci-Guyon, E., Murayama, E., Kissa, K., Briolat, V., Mordelet, E., Zapata, A., Shinomiya, H. and Herbomel, P. (2008). Origins and unconventional behavior of neutrophils in developing zebrafish. *Blood* 111, 132 LP – 141.

Li, L., Yan, B., Shi, Y. Q., Zhang, W. Q. and Wen, Z. L. (2012). Live imaging reveals differing roles of macrophages and neutrophils during zebrafish tail fin regeneration. *Journal of Biological Chemistry* 287, 25353–25360.

Livak, K. J. and Schmittgen, T. D. (2001). Analysis of relative gene expression data using real-time quantitative PCR and the 2(-Delta Delta C(T)) Method. *Methods* 25, 402–8.

McCoy, K. L., Chi, E., Engel, D., Rosse, C. and Clagett, J. (1982). Abnormal in vitro proliferation of splenic mononuclear phagocytes from autoimmune motheaten mice. *The Journal of Immunology* 128,.

McCoy, K. L., Chi, E., Engel, D. and Clagett, J. (1983). Accelerated rate of mononuclear phagocyte production in vitro by splenocytes from autoimmune motheaten mice. *The American Journal of Pathology* 112, 18.

Murayama, E., Kissa, K., Zapata, A., Mordelet, E., Briolat, V., Lin, H.-F., Handin, R. I. and Herbomel, P. (2006). Tracing hematopoietic precursor migration to successive hematopoietic organs during zebrafish development. *Immunity* 25, 963–75.

Nakayama, K. I., Takahashi, K., Shultz, L. D., Miyakawa, K. and Tomita, K. (1997). Abnormal development and differentiation of macrophages and dendritic cells in viable motheaten mutant mice deficient in haematopoietic cell phosphatase. *International Journal of Experimental Pathology* 78, 245–257.

Neel, B. G., Gu, H. and Pao, L. (2003). The 'Shp'ing news: SH2 domain-containing tyrosine phosphatases in cell signaling. *Trends Biochem Sci* 28, 284–93.

Nesterovitch, A. B., Gyorfy, Z., Hoffman, M. D., Moore, E. C., Elbuluk, N., Tryniszewska, B., Rauch, T. A., Simon, M., Kang, S., Fisher, G. J., *et al.* (2011). Alteration in the gene encoding protein tyrosine phosphatase nonreceptor type 6 (PTPN6/SHP1) may contribute to neutrophilic dermatoses. *Am J Pathol* 178, 1434–1441.

Paling, N. R. D. and Welham, M. J. (2005). Tyrosine phosphatase SHP-1 acts at different stages of development to regulate hematopoiesis. *Blood* 105, 4290–4297.

Plutzky, J., Neel, B. G. and Rosenberg, R. D. (1992). Isolation of a src homology 2-containing tyrosine phosphatase. *Proc Natl Acad Sci U S A* 89, 1123.

Ransom, D. G., Haffter, P., Odenthal, J., Brownlie, A., Vogelsang, E., Kelsh, R. N., Brand, M., van Eeden, F. J., Furutani-Seiki, M., Granato, M., *et al.* (1996). Characterization of zebrafish mutants with defects in embryonic hematopoiesis. *Development* 123,.

Roach TI, Slater SE, White LS, Zhang X, Majerus PW, Brown EJ, Thomas ML. (1998) The protein tyrosine phosphatase SHP-1 regulates integrin-mediated adhesion of macrophages. *Curr Biol.* 8, 1035-8.

Sánchez, M.-J., Holmes, A., Miles, C. and Dzierzak, E. (1996). Characterization of the First Definitive Hematopoietic Stem Cells in the AGM and Liver of the Mouse Embryo. *Immunity* 5, 513–525.

Shultz, L. D., Bailey, C. L. and Coman, D. R. (1983). Hematopoietic stem cell function in motheaten mice. *Experimental Hematology* 11, 667–680.

Shultz, L. D., Coman, D. R., Bailey, C. L., Beamer, W. G. and Sidman, C. L. (1984). Viable motheaten, a new allele at the motheaten locus. *Am J Pathol* 116, 179–92.

Shultz, L., Bailey, C. and Coman, D. (1987). Hematopoietic stem cell function in motheaten mice. - PubMed - NCBI. *Exp. Hematology* 11, 667–680.

Stadtmann A, Block H, Volmering S, Abram C, Sohlbach C, Boras M, Lowell CA, Zarbock A.(2015) Cross-Talk between Shp1 and PIPKIγ Controls Leukocyte Recruitment. *J Immunol.* 195, 1152-61.

Thisse, C. and Thisse, B. (2008). High-resolution in situ hybridization to whole-mount zebrafish embryos. *Nat Protoc* 3, 59–69.

Timms, J. F., Carlberg, K., Gu, H., Chen, H., Kamatkar, S., Nadler, M. J., Rohrschneider, L. R. and Neel, B. G. (1998). Identification of major binding proteins and substrates for the SH2-containing protein tyrosine phosphatase SHP-1 in macrophages. *Mol Cell Biol* 18, 3838–50.

Tsui, H. W., Siminovitch, K. A., de Souza, L. and Tsui, F. W. L. (1993). Motheaten and viable motheaten mice have mutations in the haematopoietic cell phosphatase gene. *Nat Genet* 4, 124–129.

Watson, H. A., Wehenkel, S., Matthews, J. and Ager, A. (2016). SHP-1: the next checkpoint target for cancer immunotherapy? *Biochemical Society Transactions* 44,.

Willett, C. E., Zapata, A. G., Hopkins, N. and Steiner, L. A. (1997). Expression of ZebrafishragGenes during Early Development Identifies the Thymus. *Developmental Biology* 182, 331–341.

Willett, C. E., Cortes, A., Zuasti, A. and Zapata, A. G. (1999). Early hematopoiesis and developing lymphoid organs in the zebrafish. *Developmental Dynamics* 214, 323–336.

Willett, C. E., Kawasaki, H., Amemiya, C. T., Lin, S. and Steiner, L. A. (2001). Ikaros expression as a marker for lymphoid progenitors during zebrafish development. *Developmental Dynamics* 222, 694–698.

Xiao W, Ando T, Wang HY, Kawakami Y, Kawakami T. (2010). Lyn- and PLC-beta3-dependent regulation of SHP-1 phosphorylation controls Stat5 activity and myelomonocytic leukemia-like disease. *Blood* 116, 6003-13.

Yu, C. C. K., Tsui, H. W., Ngan, B. Y., Shulman, M. J., Wu, G. E. and Tsui, F. W. L. (1996). B and T cells are not required for the viable motheaten phenotype. *J Exp Med* 183, 371–380.

Acknowledgements

The authors would like to thank the animal caretakers at the Hubrecht Institute for excellent care of the zebrafish.

Competing interests

The authors declare no competing or financial interests.

Author contributions

Conceptualization: P.A.B., M.A., J.d.H.; Methodology: P.A.B., M.A., J.H., J.d.H.; Validation: P.A.B., M.A.; Formal analysis: P.A.B., M.A., J.H.; Investigation: P.A.B., M.A.; Resources: P.A.B., M.A., H.P.S., J.d.H.; Data curation: P.A.B., M.A.; Writing – original draft: P.A.B., M.A., J.d.H.; Writing - review & editing: M.A., H.P.S., J.d.H.; Visualization: P.A.B., M.A.; Supervision: H.P.S., J.d.H.; Project administration: J.d.H.; Funding acquisition: H.P.S., J.d.H.

Funding

This work was funded in part by a grant from the Dutch Research Council to J.d.H. (ALW OP.234).

Oxidation of Shp2a is essential for zebrafish caudal fin-fold regeneration

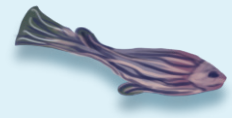

Maaike Allers[1], Niels M. Leijten[2], Jelmer Hoeksma[1], Simone Lemeer[2] and Jeroen den Hertog[1,3]

1. Hubrecht Institute-KNAW and University Medical Center Utrecht, Utrecht, the Netherlands
2. Institute Biology Leiden, Leiden University, Leiden, the Netherlands
3. Biomolecular Mass Spectrometry and Proteomics, Bijvoet Center for Biomolecular Research and Utrecht Institute of Pharmaceutical Sciences, Utrecht University, Utrecht, the Netherlands

Abstract

Src homology region 2 containing protein-tyrosine phosphatase 2 (SHP2) is a well-known phosphatase of the classical protein tyrosine phosphatase (PTP) family. SHP2 is essential for normal development and is widely expressed in numerous tissues and cell types. In zebrafish, two homologs of SHP2 exist, of which one, Shp2a, is indispensable for development. Shp2a also has an essential role in regeneration of the caudal fin-fold in zebrafish embryos. Phosphorylation of MAPK is reduced in amputated tail fin-folds of embryos lacking Shp2a and the catalytic function of Shp2a is essential for regeneration. However, which signal instigates the MAPK pathway in response to amputation is still unknown. We hypothesize that this initiating signal consists of reactive oxygen species (ROS) that are produced in response to wounding. Here, we report the generation of a Shp2a variant that is resistant to oxidation by fusion of Catalase to Shp2a, which quenches H_2O_2 in the vicinity. The Shp2a catalytic cysteine in the Shp2a-Catalase fusion protein was only minimally oxidized by H_2O_2 *in vitro*, while it retained phosphatase activity. Whereas wild type Shp2a rescued regeneration of the amputated caudal fin-fold in Shp2a knock-out embryos, the Shp2a-Catalase fusion protein did not. This shows that reversible oxidation of Shp2a is an essential step in the process of regeneration of zebrafish. We believe that the Catalase fusion we employed may be applied to many different proteins, which facilitates assessment of the effect of target protein oxidation on specific signaling pathways.

Introduction

Src homology region 2 containing protein-tyrosine phosphatase 2 (SHP2) is a well-known phosphatase of the classical protein tyrosine phosphatase (PTP) family, encoded by the gene *PTPN11*. SHP2 is comprised of two Src-homology 2 domains and one PTP domain with the conserved catalytic motif [I/V]HCSXGXGR[S/T]G. SHP2 is tightly regulated via an intramolecular interaction in that the N-terminal SH2 domain is bound to the PTP domain in SHP2's inactive state. SHP2 is activated by binding of the SH2 domains to binding partners and releasing the PTP domain. This opens up the catalytic site for phosphotyrosine containing substrates to bind and be dephosphorylated. Like for all PTPs, the dephosphorylation mechanism involves a catalytic cysteine and an assisting arginine in the PTP domain.

SHP2 functions in multiple signaling pathways. The most well-known is the MAPK/ERK pathway, in which SHP2 promotes activation of MAPK in response to a wide variety of extracellular signals. The exact role of SHP2 in the RAS-MAPK pathway is not clear, but catalytic activity of SHP2 has been shown to be required for activation of MAPK signaling. A likely candidate substrate for SHP2 is Sprouty, an inhibitor of RAS, and dephosphorylation of Sprouty may activate MAPK signaling.

SHP2 is essential for normal development and is widely expressed in numerous tissues and cell types. Knock-out mouse embryos lacking functional SHP2 fail during the blastocyst stage (Yang *et al.*, 2006). In humans, mutations in SHP2 are linked to developmental disorders like Noonan Syndrome (NS) and Noonan Syndrome with multiple lentigines (formerly known as Leopard Syndrome), as well as acute myeloid leukemia. SHP2 is also associated with many other types of cancer (Solman, Woutersen, *et al.*, 2022).

In zebrafish, two homologs of SHP2 exist, called Shp2a and Shp2b. Shp2a is indispensable for development, while Shp2b is not. Zebrafish larvae missing Shp2a develop craniofacial defects and reduced length and are embryonic lethal between 5-7 days post fertilization (dpf) (Bonetti *et al.*, 2014). A specific missense mutation in Shp2a, namely D61G, which causes NS in human patients, leads to the development of NS-specific symptoms in zebrafish (Solman, Blokzijl-Franke, *et al.*, 2022). These symptoms include reduced length and a hammerhead phenotype (broadened head), which recapitulates the symptoms of human patients with Noonan syndrome. This indicates that Shp2a has a similar, essential role in zebrafish development as SHP2 in humans.

In addition, Shp2a plays an essential role in regeneration of the caudal fin-fold in zebrafish embryos. Wildtype zebrafish, both adult and embryonic, are able to regenerate wounded body parts. Yet, mutant zebrafish embryos lacking functional Shp2a do not regenerate their caudal fin-fold following amputation (Hale & den Hertog, 2018). The phosphorylation of MAPK is reduced in the amputated tails of embryos lacking Shp2a and the catalytic function of Shp2a is essential for regeneration. However, the signal that instigates the MAPK pathway in response to amputation is still unknown.

Similarly, the signal that initiates regeneration in response to wounding is still unknown. A candidate for this signal is production of reactive oxygen species (ROS), which is upregulated in response to wounding in a wide variety of organisms, from humans to plants. Live imaging of zebrafish fins after amputation shows that production of ROS starts within 1 hour after amputation (hpa) and is gone by 24 hpa (Gauron *et al*., 2013). Inhibition of ROS production in response to fin amputation of zebrafish inhibits regeneration (Gauron *et al*., 2013; Niethammer *et al*., 2009a; Yoo *et al*., 2012). In addition, recent research shows that application of exogenous H_2O_2 is enough to rescue regeneration in axolotls after inhibition of ROS production (Carbonell-M *et al*., 2022). These data indicate that ROS may be the signal that initiates regeneration in response to wounding.

PTPs are strongly susceptible to oxidation by ROS, because their catalytic site cysteines have a low pKa. Oxidation of the catalytic cysteine leads to temporary inactivation of the PTP. The exact susceptibility of a PTP to oxidation depends on the circumstances and the kind of reactive oxygen species that causes the oxidation. Several PTPs are specifically oxidized upon amputation of the caudal fin of zebrafish, including Shp2a (Wu *et al*., 2017).

The importance of Shp2a in regeneration combined with its susceptibility to oxidation prompted us to investigate the importance of oxidation in Shp2a function during regeneration. Previous attempts to create a Shp2a mutant that was active and was resistant to oxidation, were unsuccessful. Here, we report how we created a Shp2a variant that is protected from oxidation by fusion of Catalase to Shp2a. The Shp2a-Catalase fusion protein was strongly protected from oxidation by H_2O_2 in vitro, while it retained phosphatase activity. The Shp2a-Cat fusion protein was not able to fully rescue regeneration in Shp2a knock-out embryos. This shows that oxidation of Shp2a by ROS is an essential step in the process of regeneration of zebrafish. We believe that the Catalase fusion we employed may be applied to many different proteins in different situations to determine the effect of oxidation on specific signaling pathways.

Material and methods

Zebrafish husbandry

All procedures involving experimental animals were approved by the local animal experiments committee (AVD-8010020173786). All fish were housed and handled according to local guidelines and policies in compliance with national and European law. Zebrafish were raised and maintained under a 14 hours light / 10 hours dark cycle at 28.5˚C as described by (Westerfield, 2000). Fertilized eggs were harvested and incubated at 28.5˚C in E3 medium (5 mM NaCl, 0,17 mM KCl, 0.33 mM $CaCl_2$, 0.33mM $MgSO_4$).

Generation of fusion constructs

Catalase was cloned from cDNA of 5dpf whole zebrafish embryos into multipurpose expression vector pCS2+ and bacterial expression vector pGex. We introduced a silent mutation to remove a BamHI cut-site and we deleted the final C-terminal part of Catalase to remove the nuclear localization signal. For the catalytically inactive variant, the H75F mutation was introduced using Q5 site directed mutagenesis (NEB). Vectors containing Shp2a were previously generated and described in Bonetti *et al.* 2014. A 20 peptide flexible linker (ASGAGGSEGGGSEGGTSGAT) was added C-terminally to Shp2a, as previously used by (Hayashi *et al*., 2017). The pCS2+ plasmids all contained a N-terminal eGFP followed by a peptide-2a cleavage sequence. The pGEX constructs all contained a N-terminal Glutathione-S-transferase(GST) followed by a KG linker.

Bacterial *in vitro* protein production

E. coli sub-cloning competent cells (Invitrogen #18265-017) were transformed with pGEX constructs and protein expression was induced by treating the cells with 100µM isopropyl β-D-1-thiogalactopyranoside (Invitrogen #15529019) at 25˚C overnight. Proteins were isolated by lysis of the bacterial pellet in 1 mg/ml lysozyme (Sigma #L6876-10G), aprotinin (Sigma #10981532001) and leupeptin (Sigma #11017128001) in PBS0. Protein solutions were sonicated and triton X-100 was added. The supernatant was bound to glutathione-agarose beads (Merck Millipore G4510) and eluted using a reduced glutathione buffer (50 mM Tris, 10% glycerol, 10mM reduced glutathione). Proteins were dialyzed at 4˚C in PBS using Spectra/Por Dialysis membranes (Spectrum labs #132665) overnight. Dialyzed protein was aliquoted and stored at -80˚C.

Oxidative treatment

Agarose beads were dissolved in TBS, after which 40 µl was taken to perform experiments with. The beads were washed twice with PBS0, after which the SHP2 protein or mutant was added to bind to the beads. During bead binding, dithiothreitol (DTT) was added to a

concentration of 1 mM to reduce the protein. An additional 100 µl of PBS0 was added and incubated for 30 minutes on a spinner at 4 ˚C. After bead binding the oxidative treatment was performed. Either MilliQ or H_2O_2 was added to the desired concentration and incubated for the desired time. Afterwards, the beads were washed twice with PBS0. After oxidative treatment, non-reacted cysteines were alkylated by adding N-ethylmaleimide (NEM) to a final concentration of 4 mM and incubating for 2 hours at 37 ˚C. The beads were washed twice with PBS0, after which the singly oxidized cysteines were reduced by adding 10mM DTT in PBS0 with 1% sodium deoxycholate. The beads were incubated for 30 minutes at room temperature. Subsequently, the beads were washed twice with PBS0. Finally, the now reduced cysteines were alkylated by adding 40mM iodoacetic acid (IAA). Beads were incubated at room temperature for 30 minutes. The reaction was quenched by adding 1 mM DTT, after which the beads were stored in the -80 freezer for analysis by mass spectrometry.

Digestion and desalting

The beads were centrifuged at 20,000 relative centrifugal force (rcf) for 5 minutes at 4 ˚C to pellet the beads. The supernatant was removed and 240 µl of digestion buffer was added (1.5 M Urea in 50 mM ammonium bicarbonate (AMBIC)). A predigestion step was performed by adding trypsin in a 1:100 ratio (protein:protease). The samples were incubated for four hours at 37 ˚C. A second digestion step with trypsin (1:100) was performed overnight at 37 ˚C. After digestion, the samples were diluted with 200 µl of 50 mM AMBIC and acidified by adding 12 µl of formic acid. The samples were centrifuged at 20,000 rcf for 10 minutes and 4˚C, after which they were desalted using SEPPAK SPE cartridges (Waters). Briefly, the cartridges were washed three times with 1 ml acetonitrile, followed by washing three times with 1 ml of 0.1 M acetic acid. Afterwards, samples were loaded and the flow through was passed through the cartridge again. The cartridges were then washed three times with 0.1 M acetic acid, after which the peptides were eluted by adding three times 250 µl of 0.1 M acetic acid / 80% acetonitrile. The samples were subsequently dried using a Thermo Savant SPD SpeedVac (Thermofisher scientific).

Mass spectrometric analysis

For the mass spectrometric analysis, peptides were dissolved in 2% formic acid and a volume corresponding to 2 µg was injected on a UHPLC 1290 system (Agilent) coupled to a Q Exactive HF-X mass spectrometer (Thermo Fisher Scientific). The peptides were trapped (Dr Maisch Reprosil C18, 3 µm, 2 cm x 100 µm) for 5 minutes in buffer A (0.1% formic acid) at a flow rate of 0.005 ml/min. Afterwards they were separated using an analytical column (Agilent Poroshell EC-C18, 2.7 µm, 50 cm x 75 µm). The following gradient was used: 13 – 44% buffer B (80% acetonitrile + 0.1% formic acid) in 65 minutes, 100% buffer B for 2 minutes followed by 100% buffer A for 11 minutes. A split flow was used to generate a flow rate of 300 nl/min. The Q Exactive HF-X was operated in a data

dependent acquisition mode with positive ionization. The full MS spectra were acquired from 375 to 1600 m/z at 60000 resolution, using an automatic gain control (AGC) target value of 3 x 106 charges and a maximum injection time of 20 ms. A maximum of 15 precursors were allowed to be fragmented. The dynamic exclusion was set to 12 seconds. MS/MS fragmentation spectra were obtained with a fixed first mass of 120 m/z and a resolution of 30000. An AGC target of 1 x 105 was chosen and a maximum injection time of 50 ms. The fragmentation was performed using HCD at a NCE of 27.

Quantification of oxidative modifications

The relative presence of the different oxidative modification was determined by creating extracted ion chromatograms (XIC) of the masses corresponding to the modified peptide (QEGITGAGPIVVHCSAGIGR). The following masses were chosen: NEM alkylated (572.81, 4+), IAA alkylated (741.06, 3+), sulphinic acid (732.39, 3+) and sulphonic acid (737.72, 3+). The extracted XICs were integrated in the xCalibur Qual browser (Thermo Fisher scientific, version 4.0.27.21) using the Genesis algorithm. The areas of these XICs were used to compare the intensity of the different modifications.

Phosphatase assays

Protein was dissolved in 33.3 mM 2-(N-morpholino)-ethanesulphonic acid (MES)(pH 6.0). Protein was incubated with different levels of H_2O_2 at room temperature for 30 min. Equal volume of 2x para-nitrophenylphosphate (pNPP) solution (40mM MES(pH 6.0)., 2mM DTT, 2 mM EDTA, 200M NaCl, 20mM pNPP) was added to the samples. The reaction was incubated for 30 min at 30˚C and stopped by adding 0.5M NaOH. Phosphatase activity was determined by measuring the absorption at 405 nm using a plate reader.

SDS-page

Isolated protein was diluted using gel loading buffer (Invitrogen) and resolved on a 10% acrylamide SDS-page gel (Biorad) in running buffer (25mM Tris, 0.2M Glycine, 0.1% SDS). The gels were stained with Coomassie staining for 30 min and washed overnight, before being imaged.

mRNA synthesis and micro-injections

Sense messenger RNA (mRNA) was synthesized using the mMessage machine SP6 kit (Ambion) from pCS2+ plasmids. Solutions consisting of phenol red with diluted mRNA were incubated at 65˚C for 5 min and then kept on ice. Micropipettes were created by pulling borosilicate glass capillary tubes (World Precision Instruments, Inc., 1B100-4) using a micropipette puller device (Sutter Instruments Inc., Flaming/Brown P-97). One cell-stage embryos were arranged on a 1.5% agarose/E3 microinjection mold and micro-injected with 1 nanoliter of the mRNA solutions.

Regeneration
Zebrafish embryos were amputated at the tail as previously described (Hale & den Hertog, 2016). Amputations were performed at 2 dpf and regeneration was analyzed at 5 dpf. Regenerated tails were imaged and whole embryos were lysed for genotyping. Regeneration was quantified by measuring the length from the tip of the notochord to the end of the fin-fold in ImageJ.

Embryonic development
Zebrafish embryos were injected at the one cell stage and left to develop at 28.5˚C. At 2dpf and 5dpf the embryos were anesthetized using tricaine methanesulfonate and mounted in 2% methylcellulose (Sigma) on glass indented slides. They were imaged using a Leica M165FC connected to a DFC420C camera. Images were processed using ImageJ. They were scored for 5 stages from WT till death. Moderately affected included embryos with a deflated swim bladder, smaller eyes or a lightly curved body. Intermediately affected embryos included embryos with heart oedema or craniofacial defects. Severely affected embryos included embryos that were missing body parts or were otherwise strongly malformed.

Results

Catalase fusion protects Shp2a from oxidation
We created a fusion protein, consisting of Shp2a fused to Catalase C-terminally. We used a 20-peptide flexible linker to minimize the perturbation of folding and interaction with binding partners of Shp2a. By ensuring that a Catalase was constantly in the vicinity of Shp2a, we expected to protect Shp2a from oxidation by hydrogen peroxide. As a control, we created the same fusion protein with a single point mutation in Catalase, leading to a functionally inactive Catalase. This Shp2a – inactive Catalase complex should function comparable to WT Shp2a, since the Shp2a is not protected from oxidation by mutant Catalase.

To assess whether the Catalase is able to protect Shp2a from oxidation by hydrogen peroxide (H_2O_2), we tested the oxidation of Shp2a after treatment with H_2O_2 by mass-spectrometry. For this, we incubated the Shp2a proteins with water or H_2O_2, followed by a differential alkylation experiment. After incubation with different concentrations of H_2O_2 for 2 hours, we alkylated the remaining free thiols by N-ethylmaleimide (NEM). Subsequently, we reduced reversibly oxidized thiols by DTT and then alkylated those using iodoacetic acid (IAA) (Figure 1). After digesting, LC-MS/MS was performed to detect the cysteine containing peptide with the different modifications.

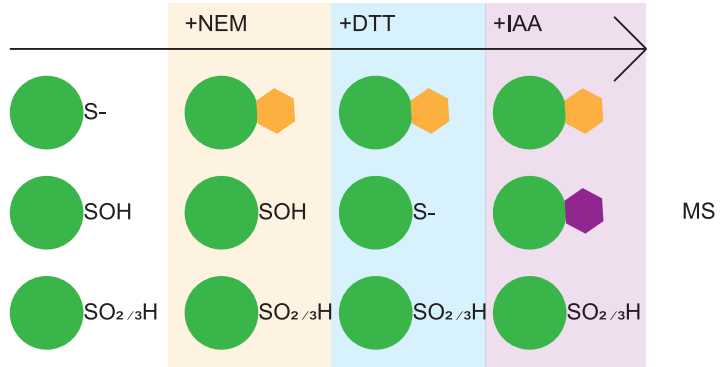

Figure 1: Schematic representation of the treatment of Shp2 before MS analysis. The oxidation state of proteins consists of a mixture of proteins in which the cysteines are reduced (S-), reversibly oxidized (SOH) or irreversibly oxidized ($SO_{2/3}H$). Bacterially expressed proteins were treated with N-ethylmaleimide (NEM), which alkylated the reduced cysteines. Subsequently, DTT was added, which reduced the reversibly oxidized cysteines. These, now reduced, cysteines were alkylated by addition of iodoacidic acid (IAA). The irreversibly oxidized cysteines were not affected by any treatment. Finally, all peptide populations were measured by mass spectrometry.

We were able to distinguish the percentage of non-oxidized Shp2a, reversibly oxidized Shp2a and irreversibly oxidized Shp2a. For WT Shp2a, incubation with 0.25 mM H_2O_2 led to 50% reversibly oxidized Shp2a, and almost 20% irreversibly oxidized Shp2a. Increasing the H_2O_2 concentration to 1mM, led to 40% irreversibly oxidized and 40% reversibly oxidized Shp2a. The Shp2a – inactive catalase fusion (Shp2a-mCatalase) showed similar results, with 20% being irreversibly oxidized and 35% being reversibly oxidized in the 0.25 mM H_2O_2 condition, and 45% irreversibly and 35% reversibly oxidized in the 1 mM H_2O_2 condition. The Shp2a-Catalase fusion protein showed much less oxidation, with approximately 20% of the Shp2a being reversibly oxidized in all conditions, and only 10% and 25% being irreversibly oxidized in the 0.25 mM and 1 mM H_2O_2 conditions, respectively (Figure 2A,B). This indicated that *in vitro*, Shp2a–Catalase is significantly protected against oxidation.

Figure 2: Shp2a-Catalase is protected from oxidation *in vitro*. A: Extracted ion chromatograms for wt Shp2a, Shp2a-Catalase and Shp2a-mCatalase upon treatment with milliQ (light grey), 0.25 mM H_2O_2 (dark grey) or 1 mM H_2O_2 (black). The number of asterisks indicates the oxidation status of the peptide in the peak as indicated in the inset. B: Bargraph representation of the proportion of reduced and oxidized WT Shp2a, Shp2a-Catalase and Shp2a-mCatalase upon treatment with milliQ, 0.25 mm H_2O_2 or 1 mm H_2O_2. For statistical analysis, the triply and doubly oxidized categories were combined together and counted as 'irreversibly oxidized', while the singly oxidized category is 'reversibly oxidized'. A Chi-square test was performed on the differences in proportions of 'reduced', 'reversibly oxidized' and 'irreversibly oxidized' in the 0.25mM H_2O_2 and the 1mM H_2O_2 categories compared to the milliQ treated category. The data from Shp2a WT was indicated as the expected proportion that responded in reaction to the treatment. The results from the Chi-square test indicated a strong statistically significant difference in the proportions that changed in response to both the 0.25mM H_2O_2 and the 1mM H_2O_2 treatment of Shp2a-Catalase compared to WT Shp2a (p-values = 5.9e-10 and 2.2e-5). For the Shp2a-mCatalase, the Chi-square test indicated a significant difference in response to 0.25mM H_2O_2 treatment (p-value = 1.3e-5), but no difference between WT Shp2a and Shp2a-mCatalase in response to 1mM H_2O_2 treatment. ►

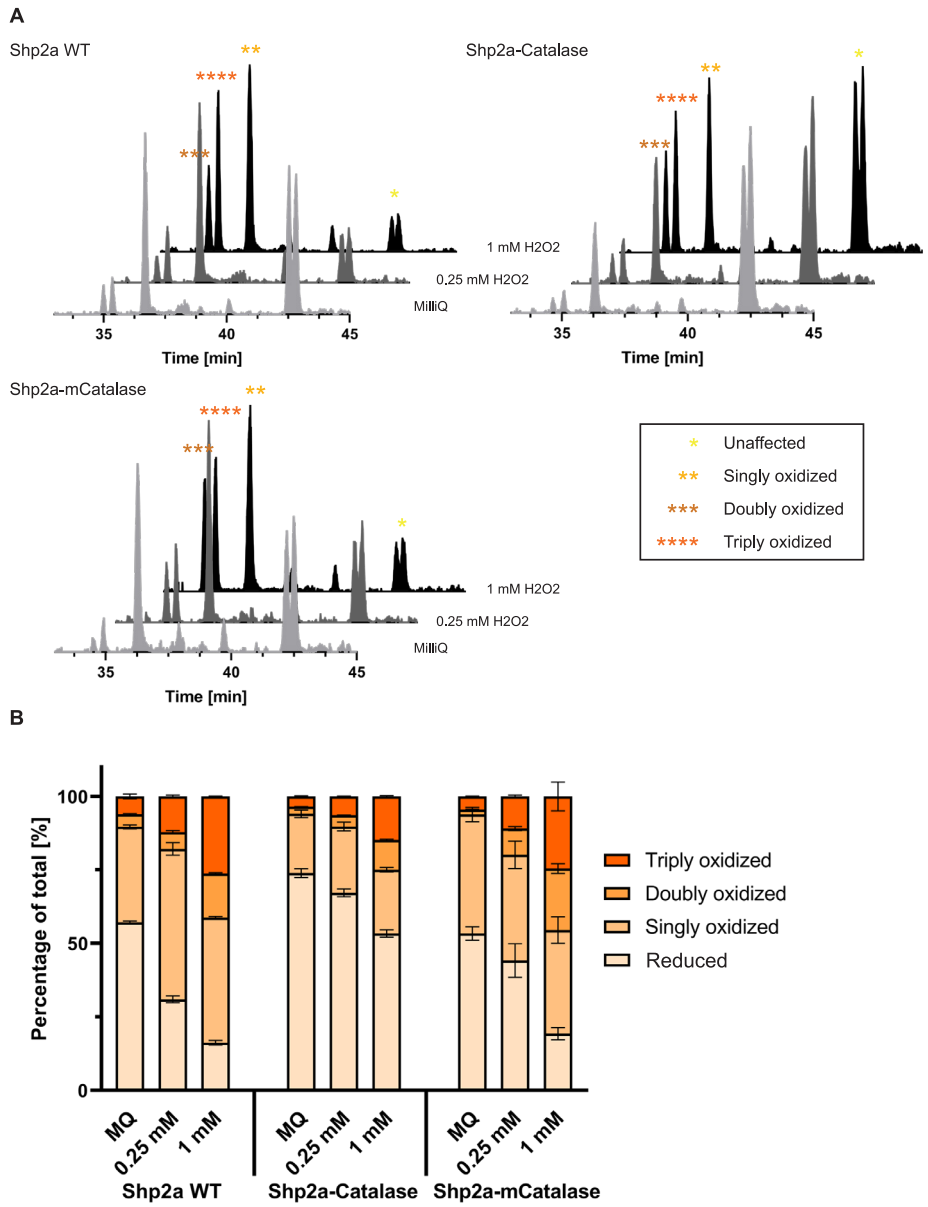

Persistent Shp2a catalytic activity by Catalase fusion in oxidizing conditions

Next, we investigated whether the Shp2a-Catalase fusion still showed phosphatase activity. We tested the activity of our Shp2a-catalase fusion protein *in vitro* using a phosphatase activity assay. Both Shp2a-Catalase and Shp2a-mCatalase were able to dephosphorylate para-nitrophenylphosphate (pNPP), a widely used chromogenic substrate. Incubation for 30 min with 1 mM H_2O_2 led to a decrease in phosphatase activity of WT Shp2a to 50% of WT Shp2a treated with water, when the samples were reduced with DTT prior to activity testing (Figure 3A). When the reduction step was omitted, phosphatase activity was reduced to less than 20%. This indicates that 30 min 1 mM H_2O_2 incubation led to 30% of the WT Shp2a being reversibly oxidized, and 50% of the WT Shp2a being irreversibly oxidized. Using a lower concentration of H_2O_2 (0.25 mM), resulted in 35% irreversibly oxidized Shp2a and 20% reversibly oxidized Shp2a (Figure 3A).

Remarkably, the catalytic activity of Shp2a-Catalase fusion protein was only 5% reduced upon treatment with 0.25 mM H_2O_2 for 30 min, which was reversible. In response to 1 mM H_2O_2, catalytic activity was reduced by 10%. No irreversible inactivation was detected of the Shp2a-Catalase fusion protein (Figure 3A). Treatment of the Shp2a–mCatalase fusion protein led to a 25% reversible and 20% irreversible reduction in Shp2a activity when incubated with 0.25 mM H_2O_2 for 30 min, similar to WT Shp2a. Treatment with 1 mM H_2O_2 resulted in 25% irreversible and 55% reversible reduction in activity of the Shp2a-mCatalase fusion (Figure 3A). These data indicate that Shp2a was resistant to H_2O_2-mediated oxidation when fused to Catalase. To verify the size of Shp2a, Shp2a-Catalase and Shp2a-mCatalase protein, we ran these proteins on SDS-page gel and stained with Coomassie blue (Figure 3B).

To control for the possibility that Catalase was scavenging all the H_2O_2 in the vials, we included Shp2a WT mixed with free Catalase or mutant Catalase. Neither the Catalase nor the mutant Catalase protein was able to protect Shp2a from inactivation by the H_2O_2 (Figure 3A). This showed that the close proximity of Shp2a to Catalase in the Shp2a-Catalase fusion protein was essential to protect Shp2a from oxidation.

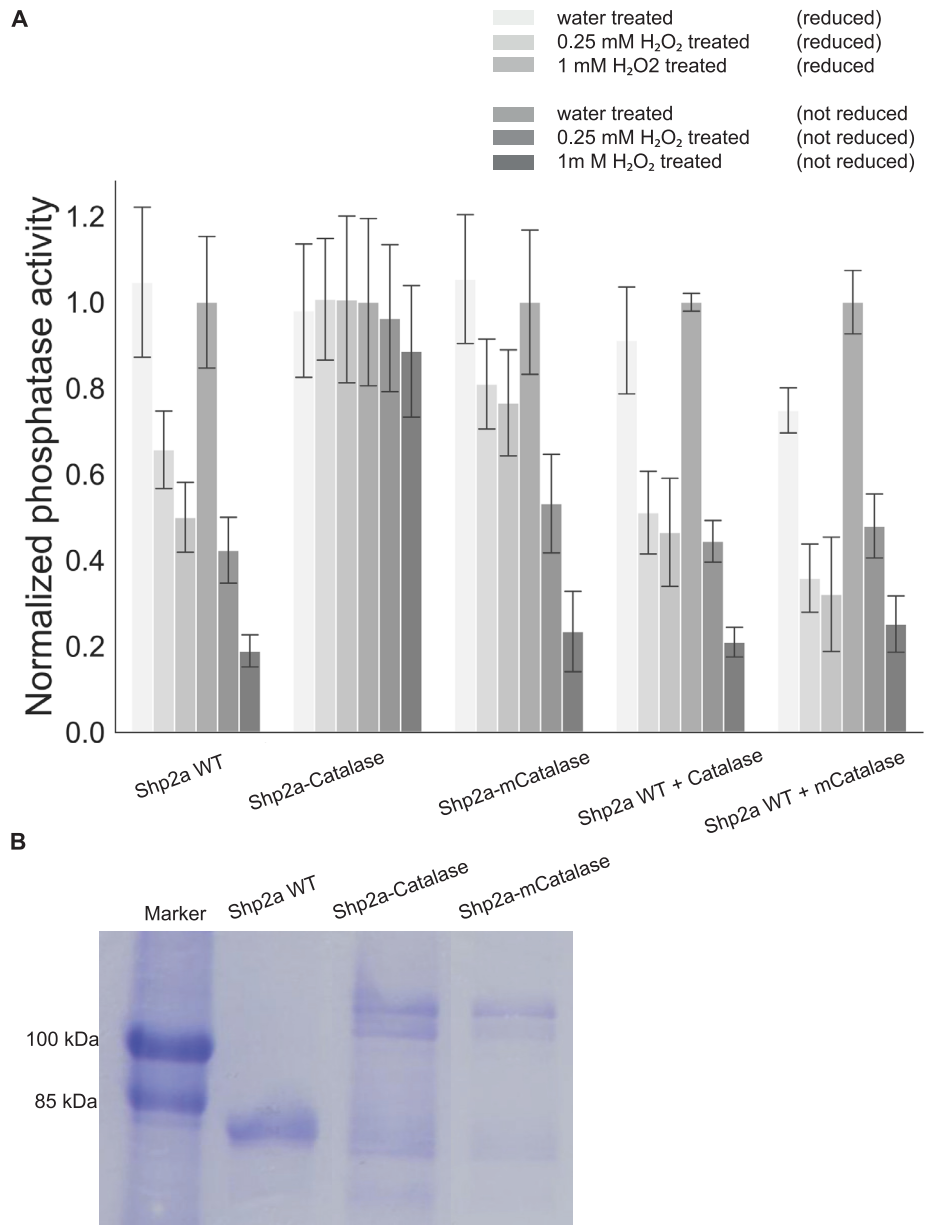

◂ Figure 3: Shp2a-Catalase maintains phosphatase activity upon treatment with H_2O_2 *in vitro*. A: Bacterially expressed Shp2a-WT, Shp2a-Catalase, Shp2a-mCatalase and mixtures of Shp2a with free Catalase or mCatalase were treated for 30 min. with milliQ (white), 0.25 mM H_2O_2 (light grey) or 1 mM H_2O_2 (dark grey). Half of the samples was reduced with DTT (lighter greys), which reactivated reversibly inactivated Shp2a. The other half of the samples (darker grey) was not reduced and hence only the non-oxidized Shp2a was active. Subsequently, PTP activity assays were done using *para*-nitrophenylphosphate for 30 min at 30˚C. Hydrolysis of para-nitrophenylphosphate was measured and normalized to the average phosphatase activity of the respective proteins in 0 mM H_2O_2, non-reduced condition. The difference in the activity between the reduced and the non-reduced bars indicates the fraction of Shp2a that was reversibly oxidized. The error bars indicate standard deviation. n = 3 B: Coomassie blue stained gel was imaged to show the size of the expressed proteins.

Shp2a oxidation level affects regeneration ability of zebrafish embryos

Oxidation-resistant Shp2a fusion proteins allowed us to investigate the role of Shp2a oxidation in vivo. It is well known that reactive oxygen species (ROS), including H_2O_2, are produced in response to wounding and that ROS are essential for regeneration in zebrafish (Gauron *et al.*, 2013; Niethammer *et al.*, 2009b; Yoo *et al.*, 2012). We have shown that Shp2a is oxidized in response to wounding and that Shp2a is required for normal caudal fin-fold regeneration in zebrafish embryos (Wu *et al.*, 2017). Zebrafish knock-out embryos lacking functional Shp2 do not regenerate their caudal fin-fold upon amputation. Expression of Shp2a rescues this defect. Catalytic activity of Shp2a is required, because expression of catalytically inactive Shp2a-R468M does not rescue regeneration in Shp2 knock-out embryos (Hale *et al.*, 2018).

We investigated the capacity of the Shp2a-Catalase fusions to rescue regeneration in Shp2 mutant embryos. As a control, we first injected wild type embryos with mRNA encoding free Catalase, Shp2a-Catalase, Shp2a, mCatalase or Shp2a-mCatalase. None of these affected caudal fin-fold regeneration in wild type embryos (Figure 4A,B).

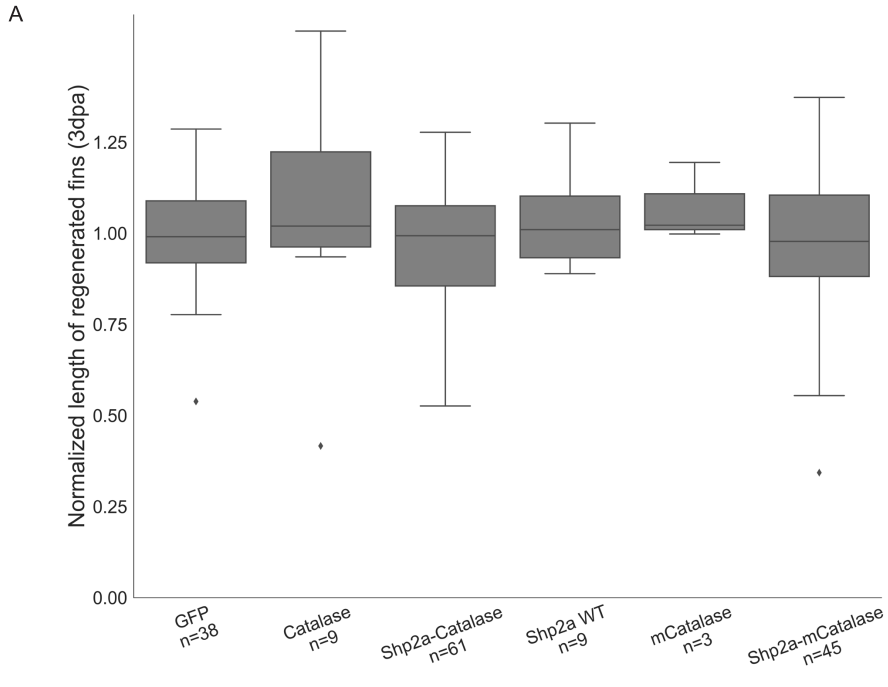

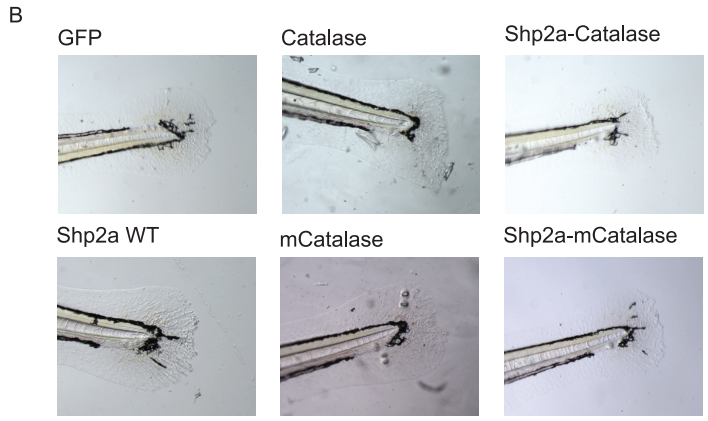

Figure 4 Injection of mRNA encoding Shp2a, (mutant) Catalase or fusion proteins does not affect tail fin-fold regeneration in control, WT embryos. A: Shp2a WT embryos were microinjected at the one-cell stage with constructs encoding proteins as indicated. The tail fin-fold was amputated at the base of the notochord 2 days post injection. The embryos were allowed to recover for three days and then the tail fin-folds were imaged. The length of the tail fins was measured from the tip of the notochord to the end of the tail fin. Lengths were normalized compared to the average length of the regenerated tail fin of WT embryos. Data from 5 experiments were collected. An ANOVA test indicated no significant differences in regeneration of the tail fin-fold between any of the microinjected embryos and control WT embryos. B: Representative pictures of the regenerated tail fins.

Next, we micro-injected embryos of an incross of Shp2a+/-Shp2b-/- fish at the one-cell stage with synthetic mRNA encoding Shp2a and fusion proteins. At 2dpi embryos were cut at the base of the tail fin-fold. Fish were allowed to recover for three days, which is sufficient time for wild type siblings to regenerate the amputated caudal fin-folds. Three days after amputation, regeneration was assessed and the genotype of the embryos was established by sequencing. As reported before, injecting mRNA encoding WT Shp2a largely rescued regeneration in Shp2 mutant embryos, whereas injection of mRNA encoding GFP did not (Figure 5 A,B). Shp2a-Catalase fusion protein did not rescue regeneration, in that no significant difference was detected between the length of the regenerated fins of Shp2a-Catalase injected embryos and GFP injected embryos. We verified correct micro-injection of all synthetic mRNAs and correct expression at 2 days post injection by assessment of GFP expression. All mRNAs encoded GFP fused to the target sequences via self-cleaving peptide 2A. The presence of GFP in all injected embryos indicated that the proteins were expressed as intended in all embryos (Figure 6). As a control, Shp2a WT was injected together with free Catalase, which rescued regeneration, like Shp2a by itself, i.e. no significant difference was observed between Shp2a by itself and Shp2a + Catalase (Figure 5A,B). There was a significant difference between Shp2a WT + free Catalase and Shp2a-Catalase fusion protein. This indicates that oxidation-resistant Shp2a-Catalase fusion protein did not rescue regeneration of the amputated tail fin-fold, and hence that apparently oxidation of Shp2a is required for normal regeneration of the caudal fin-fold.

As a control, we used Shp2a-mCatalase and free mCatalase. Shp2a-mCatalase was not protected from oxidation (Figure 1B, 2A). Microinjection of synthetic mRNA encoding Shp2a-mCatalase rescued caudal fin-fold regeneration significantly better than GFP, yet not as well as Shp2a by itself or Shp2a + free mCatalase (Figure 5A, B). Although it appeared that Shp2a-mCatalase rescued regeneration better than Shp2a-Catalase, the effect was not significantly different. It appeared that Shp2a-mCatalase had an intermediate effect. All in all, our data suggest that oxidation of Shp2a is required for normal regeneration of the caudal fin-fold in zebrafish embryos.

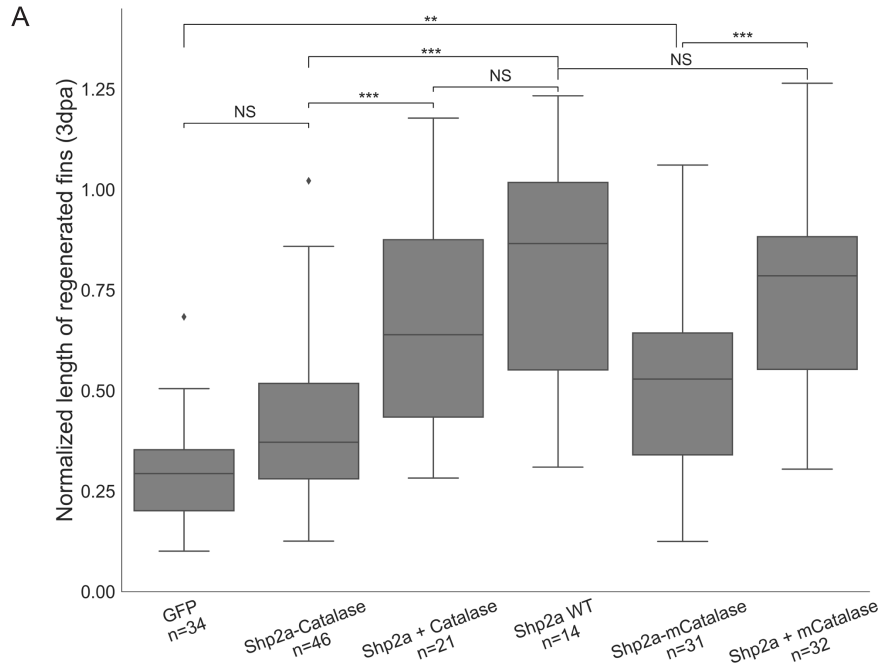

Figure 5: Shp2a-Catalase fusion protein does not rescue tail fin-fold regeneration in Shp2a KO embryos. A: Incrosses of Shp2a+/-Shp2b-/- fish were micro-injected with mRNA encoding the indicated proteins. The tail fin-fold of embryos was amputated 2 days post injection and the embryos were allowed to recover for three days. The tail fin-folds were imaged and the embryos were genotyped by sequencing. The length of the tail fin-folds of Shp2a-/-Shp2b-/- embryos was measured from the tip of the notochord to the end of the tail fin. Lengths were normalized compared to the average length of the regenerated tail fin of WT embryos. Data from 5 experiments were collected. The total number of embryos is indicated (n). A Tuckey post hoc test was performed to assess significant differences between categories, as an ANOVA test indicated that there were significant differences. The most relevant results from the Tuckey post hoc test are represented here(***, $p<0.001$; **, $p<0.01$; NS, not significant). B: Representative pictures of the regenerated tail fin-folds of injected Shp2a-/-Shp2b-/- embryos are shown.

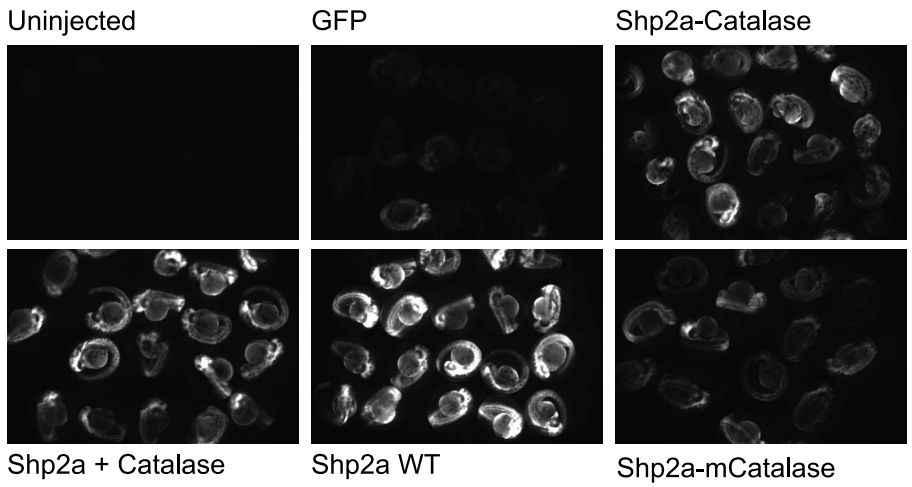

Figure 6: Successful micro-injection was monitored at 2 dpi. Representative pictures are shown of GFP expression at 2 days post injection with mRNA encoding the indicated proteins. The constructs encoded GFP by itself or GFP followed by a peptide 2A self-cleaving peptide and the indicated protein.

Discussion

We created a version of Shp2a that was resistant to oxidation, while it preserved its phosphatase activity. This Shp2a-Catalase fusion protein showed much less oxidation *in vitro* and its phosphatase activity remained around 95% after treatment with H_2O_2. This was in stark contrast with the control Shp2a-mCatalase, which was oxidized up to 80% and its activity decreased to 25%. *In vivo* we show that Shp2a-Catalase did not efficiently rescue tail fin regeneration in zebrafish embryos. This shows for the first time that oxidation of Shp2a in response to amputation was required for the function of Shp2a in regeneration. Previously, we had already shown that Shp2a becomes oxidized in response to caudal fin amputation (Wu *et al.*, 2017) and that Shp2a catalytic activity is required for regeneration (Hale *et al.*, 2018). Our current data put an end to the apparent paradox that Shp2a catalytic activity is required and Shp2a is oxidized, which inhibits its activity. Apparently, Shp2a is required for regeneration and needs to be inactivated transiently by oxidation for normal regeneration. It is possible that a negative feedback-loop of downstream signaling, e.g. the MAPK pathway, is transiently inhibited by inhibition of Shp2a, which in turn results in a strong boost in MAPK activity later on. In the case of Shp2a-Catalase, Shp2a activity remains high, the negative feedback loop remains active and there is no strong boost of activity later on. It is unlikely that Shp2a has a phosphatase-independent scaffolding role as an adaptor protein in regeneration, because phosphatase activity is required for regeneration. The exact mechanism underlying downstream signaling of transiently oxidized Shp2a remains to be determined.

We used Shp2a-mCatalase, which is not resistant to oxidation by H_2O_2 as a control. Whereas expression of Shp2a-mCatalase induced a significant increase in the length of regenerated tail fins compared to GFP injected embryos, there was no significant difference in regeneration of the caudal fin-fold compared to expression of oxidation-resistant Shp2a-Catalase. Catalase forms tetramers. A possible explanation for the observed partial rescue of Shp2a-mCatalase is that Shp2a-mCatalase may form heterotetramers with endogenous wild type Catalase, which is abundantly expressed. That way, Shp2a-mCatalase may be partially resistant to oxidation, due to wild type Catalase in the complex, which quenches H_2O_2 in the vicinity.

Of course, the Shp2a-Catalase complex is much larger than WT Shp2a by itself and there is previous data indicating that the specific localization of Shp2a in the cell is important for its function. However, Shp2a-mCatalase partially rescued loss of Shp2a in regeneration. We consider that this partial rescue of regeneration of the tail fin is a strong indicator that the localization of Shp2a-Catalase/Shp2a-mCatalase is not blocking its function.

The nature of the exact ROS molecule that oxidizes PTP's *in vivo* is still unknown. There is data that indicates that the molecule should be small enough to enter the catalytic site, since bigger oxidants fail to oxidize certain PTPs (Denu & Tanner, 1998). For example, SHP2 is oxidized by exogenous H_2O_2, which correlates with an increase in MAPK phosphorylation in cells (T.-C. Meng *et al*., 2002). In contrast, treatment with tert-Butyl hydroperoxide, which is a bigger molecule than H_2O_2, hardly affects SHP2 oxidation and MAPK phosphorylation (T. C. Meng *et al*., 2002). Yet, purified peroxidized lipid 15-HETE oxidizes the PTPs SHP1, PTP-H1 and TC-PTP *in vitro* more efficiently than H_2O_2 (Conrad *et al*., 2010). Perhaps lipids are flexible or narrow enough to reach the catalytic cysteine. It has been proposed that oxidation by H_2O_2 may be too slow to play an extensive role *in vivo* and superoxide may be responsible for oxidation of PTPs (F.-G. Meng & Zhang, 2013). Yet, amputation of the caudal fin-fold of zebrafish in particular induces the production of H_2O_2 (Niethammer *et al*., 2009b) and under these conditions, PTPs are oxidized. Moreover, it was shown that only the H_2O_2 producing NOX is necessary for H_2O_2 gradient in response to wounding (Niethammer *et al*., 2009b).

Subcellular localization of PTPs and ROS-producing proteins may be the explanation for how H_2O_2 can oxidize its targets. SHP2 localizes to specific endosomes in a complex named the redoxosome, where both the ROS producing proteins as well as the oxidation targets are localized together (Tsutsumi *et al*., 2017). Hence, the concentration of locally produced H_2O_2 may be high enough to generate the required speed of oxidation, or perhaps superoxide and H_2O_2 work in tandem to oxidize PTPs in redoxosomes. In summary, we consider H_2O_2 to be one of the main oxidants of PTPs *in vivo,* which is in line with our finding that the fusion of Shp2a with catalase protects Shp2a against oxidation.

To conclude, we have shown that oxidation of Shp2a plays an essential role in its function during tail fin-fold regeneration in zebrafish embryos. We believe that our results provide a strong indication that oxidation of Shp2 in response to the burst of ROS that is produced upon amputation, is the start signal for regeneration. Fusion of Catalase could be useful to test the role of oxidation of many more PTPs and other proteins. We believe that research along those lines could shed more light on the role of oxidation in signaling pathways.

Literature list

Bonetti, M., Rodriguez-Martinez, V., Paardekooper Overman, J., Overvoorde, J., van Eekelen, M., Jopling, C., & Hertog, J. den. (2014). Distinct and Overlapping Functions of ptpn11 Genes in Zebrafish Development. *PLoS ONE*, *9*(4), e94884. https://doi.org/10.1371/journal.pone.0094884

Carbonell-M, B., Zapata Cardona, J., & Delgado, J. P. (2022). Post-amputation reactive oxygen species production is necessary for axolotls limb regeneration. *Frontiers in Cell and Developmental Biology*, *0*, 1690. https://doi.org/10.3389/FCELL.2022.921520

Conrad, M., Sandin, Å., Förster, H., Seiler, A., Frijhoff, J., Dagnell, M., Bornkamm, G. W., Rådmark, O., Van Huijsduijnen, R. H., Aspenström, P., Böhmer, F., & Östman, A. (2010). 12/15-Lipoxygenase-derived lipid peroxides control receptor tyrosine kinase signaling through oxidation of protein tyrosine phosphatases. *Proceedings of the National Academy of Sciences of the United States of America*, *107*(36), 15774–15779. https://doi.org/10.1073/PNAS.1007909107/-/DCSUPPLEMENTAL

Denu, J. M., & Tanner, K. G. (1998). Specific and reversible inactivation of protein tyrosine phosphatases by hydrogen peroxide: Evidence for a sulfenic acid intermediate and implications for redox regulation. *Biochemistry*, *37*(16), 5633–5642. https://doi.org/10.1021/BI973035T/ASSET/IMAGES/LARGE/BI973035TH00002.JPEG

Gauron, C., Rampon, C., Bouzaffour, M., Ipendey, E., Teillon, J., Volovitch, M., & Vriz, S. (2013). Sustained production of ROS triggers compensatory proliferation and is required for regeneration to proceed. *Scientific Reports*, *3*(1), 2084. https://doi.org/10.1038/srep02084

Hale, A. J., & den Hertog, J. (2016). Studying Protein-Tyrosine Phosphatases in Zebrafish. *Methods in Molecular Biology (Clifton, N.J.)*, *1447*, 351–372. https://doi.org/10.1007/978-1-4939-3746-2_19

Hale, A. J., & den Hertog, J. (2018). Shp2-Mitogen-Activated Protein Kinase Signaling Drives Proliferation during Zebrafish Embryo Caudal Fin Fold Regeneration. *Molecular and Cellular Biology*, *38*(4), e00515-17. https://doi.org/10.1128/MCB.00515-17

Hayashi, S., Nakazaki, Y., Kagii, K., Imamura, H., & Watanabe, Y. H. (2017). Fusion protein analysis reveals the precise regulation between Hsp70 and Hsp100 during protein disaggregation. *Scientific Reports 2017 7:1*, *7*(1), 1–14. https://doi.org/10.1038/s41598-017-08917-8

Meng, F.-G., & Zhang, Z.-Y. (2013). Redox regulation of protein tyrosine phosphatase activity by hydroxyl radical. *Biochimica et Biophysica Acta (BBA) - Proteins and Proteomics*, *1834*(1), 464–469. https://doi.org/10.1016/j.bbapap.2012.06.018

Meng, T.-C., Fukada, T., & Tonks, N. K. (2002). Reversible oxidation and inactivation of protein tyrosine phosphatases in vivo. *Molecular Cell*, *9*(2), 387–399. http://www.ncbi.nlm.nih.gov/pubmed/11864611

Meng, T. C., Fukada, T., & Tonks, N. K. (2002). Reversible Oxidation and Inactivation of Protein Tyrosine Phosphatases In Vivo. *Molecular Cell*, *9*(2), 387–399. https://doi.org/10.1016/S1097-2765(02)00445-8

Niethammer, P., Grabher, C., Look, A. T., & Mitchison, T. J. (2009a). A tissue-scale gradient of hydrogen peroxide mediates rapid wound detection in zebrafish. *Nature*, *459*(7249), 996–999. https://doi.org/10.1038/nature08119

Niethammer, P., Grabher, C., Look, A. T., & Mitchison, T. J. (2009b). A tissue-scale gradient of hydrogen peroxide mediates rapid wound detection in zebrafish. *Nature*, *459*(7249), 996–999. https://doi.org/10.1038/nature08119

Solman, M., Blokzijl-Franke, S., Piques, F., Yan, C., Yang, Q., Strullu, M., Kamel, S. M., Ak, P., Bakkers, J., Langenau, D. M., Cavé, H., & Den Hertog, J. (2022). Inflammatory response in hematopoietic stem and progenitor cells triggered by activating SHP2 mutations evokes blood defects. *ELife*, *11*. https://doi.org/10.7554/ELIFE.73040

Solman, M., Woutersen, D. T. J., & den Hertog, J. (2022). Modeling (not so) rare developmental disorders associated with mutations in the protein-tyrosine phosphatase SHP2. *Frontiers in Cell and Developmental Biology*, *10*, 1046415. https://doi.org/10.3389/FCELL.2022.1046415/BIBTEX

Tsutsumi, R., Harizanova, J., Stockert, R., Schröder, K., Bastiaens, P. I. H., & Neel, B. G. (2017). Assay to visualize specific protein oxidation reveals spatio-temporal regulation of SHP2. *Nature Communications*, *8*(1). https://doi.org/10.1038/s41467-017-00503-w

Westerfield, M. (2000). *The Zebrafish Book: A Guide for the Laboratory Use of Zebrafish (Danio Rerio)* (4th ed.). Universitu of Oregon Press. https://books.google.nl/books/about/The_Zebrafish_Book.html?id=Iy8PngEACAAJ&redir_esc=y

Wu, W., Hale, A. J., Lemeer, S., & den Hertog, J. (2017). Differential oxidation of protein-tyrosine phosphatases during zebrafish caudal fin regeneration. *Scientific Reports*, *7*(1), 8460. https://doi.org/10.1038/s41598-017-07109-8

Yang, W., Klaman, L. D., Chen, B., Araki, T., Harada, H., Thomas, S. M., George, E. L., & Neel, B. G. (2006). An Shp2/SFK/Ras/Erk signaling pathway controls trophoblast stem cell survival. *Developmental Cell*, *10*(3), 317–327. https://doi.org/10.1016/J.DEVCEL.2006.01.002

Yoo, S. K., Freisinger, C. M., LeBert, D. C., & Huttenlocher, A. (2012). Early redox, Src family kinase, and calcium signaling integrate wound responses and tissue regeneration in zebrafish. *The Journal of Cell Biology*, *199*(2), 225–234. https://doi.org/10.1083/jcb.201203154

Acknowledgements

The authors would like to thank the animal caretakers at the Hubrecht Institute for excellent care of the zebrafish.

Author contributions

Conceptualization: M.A., J.H., N.L., J.d.H., S.M.; Methodology: M.A,J.H., N.L. J.d.H., S.L.; Validation: M.A., N.L.; Formal analysis: M.A., N.L.; Investigation: M.A., J.H., N.L.; Resources: M.A.,J.H., N.L., J.d.H., S.L.; Data curation: M.A., N.L.; Writing – original draft: M.A., J.d.H.; Writing - review & editing: M.A., J.d.H.; Visualization: M.A., N.L.; Supervision: J.d.H., S.L.; Project administration: J.d.H., S.L.; Funding acquisition: J.d.H, S.L..

Funding

This work was funded in part by a grant from the Dutch Research Council to J.d.H. (ALW OP.234).

Summarizing discussion

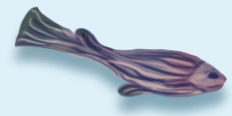

Summarizing discussion

It has been shown in many different species that a burst of Reactive Oxygen Species (ROS) is produced upon injury. This burst of ROS plays an important role in wound healing and regeneration (Carbonell-M *et al*., 2022; Ferreira *et al*., 2016; Gauron *et al*., 2013; Hunter *et al*., 2018; Love *et al*., 2013; Niethammer *et al*., 2009; Pirotte *et al*., 2015; Roy *et al*., 2006). However, it is not extensively known how ROS functions to promote regeneration. While one of the functions of the ROS gradient is to attract macrophages to the wound, this is not enough to explain the extensive role of the ROS burst in regeneration. We hypothesized that the ROS could start a signaling cascade by oxidizing Protein Tyrosine Phosphatases (PTPs).

PTPs are a family of proteins that all share a conserved active site with a catalytic cysteine that has a low pKa and is therefore highly susceptible to oxidation (Denu & Tanner, 1998; Meng *et al*., 2002; Östman *et al*., 2011; Peters *et al*., 1998). Previously, eight PTPs were identified that are specifically oxidized in response to amputation of the tail fin of adult zebrafish (Wu *et al*., 2017). One of these PTPs, Shp2a, is essential for regeneration of the caudal fin-fold in zebrafish embryos (Hale & den Hertog, 2018). The work described in this thesis contributes to the knowledge concerning the role of PTPs in zebrafish development and regeneration. We describe that regeneration was not affected by Crispr-CAS9 mediated knockout of the identified PTPs or their paralogs, unlike the Shp2a knockout. However, we did find that a knockout of *ptpn4a* led to a juvenile growth defect and deadly seizures in the majority of the population, while a knockout of *ptpn6* led to excessive inflammation and complete lethality. In addition, we found that inhibition of the oxidation of Shp2a upon injury diminished regeneration. Below we discuss our major findings.

A panel of PTP knock-out lines does not show defects during regeneration or embryonic development

A mass spectrometry-based screening method of the oxidation status of PTPs before and after amputation of the caudal fin in zebrafish, led to the identification of eight PTPs that are specifically oxidized in response to amputation. These PTPs are Shp2a (*ptpn11a*), Shp2b (*ptpn11b*), Ptp1b (*ptpn1*), TC-Ptpa (*ptpn2a*), PTP-Meg1b (*ptpn4b*), PTP-Meg2a (*ptpn9a*), Ptpεa (*ptpr εa)* and Sap1 (*ptprh1*) (Wu *et al*., 2017). In **chapter 2** we describe the investigation of zebrafish lacking the function of *ptpn1*, *ptpn2a*, *ptpn2b*, *ptpn4a*, *ptpn4b*, *ptpn9a*, *ptpn9b*, *ptpr*εa, *ptpr εb*, *ptprh1* and *ptprh2*. We also investigated double and triple mutants lacking several combinations of paralogs. None of these mutant lines showed defects in regeneration of the caudal fin-fold. In addition, the only line that showed developmental defects was the *ptpn4a* mutant line. The other mutant lines showed

no mortality or morphological defects. We showed that the introduced premature stopcodons in *ptpn2a, ptpn2b* and *ptpng9b* induced nonsense-mediated decay, as the level of targeted mRNA transcripts was lower in the mutant zebrafish compared to their WT siblings (Nickless *et al*., 2017). However, the other lines showed no evidence of nonsense-mediated decay, with one line from *ptpn4b* and one line from *ptprh2* even showing a strong upregulation of the affected mRNA transcript.

We did not recapitulate all the phenotypes we expected based on previous results with mouse mutants or transient knockdowns of the target PTPs. The most clear example of this is the *ptpn2a-/- ptpn2b -/-* mutant line, where we expected a strong effect on the differentiation of T-cells, based on the mouse *Ptpn2-/-* line (Pike *et al*., 2017; Wiede *et al*., 2012, 2014). Instead we found no effect on T-cell development in the *ptpn2a-/- ptpn2b-/-* line. We believe this is possibly caused by transcriptional adaptation, a process during which fragments of the decayed mRNA transcript bind to similar genes and cause their upregulation, thereby compensating for the loss of the original mRNA (El-Brolosy *et al*., 2019). This hypothesis is supported by the fact that we found evidence that the mRNA transcripts of *ptpn2a* and *ptpn2b* were affected by nonsense-mediated decay. Hence, the mRNA fragments might cause compensation by binding to similar genes and upregulating their expression. In mice, it has been shown that upregulation of *Ptpn23* compensates for the loss of *Ptpn2* in intestinal cells (Ulugöl *et al*., 2019). It would be highly interesting to investigate if in zebrafish, PTPs can compensate for the loss of other PTPs in a similar manner. This compensation might occur in the entire organism, but it is a strong possibility that the exact genes that cause compensation differ between different cell types. After all, PTPs are differentially expressed and the exact signaling pathways and roles of the PTPs often differ between different cell types, and PTPN2 has been implicated in multiple signaling pathways *in vitro* (Shields *et al*., 2008; Simoncic *et al*., 2002; ten Hoeve *et al*., 2002).

We also expected a phenotype in the *ptpn9a* mutant line. Based on previous results by *in vitro* inhibition of PTPN9 and a transient knockdown of *ptpn9a* by morpholinos (Bu *et al*., 2014; Xu *et al*., 2003), we expected to find a reduced number of red blood cells in the *ptpn9a* mutant line. We did not see this expected effect in our *ptpn9a* mutant line, but neither did we find evidence for nonsense-mediated decay of *ptpn9a* mRNA transcripts. This could indicate that there are other methods of genetic compensation at play.

Knock-out of Ptpn4a causes lethal neurological defects late during development in zebrafish

In **chapter 3** we further described the developmental defects in the *ptpn4a-/-* zebrafish line. We showed that zebrafish with a specific loss-of-function mutation in *ptpn4a* displayed no morphological defects at 5dpf, but 90% did not survive beyond the juvenile stage. The mutant zebrafish were smaller than their WT siblings until they were 7 weeks old. However, the minority of mutant zebrafish that survived their juvenile weeks, caught up with their WT siblings in length and displayed normal adulthood and fertility.

We were not able to definitively prove the exact cause of death, but we have observed several *ptpn4a-/-* fish undergoing an epileptic-like seizure, always followed by death. We did not observe these seizures in their WT siblings, nor did we observe a zebrafish undergoing a seizure and survive. Therefore, we believe these seizures were the cause of death for the majority of the *ptpn4-/-* zebrafish. It is highly interesting that these seizures and mortality only occurred during the juvenile stage. It indicates that in zebrafish, the role of Ptpn4a in brain development is essential during the juvenile stage. This corresponds partly to the observations in human patients, since in at least a couple human patients the first symptoms developed after their first birthday, indicating that Ptpn4 is not yet essential directly after birth (Williamson *et al*., 2015). On the other hand, *PTPN4* has a high Loss-of-Function (LoF) intolerance, as there are less LoF mutations present in the normal population than you would expect (Lek *et al*., 2016). This could indicate that a fraction of the embryos/fetuses with *PTPN4* mutations do not reach the end of pregnancy, which suggests that Ptpn4 could be highly important during early human development too.

Furthermore, in human patients we can make a distinction between patients with *PTPN4* LoF mutations and patients with missense mutations. As far as we know now, patients with LoF mutations in *PTPN4* are in the 1st or 2nd percentile for height and undergo epileptic seizures (Chmielewska *et al*., 2021). This corresponds to the symptoms in our zebrafish line with a LoF mutation in *ptpn4a*. On the other hand, patients with missense mutations often do not show these symptoms. However, they do show intellectual disability. Two of these patients have a missense mutation in *PTPN4* in the FERM domain (L72S and G239A, respectively). These mutations prevent the correct localization of Ptpn4 to the dendritic spines of neuronal cells *in vitro* (Chmielewska *et al*., 2021; Szczałuba *et al*., 2018). This suggests that correct localization of Ptpn4 to the synapses of neurons is essential for correct neurological development. This is further corroborated by the observation thatin RETT syndromethe dendritic spines are also affected (Chapleau *et al*., 2009, 2012; Landi *et al*., 2011). Since *PTPN4* is a target of the transcription factor MECP2, which is the main gene causing RETT syndrome, this strengthens the relation between correct *PTPN4* expression and correct dendritic spines.

To summarize, from our data and data previously published, we conclude that Ptpn4 is essential for correct neurological development. LoF mutations in *PTPN4 / ptpn4a* result in epileptic seizures and growth deficiency in the toddler (human) / juvenile (zebrafish)

stage. In human patients, missense mutations in *PTPN4* result in intellectual disability, most likely because Ptpn4 fails to correctly localize to the dendritic spines. In addition, mutations in *PTPN4 may* result in miscarriages, as evidenced by the high LoF intolerance.

The exact target and pathway in which *Ptpn4a* functions to affect body growth and prevention of epileptic seizures are still unknown and it would be highly interesting to investigate this further. While the target of *Ptpn4a* at the synapses is identified as the NMDAR subunits GluN2A and GluN2B (Espinoza *et al*., 2020), it is likely that the growth deficiency, and possibly also the seizures, are due to the role of *Ptpn4a* in another pathway.

Surprisingly, a second line with a different LoF mutation in *ptpn4a* showed no mortality or growth defects initially. We investigated if this line had other PTPs up- or downregulated to compensate for the loss of *Ptpn4a* and found an upregulation of *ptpn2a* in the *ptpn4a* line 2. Interestingly, *ptpn2a* was downregulated in the *ptpn4a* line 1. We were interested to combine the *ptpn4a-/-* line 2 with a knock-out of *ptpn2a*, but when we did those experiments, we found that the original *ptpn4a-/-* line 2 had lost the ability to compensate for the loss of *ptpn4a* and now also showed mortality in the juvenile stage. Furthermore, the offspring of the surviving adults of *ptpn4a-/-* line 1 showed a strongly decreased mortality. Loss of genetic pressure, like in the heterozygous *ptpn4a+/-* line 2, may lead to loss of genetic compensation. Together, these observations indicate that zebrafish can compensate for the loss of *ptpn4a*, but that this compensation is not static but variable.

Loss of Shp1 impairs myeloid cell function and causes lethal inflammation in zebrafish larvae

In **chapter 4** we show that zebrafish with a knock-out of *ptpn6* displayed a fully penetrant phenotype and complete mortality in the late larval stage. The mutant larvae grew to be smaller, skinnier and curved compared to their WT siblings during the larval stage. They developed lethal hyperinflammation, characterized by skin lesions and strong neutrophil infiltration of the gills. It is interesting to note that there are differences between the phenotypes caused by the genetic knock-out and a previously performed morpholino-mediated knockdown. Zebrafish with a morpholino-mediated knockdown of Shp1, the protein product of the *ptpn6* gene, present with stronger and earlier defects than the genetic knock-out (Kanwal *et al*., 2013). Even so, the kind of symptoms in the genetic knock-out and the morpholino mediated knockdown are highly similar, indicating that the symptoms are specifically caused by the deletion of functional Shp1. One possibility is that the symptoms arise earlier in

the morpholino mediated knockdown. Splice site-directed morpholinos block splicing and ATG-directed morpholinos block translation, both resulting in an instantaneous block of protein production. The genetic knock-out is not instantaneous, because there is still maternal *ptpn6* mRNA present, which may be translated, resulting in protein production. Therefore, the effects of the genetic knock-out may lag behind the morpholino-mediated knockdown. Another explanation for the observed difference is that the morpholinos may induce a general inflammatory response, which may worsen the inflammation caused by the loss of Shp1.

The phenotype of the *ptpn6* knockout zebrafish is very similar to the *motheaten* appearance and lethal pneumonitis found in *motheaten* mice (Green and Shultz, 1975; Jiao *et al*., 1997). It also supports the sporadic cases of humans that present with mutations in *PTPN6,* which have been associated with neutrophilic dermatoses, and emphysema (Nesterovitch *et al*., 2011; Bossé *et al*., 2019). These observations support the notion that our *ptpn6* knockout zebrafish model is ideal to study the effect of loss of Shp1 during embryonic development.

We show that the number of emerging HSPCs was reduced in *ptpn6* mutants, which was compensated by increased proliferation of HSPCs later on. These observations are corroborated by the finding that knock-out of Shp1 in HSPCs causes enhanced proliferation in mouse embryos (Jiang *et al*., 2018). This is in contrast with an earlier report that found no effect of loss of Shp1 on HSPCs in mice, but we believe the authors might have missed the effect due to the enhanced proliferation that compensates for the reduced number of emerging HSPCs (Shultz *et al*., 1983).

We also show an increased number of macrophages and a decreased number of neutrophils in the *ptpn6* knockout zebrafish. An increased number of macrophages has also been reported in mice lacking SHP1 on several occasions and in several manners (McCoy *et al*., 1982, 1983; Nakayama *et al*., 1997; Paling & Welham, 2005). The increased number of macrophages therefore seems to be a consistent effect of loss of Shp1. It could be the result of the same mechanism that causes enhanced proliferation of HSPCs. However, the reduced number of neutrophils might indicate a skewing of the development of HSPCs towards macrophages and away from neutrophils. The reduced number of neutrophils has not been reported in mice lacking SHP1. It would be highly interesting to compare the neutrophil development in mice lacking SHP1 with zebrafish lacking Shp1. This could shed light on the question if the enhanced number of macrophages always comes at a loss of the number of neutrophils, or if the reduced number of neutrophils is a free-standing effect of Shp1 loss.

Finally, we also show that the directional migration of macrophages and neutrophils is affected upon wounding of the zebrafish larvae. The meandering index of neutrophils was strongly reduced, indicating that the neutrophils struggle to migrate towards the target. This could be due to increased neutrophil adhesion, as reported in motheaten mice lacking functional SHP1 (Stadtmann *et al.*, 2015). For macrophages, both the meandering index and the wound persistence were reduced. It was surprising that we found a lower number of macrophages at the wound edge in *ptpn6* mutant zebrafish, as there is an increased number of macrophages present in the embryo as a whole. However, macrophages were located primarily in the anterior region of the embryo. The reduced wound persistence and the strong anterior localization of the macrophages might indicate affected cell adhesion in the macrophages. It would be highly interesting to investigate this further, as the behaviour of neutrophils and macrophages may play a major role in the development of hyperinflammation and lethal pneumonitis.

Oxidation of Shp2a is essential for its function during caudal fin-fold regeneration

Finally, we were interested in further investigation of Shp2a, which was shown previously to be essential for regeneration of the caudal fin-fold of zebrafish embryos (Hale & den Hertog, 2018). In **chapter 5** we describe a fusion protein consisting of Shp2a and Catalase, linked by a flexible linker. We show that Catalase protected Shp2a from oxidation by H_2O_2 *in vitro*, and that this protection resulted in persistent Shp2a activity under oxidizing conditions. We show that the fusion protein Shp2a-Catalase was not able to efficiently rescue regeneration in zebrafish embryos lacking functional Shp2a. Since the Shp2a-Catalase fusion displayed catalytic activity, the inability of the Shp2a-Catalase fusion to rescue loss of Shp2 in zebrafish embryos, could not be explained by the suggestion that Shp2a-Catalase did not dephosphorylate its targets due to the link with Catalase.

Perhaps the Shp2a-Catalase complex did not localize to the correct position in the cell for Shp2a function, as it has been shown that Shp2a localizes to very specific redoxosomes (Tsutsumi *et al.*, 2017). To control for this, we generated a Shp2a-Catalase fusion protein with a mutation in Catalase, mCatalase, that does not affect its structure, but does abolish all Catalase activity. The Shp2a-mCatalase fusion was catalytically active and was susceptible to oxidation, like wild type Shp2a. We show that this Shp2a-mCatalase protein complex was able to partially rescue regeneration, indicating that Shp2a likely localized to the correct subcellular location and was able to perform its essential role in the signaling pathway, despite the fusion of mCatalase.

Since the lack of rescue by Shp2a-Catalase was apparently not due to a lack of Shp2a catalytic activity or due to Catalase preventing correct localization of Shp2a, we conclude that temporary oxidation-mediated inactivation of Shp2a is essential for its role during regeneration. Prevention of oxidation of Shp2a during regeneration by the attached Catalase abolished the rescue ability of the Shp2a protein. This observation solves the apparent paradox that was present until now, as it is known that catalytic activity of Shp2a is essential for regeneration, but also that Shp2a becomes oxidized (inactivated) during regeneration. We hypothesize that transient oxidation of Shp2a is necessary to suppress a negative feedback-loop of downstream signaling, e.g. the MAPK pathway, which in turn results in a strong boost in MAPK activity later on. We believe it would be highly interesting to investigate the downstream signaling using our Shp2a-Catalase protein, as this may shed light on the exact signaling pathway that is essential for regeneration.

Concluding remarks

It has been shown in many different species that a burst of ROS is produced upon injury. We hypothesized that the ROS could start a signaling cascade by oxidizing PTPs. In chapter 2 we describe how we generated zebrafish knockouts of 6 PTPs that were shown previously to be oxidized upon amputation of the caudal fin and their paralogs. We show that these PTPs were not essential for regeneration. In addition, we did not recapitulate all the phenotypes we expected based on previous results with mouse mutants or transient knockdowns of the target PTPs. We hypothesize that this is due to genetic compensation.

In chapter 3 we describe our investigation of zebrafish with a knockout of *ptpn4a*. We show that the majority of the mutant zebrafish died at the juvenile stage and suffered from epileptic seizures. This corresponds to human patients who suffer from intellectual disability and epileptic seizures due to nonsense mutations in *PTPN4*. We show that a minority of the mutant zebrafish compensated for the loss of Ptpn4a and survived, but also that a separate knockout line lost its compensation ability over time and showed enhanced lethality at the juvenile stage.

In chapter 4 we describe our investigation of zebrafish with a knockout of *ptpn6*. We show that these mutant zebrafish displayed fully penetrant mortality at the larval stage and died from lethal hyperinflammation. This corresponds to the phenotype of the *motheaten* mice lacking Shp1 and human patients suffering from neutrophilic dermatoses and emphysema. We show that loss of Shp1 led to a reduced number of emerging HSPCs, increased HSPC proliferation, an increased number of macrophages and a decreased number of neutrophils. In addition, we show that loss of Shp1 affected the behavior of neutrophils and macrophages and led to reduced directional migration upon wounding.

In chapter 5 we describe how we investigated the role of oxidation of Shp2a during regeneration, by creating a fusion protein consisting of Shp2a linked with Catalase. Due to the close vicinity, the Catalase protected Shp2a from oxidation. We show that by inhibiting oxidation of Shp2a, we inhibited regeneration. This indicates that transient oxidation of Shp2a is an essential step in the signaling cascade that results in regeneration. This research puts an end to the apparent paradox that Shp2a is oxidized during regeneration, but that catalytic activity of Shp2a is essential for regeneration to proceed. We hypothesize that transient oxidation of Shp2a leads to a reduction of a negative feedback loop, resulting in increased signaling activity once Shp2a is reduced again. On the other hand, it would also be possible that Shp2a needs to be inactive to allow for correct signaling during this specific time period to induce regeneration. It would be highly interesting to investigate which signaling pathways are affected by the Shp2a-Catalase fusion protein.

Recently, genetic compensation has been gaining attention as a mechanism for knock-out lines to compensate for the loss-of-function of the target protein. This has caused experiments to result in non-reproducible effects or understatement of the importance of certain proteins. Several papers have been published about this phenomenon (El-Brolosy *et al*., 2019; Salanga & Salanga, 2021). We believe genetic compensation has also affected the results we generated in chapters 2 and 3, resulting in the lack of phenotypes in mutant zebrafish. On the other hand, the results we generated in chapter 4 and 5 show that genetic knockouts can still be a very strong tool in investigating the effect of the loss of a particular protein. More research is needed to unravel the mechanism of genetic compensation, which in the future will allow to determine if a lack of phenotype is due to genetic compensation or because the target protein is simply not essential. In this respect, it would be highly interesting to investigate humans carrying lethal mutations who do not show any disease symptoms. For instance, 13 humans were identified in 2016 carrying mendelian mutations that should have caused severe illness (Chen *et al*., 2016). It would be interesting to analyze these patients in depth for genetic compensation mechanisms.

Literature list

Bu, Y., Su, F., Wang, X., Gao, H., Lei, L., Chang, N., Wu, Q., Hu, K., Zhu, X., Chang, Z., Meng, K., & Xiong, J.-W. (2014). Protein tyrosine phosphatase PTPN9 regulates erythroid cell development through STAT3 dephosphorylation in zebrafish. *Journal of Cell Science*, *127*(Pt 12), 2761–2770. https://doi.org/10.1242/jcs.145367

Carbonell-M, B., Zapata Cardona, J., & Delgado, J. P. (2022). Post-amputation reactive oxygen species production is necessary for axolotls limb regeneration. *Frontiers in Cell and Developmental Biology*, *0*, 1690. https://doi.org/10.3389/FCELL.2022.921520

Chapleau, C. A., Boggio, E. M., Calfa, G., Percy, A. K., Giustetto, M., & Pozzo-Miller, L. (2012). Hippocampal CA1 Pyramidal Neurons of Mecp2 Mutant Mice Show a Dendritic Spine Phenotype Only in the Presymptomatic Stage. *Neural Plasticity*, *2012*. https://doi.org/10.1155/2012/976164

Chapleau, C. A., Calfa, G. D., Lane, M. C., Albertson, A. J., Larimore, J. L., Kudo, S., Armstrong, D. L., Percy, A. K., & Pozzo-Miller, L. (2009). Dendritic spine pathologies in hippocampal pyramidal neurons from Rett syndrome brain and after expression of Rett-associated MECP2 mutations. *Neurobiology of Disease*, *35*(2), 219–233. https://doi.org/10.1016/J.NBD.2009.05.001

Chen, R., Shi, L., Hakenberg, J., Naughton, B., Sklar, P., Zhang, J., Zhou, H., Tian, L., Prakash, O., Lemire, M., Sleiman, P., Cheng, W. Y., Chen, W., Shah, H., Shen, Y., Fromer, M., Omberg, L., Deardorff, M. A., Zackai, E., … Friend, S. H. (2016). Analysis of 589,306 genomes identifies individuals resilient to severe Mendelian childhood diseases. *Nature Biotechnology*, *34*(5), 531–538. https://doi.org/10.1038/NBT.3514

Chmielewska, J. J., Burkardt, D., Granadillo, J. L., Slaugh, R., Morgan, S., Rotenberg, J., Keren, B., Mignot, C., Escobar, L., Turnpenny, P., Zuteck, M., Seaver, L. H., Ploski, R., Dziembowska, M., Wynshaw-Boris, A., & Adegbola, A. (2021). PTPN4 germline variants result in aberrant neurodevelopment and growth. *Human Genetics and Genomics Advances*, *2*(3), 100033. https://doi.org/10.1016/J.XHGG.2021.100033

Denu, J. M., & Tanner, K. G. (1998). Specific and reversible inactivation of protein tyrosine phosphatases by hydrogen peroxide: Evidence for a sulfenic acid intermediate and implications for redox regulation. *Biochemistry*, *37*(16), 5633–5642. https://doi.org/10.1021/BI973035T/ASSET/IMAGES/LARGE/BI973035TH00002.JPEG

El-Brolosy, M. A., Kontarakis, Z., Rossi, A., Kuenne, C., Günther, S., Fukuda, N., Kikhi, K., Boezio, G. L. M., Takacs, C. M., Lai, S. L., Fukuda, R., Gerri, C., Giraldez, A. J., & Stainier, D. Y. R. (2019). Genetic compensation triggered by mutant mRNA degradation. *Nature*, *568*(7751), 193–197. https://doi.org/10.1038/s41586-019-1064-z

Espinoza, S., Arredondo, S. B., Barake, F., Carvajal, F., Guerrero, F. G., Segovia-Miranda, F., Valenzuela, D. M., Wyneken, U., Rojas-Fernández, A., Cerpa, W., Massardo, L., Varela-Nallar, L., & González, A. (2020). Neuronal surface P antigen (NSPA) modulates postsynaptic NMDAR stability through ubiquitination of tyrosine phosphatase PTPMEG. *BMC Biology*, *18*(1). https://doi.org/10.1186/s12915-020-00877-2

Ferreira, F., Luxardi, G., Reid, B., & Zhao, M. (2016). Early bioelectric activities mediate redox-modulated regeneration. *Development*, *143*(24), 4582–4594. https://doi.org/10.1242/dev.142034

Gauron, C., Rampon, C., Bouzaffour, M., Ipendey, E., Teillon, J., Volovitch, M., & Vriz, S. (2013). Sustained production of ROS triggers compensatory proliferation and is required for regeneration to proceed. *Scientific Reports*, *3*(1), 2084. https://doi.org/10.1038/srep02084

Hale, A. J., & den Hertog, J. (2018). Shp2-Mitogen-Activated Protein Kinase Signaling Drives Proliferation during Zebrafish Embryo Caudal Fin Fold Regeneration. *Molecular and Cellular Biology*, *38*(4), e00515-17. https://doi.org/10.1128/MCB.00515-17

Hunter, M. V, Willoughby, P. M., Bruce, A. E. E., & Fernandez-Gonzalez, R. (2018). Oxidative Stress Orchestrates Cell Polarity to Promote Embryonic Wound Healing. *Developmental Cell*, *47*(3), 377-387.e4. https://doi.org/10.1016/j.devcel.2018.10.013

Kanwal, Z., Zakrzewska, A., den Hertog, J., Spaink, H. P., Schaaf, M. J. M., & Meijer, A. H. (2013). Deficiency in hematopoietic phosphatase ptpn6/Shp1 hyperactivates the innate immune system and impairs control of bacterial infections in zebrafish embryos. *Journal of Immunology*, *190*(4), 1631–1645. https://doi.org/10.4049/jimmunol.1200551

Landi, S., Putignano, E., Boggio, E. M., Giustetto, M., Pizzorusso, T., & Ratto, G. M. (2011). The short-time structural plasticity of dendritic spines is altered in a model of Rett syndrome. *Scientific Reports*, *1*(1), 1–7. https://doi.org/10.1038/srep00045

Lek, M., Karczewski, K. J., Minikel, E. V., Samocha, K. E., Banks, E., Fennell, T., O'Donnell-Luria, A. H., Ware, J. S., Hill, A. J., Cummings, B. B., Tukiainen, T., Birnbaum, D. P., Kosmicki, J. A., Duncan, L. E., Estrada, K., Zhao, F., Zou, J., Pierce-Hoffman, E., Berghout, J., … Williams, A. L. (2016). Analysis of protein-coding genetic variation in 60,706 humans. *Nature*, *536*(7616), 285–291. https://doi.org/10.1038/NATURE19057

Love, N. R., Chen, Y., Ishibashi, S., Kritsiligkou, P., Lea, R., Koh, Y., Gallop, J. L., Dorey, K., & Amaya, E. (2013). Amputation-induced reactive oxygen species are required for successful Xenopus tadpole tail regeneration. *Nature Cell Biology*, *15*(2), 222–228. https://doi.org/10.1038/ncb2659

McCoy, K. L., Chi, E., Engel, D., & Clagett, J. (1983). Accelerated rate of mononuclear phagocyte production in vitro by splenocytes from autoimmune motheaten mice. *The American Journal of Pathology*, *112*(1), 18. /pmc/articles/PMC1916321/?report=abstract

McCoy, K. L., Chi, E., Engel, D., Rosse, C., & Clagett, J. (1982). Abnormal in vitro proliferation of splenic mononuclear phagocytes from autoimmune motheaten mice. *The Journal of Immunology*, *128*(4).

Meng, T. C., Fukada, T., & Tonks, N. K. (2002). Reversible Oxidation and Inactivation of Protein Tyrosine Phosphatases In Vivo. *Molecular Cell*, *9*(2), 387–399. https://doi.org/10.1016/S1097-2765(02)00445-8

Nakayama, K. I., Takahashi, K., Shultz, L. D., Miyakawa, K., & Tomita, K. (1997). Abnormal development and differentiation of macrophages and dendritic cells in viable motheaten mutant mice deficient in haematopoietic cell phosphatase. *International Journal of Experimental Pathology*, *78*(4), 245–257. https://doi.org/10.1046/j.1365-2613.1997.250358.x

Nickless, A., Bailis, J. M., & You, Z. (2017). Control of gene expression through the nonsense-mediated RNA decay pathway. *Cell & Bioscience 2017 7:1*, *7*(1), 1–12. https://doi.org/10.1186/S13578-017-0153-7

Niethammer, P., Grabher, C., Look, A. T., & Mitchison, T. J. (2009). A tissue-scale gradient of hydrogen peroxide mediates rapid wound detection in zebrafish. *Nature*, *459*(7249), 996–999. https://doi.org/10.1038/nature08119

Östman, A., Frijhoff, J., Sandin, Å., & Böhmer, F.-D. (2011). Regulation of protein tyrosine phosphatases by reversible oxidation. *The Journal of Biochemistry*, *150*(4), 345–356. https://doi.org/10.1093/jb/mvr104

Paling, N. R. D., & Welham, M. J. (2005). Tyrosine phosphatase SHP-1 acts at different stages of development to regulate hematopoiesis. *Blood*, *105*(11), 4290–4297. https://doi.org/10.1182/BLOOD-2004-08-3271

Peters, G. H., Frimurer, T. M., & Olsen, O. H. (1998). Electrostatic evaluation of the signature motif (H/V)CX5R(S/T) in protein-tyrosine phosphatases. *Biochemistry*, *37*(16), 5383–5393. https://doi.org/10.1021/Bi971187l

Pike, K. A., Hatzihristidis, T., Bussières-Marmen, S., Robert, F., Desai, N., Miranda-Saavedra, D., Pelletier, J., & Tremblay, M. L. (2017). TC-PTP regulates the IL-7 transcriptional response during murine early T cell development. *Scientific Reports*, *7*(1), 13275. https://doi.org/10.1038/s41598-017-13673-w

Pirotte, N., Stevens, A. S., Fraguas, S., Plusquin, M., Van Roten, A., Van Belleghem, F., Paesen, R., Ameloot, M., Cebrià, F., Artois, T., & Smeets, K. (2015). Reactive oxygen species in planarian regeneration: An upstream necessity for correct patterning and brain formation. *Oxidative Medicine and Cellular Longevity*. https://doi.org/10.1155/2015/392476

Roy, S., Khanna, S., Nallu, K., Hunt, T. K., & Sen, C. K. (2006). Dermal wound healing is subject to redox control. *Molecular Therapy*, *13*(1), 211–220. https://doi.org/10.1016/j.ymthe.2005.07.684

Salanga, C. M., & Salanga, M. C. (2021). Genotype to Phenotype: CRISPR Gene Editing Reveals Genetic Compensation as a Mechanism for Phenotypic Disjunction of Morphants and Mutants. *International Journal of Molecular Sciences*, *22*(7). https://doi.org/10.3390/IJMS22073472

Shields, B. J., Court, N. W., Hauser, C., Bukczynska, P. E., & Tiganis, T. (2008). Cell cycle-dependent regulation of SFK, JAK1 and STAT3 signaling by the protein tyrosine phosphatase TCPTP. *Cell Cycle*, *7*(21), 3405–3416. https://doi.org/10.4161/cc.7.21.6950

Shultz, L. D., Bailey, C. L., & Coman, D. R. (1983). Hematopoietic stem cell function in motheaten mice. *Experimental Hematology*, *11*(7), 667–680. https://europepmc.org/article/med/6350031

Simoncic, P. D., Lee-Loy, A., Barber, D. L., Tremblay, M. L., & McGlade, C. J. (2002). The T cell protein tyrosine phosphatase is a negative regulator of janus family kinases 1 and 3. *Current Biology : CB*, *12*(6), 446–453. http://www.ncbi.nlm.nih.gov/pubmed/11909529

Szczałuba, K., Chmielewska, J. J., Sokolowska, O., Rydzanicz, M., Szymańska, K., Feleszko, W., Włodarski, P., Biernacka, A., Murcia Pienkowski, V., Walczak, A., Bargeł, E., Królewczyk, K., Nowacka, A., Stawiński, P., Nowis, D., Dziembowska, M., & Płoski, R. (2018). Neurodevelopmental phenotype caused by a de novo PTPN4 single nucleotide variant disrupting protein localization in neuronal dendritic spines. *Clinical Genetics*, *94*(6), 581–585. https://doi.org/10.1111/cge.13450

ten Hoeve, J., de Jesus Ibarra-Sanchez, M., Fu, Y., Zhu, W., Tremblay, M., David, M., & Shuai, K. (2002). Identification of a nuclear Stat1 protein tyrosine phosphatase. *Molecular and Cellular Biology*, *22*(16), 5662–5668. http://www.ncbi.nlm.nih.gov/pubmed/12138178

Tsutsumi, R., Harizanova, J., Stockert, R., Schröder, K., Bastiaens, P. I. H., & Neel, B. G. (2017). Assay to visualize specific protein oxidation reveals spatio-temporal regulation of SHP2. *Nature Communications*, *8*(1). https://doi.org/10.1038/s41467-017-00503-w

Ulugöl, S., Hering, L., Manzini, R., Montalban Arques, A., Gottier, C., Lang, S., Scharl, M., & Spalinger, M. R. (2019). Deletion of Protein Tyrosine Phosphatase Nonreceptor Type 2 in Intestinal Epithelial Cells Results in Upregulation of the Related Phosphatase Protein Tyrosine Phosphatase Nonreceptor Type 23. *Inflammatory Intestinal Diseases*, *4*(1), 14–26. https://doi.org/10.1159/000499157

Wiede, F., Chew, S. H., van Vliet, C., Poulton, I. J., Kyparissoudis, K., Sasmono, T., Loh, K., Tremblay, M. L., Godfrey, D. I., Sims, N. A., & Tiganis, T. (2012). Strain-Dependent Differences in Bone Development, Myeloid Hyperplasia, Morbidity and Mortality in Ptpn2-Deficient Mice. *PLoS ONE*, *7*(5), e36703. https://doi.org/10.1371/journal.pone.0036703

Wiede, F., La Gruta, N. L., & Tiganis, T. (2014). PTPN2 attenuates T-cell lymphopenia-induced proliferation. *Nature Communications*, *5*, 3073. https://doi.org/10.1038/ncomms4073

Williamson, S. L., Ellaway, C. J., Peters, G. B., Pelka, G. J., Tam, P. P., & Christodoulou, J. (2015). Deletion of protein tyrosine phosphatase, non-receptor type 4 (PTPN4) in twins with a Rett syndrome-like phenotype. *European Journal of Human Genetics*, *23*(9), 1171–1175. https://doi.org/10.1038/ejhg.2014.249

Wu, W., Hale, A. J., Lemeer, S., & den Hertog, J. (2017). Differential oxidation of protein-tyrosine phosphatases during zebrafish caudal fin regeneration. *Scientific Reports*, *7*(1), 8460. https://doi.org/10.1038/s41598-017-07109-8

Xu, M. -j., Sui, X., Zhao, R., Dai, C., Krantz, S. B., & Zhao, Z. J. (2003). PTP-MEG2 is activated in polycythemia vera erythroid progenitor cells and is required for growth and expansion of erythroid cells. *Blood*, *102*(13), 4354–4360. https://doi.org/10.1182/blood-2003-04-1308

English summary

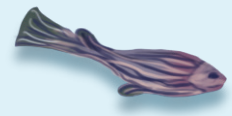

English summary

Protein tyrosine phosphatases (PTPs) have a central role in cell signaling with diverse functions in cell proliferation, migration, differentiation and apoptosis. These enzymes regulate a multitude of functions by dephosphorylating their target proteins, thereby balancing the activity of kinases. Together, kinases and PTPs guard a balance in innumerable cell signaling pathways. Loss of this balance has been linked to a plethora of human diseases, including cancer. PTPs are highly susceptible to oxidation, due to the low pKa of their active sites. Their reactive cysteine gets oxidized, which leads to the temporary inactivation of the PTP. The focus of this thesis is on several members of the classical PTP subfamily.

It has been shown in many different species that a burst of Reactive Oxygen Species (ROS) is produced upon injury. This burst of ROS plays an important role in wound healing and regeneration. However, it is not extensively known how ROS function to promote regeneration. We hypothesized that the ROS could start a signaling cascade by oxidizing PTPs. Previously, eight PTPs were identified that were specifically oxidized in response to amputation of the tail fin of adult zebrafish. One of these PTPs, Shp2a, was shown to be essential for regeneration. In **chapter 1** we give a general overview of the subjects discussed in this introduction, namely PTPs and the production of ROS upon injury. In addition, we give a summarizing introduction on the current state of knowledge of all PTPs discussed in this thesis.

In **chapter 2** we describe how we generated zebrafish knockouts of 6 PTPs that were shown previously to be oxidized upon amputation of the caudal fin and their paralogs. We show that these PTPs were not essential for regeneration. In addition, we did not recapitulate all the phenotypes we expected based on previous results with mouse mutants or transient knockdowns of the target PTPs. We hypothesize that this is due to genetic compensation.

In **chapter 3** we describe our investigation of zebrafish with a knockout of *ptpn4a*. We show that the majority of the mutant zebrafish died at the juvenile stage and suffered from epileptic seizures. This corresponds to human patients who suffer from intellectual disability and epileptic seizures due to nonsense mutations in *PTPN4*. We show that a minority of the mutant zebrafish compensated for the loss of Ptpn4a and survived, but also that a separate knockout line lost its compensation ability over time and showed enhanced lethality at the juvenile stage.

In **chapter 4** we describe our investigation of zebrafish with a knockout of *ptpn6*. We show that these mutant zebrafish displayed fully penetrant mortality at the larval stage and died from lethal hyperinflammation. This corresponds to the phenotype of the *motheaten* mice lacking SHP1 and human patients suffering from neutrophilic dermatoses and emphysema. We show that loss of Shp1 led to a reduced number of emerging HSPCs, increased HSPC proliferation, an increased number of macrophages and a decreased number of neutrophils. In addition, we show that loss of Shp1 affected the behavior of neutrophils and macrophages and led to reduced directional migration upon wounding.

In **chapter 5** we describe how we investigated the role of oxidation of Shp2a during regeneration, by creating a fusion protein consisting of Shp2a linked with Catalase. Due to the close vicinity, the Catalase protected Shp2a from oxidation. We show that by inhibiting oxidation of Shp2a, we inhibited regeneration. This indicates that transient oxidation of Shp2a is an essential step in the signaling cascade that results in regeneration. This research puts an end to the apparent paradox that Shp2a is oxidized during regeneration, but that catalytic activity of Shp2a is essential for regeneration to proceed. We hypothesize that transient oxidation of Shp2a leads to a reduction of a negative feedback loop, resulting in increased signaling activity once Shp2a is reduced again.

In **chapter 6** we discuss the findings we described in chapters 2 through 5 and what these findings mean for further research.

Nederlandse samenvatting

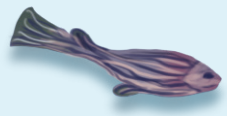

Nederlandse samenvatting

Deze thesis beschrijft onderzoek naar een aantal proteine tyrosine fosfatases (PTPs). PTPs zijn een familie van eiwitten die fosfaatgroepen van tyrosine in eiwitten kunnen verwijderen. Op deze wijze zijn fosfatases de tegenhangers van de meer bekende kinases, die fosfaatgroepen kunnen aanbrengen op aminozuren. Door het aanbrengen of verwijderen van fosfaatgroepen op eiwitten, beïnvloeden kinases en fosfatases de activiteit van de eiwitten en daarmee de signalering in cellen. Genetische fouten in kinases of fosfatases leiden tot een disbalans in deze signalering en eindigen vaak in ziektes, zoals kanker.

Alle PTPs hebben een sterk vergelijkbare actieve pocket, met diep binnenin de actieve cysteïne. Deze cysteïne is erg gevoelig voor een proces genaamd oxidatie. Door oxidatie is de cysteïne niet meer in staat om fosfaatgroepen aan te vallen, en dus is de fosfatase tijdelijk inactief. De cysteïne kan weer gereduceerd worden door reducerende eiwitten, zoals thioredoxine, en is vervolgens weer actief zoals eerder. Er is nog niet veel bekend over de precieze rol van oxidatie van eiwitten in signalering processen of over hoe dit gereguleerd wordt.

Oxidatie kan plaatsvinden door onstabiele moleculen die elektronen van andere moleculen kunnen aantrekken. We noemen deze moleculen reactieve zuurstofcomponenten (Reactive Oxygen Species, ROS) of vrije radicalen. ROS worden vaak weggez*et als* moleculen die ontstaan als schadelijk bijproduct en enkel schade veroorzaken. Echter, we weten dat ROS ook actief worden geproduceerd door cellen in bepaalde situaties. Een belangrijk voorbeeld is dat ROS worden geproduceerd in reactie op een verwonding. Dit is gevonden in allerlei organismes van simpele rondwormen tot muizen. Het wegvangen van de ROS of het blokkeren van de productie leidt tot verslechterde wondgenezing. Er is nog weinig bekend over de rol van deze ROS.

Wij vermoeden dat de ROS die geproduceerd worden bij wondgenezing, PTPs kunnen oxideren en op die manier de cel signalering beïnvloeden. Om dit te onderzoeken maken we gebruik van zebravissen. Zebravissen zijn erg bruikbaar als onderzoekmodel, omdat ze veel eitjes leggen en die eitjes zijn ook nog eens doorzichtig. Daardoor kunnen wij in zebravis-eitjes de volledige ontwikkeling van een bevruchte cel tot een larve volgen en goed onderzoeken. Zebravissen zijn ook erg goed in wondgenezing, zo goed dat beschadigde ledematen en organen kunnen terug groeien. Dit heet regeneratie. Er wordt veel onderzoek gedaan naar regeneratie, omdat we hopen dat we met die kennis de wondgenezing in mensen kunnen verbeteren. Vandaar dat we het interessant vinden om te onderzoeken welke rol de oxidatie door ROS van PTPs speelt in regeneratie.

Uit eerder onderzoek is gebleken dat 8 PTPs worden geoxideerd in reactie op amputatie van de staartvin van een zebravis. Van deze 8 PTPs bleek 1 PTP, namelijk Shp2a essentieel te zijn voor de correcte regeneratie van de staart van zebravis embryo's. In hoofdstuk 2 onderzoeken wij de overige 6 PTPs, die nog niet eerder waren onderzocht in regeneratie. We hebben met CRISPR-Cas9 de genen van de 6 PTPs aangepast, zodat er geen functioneel eiwit meer geproduceerd kan worden. We hebben dit ook gedaan voor 5 kopieën van de originele genen, zogenaamde paraloge genen. Regeneratie is niet verminderd in de zebravissen die deze eiwitten missen, dus de 6 PTPs, waar ons onderzoek zich op richtte, zijn niet essentieel voor regeneratie. Van te voren verwachtten we dat sommige zebravislijnen ziek zouden worden, omdat ze een essentieel eiwit zouden missen. Bijna al onze zebravis lijnen bleken echter gezond te zijn. Dit komt niet overeen met andere onderzoeken in muizen of in zebravissen, waar ze een andere methode hebben gebruikt om het eiwit te verminderen. Wij denken dat het gebrek aan fenotype in onze mutanten komt door een proces genaamd genetische compensatie. Bij dit proces reageert de cel op het verlies van een gen, door andere genen meer of minder te produceren en op die manier de balans te herstellen.

In hoofdstuk 3 onderzoeken we onze zebravislijn die een mutatie heeft in *ptpn4a*. We laten zien dat het grootste deel van de zebravissen met deze mutatie sterft tijdens de juveniele fase, en dat ze epileptische aanvallen ondergaan. Dit komt overeen met wat we weten van humane patiënten met een inactiverende mutatie in *PTPN4*. Zij hebben een verstandelijke beperking en last van epileptische aanvallen. We laten ook zien dat een minderheid van onze mutante zebravissen de larvale fase overleeft en leert te compenseren voor het verlies van Ptpn4a. Bovendien hebben we een tweede zebravislijn met een mutatie in *ptpn4a*, die in eerste instantie nog volledig gezond was. Pas na een paar jaar werden de mutante zebravissen van deze tweede lijn na vele uitkruisingen ook ziek en bleek de lijn dus haar compensatie voor het verlies van Ptpn4a verloren te zijn. Deze data laten zien dat genetische compensatie niet een statische situatie is, maar kan worden gecreëerd en weer wordt verloren.

In hoofdstuk 4 beschrijven we ons onderzoek naar onze zebravislijn met een mutatie in *ptpn6*. We laten zien dat deze mutatie leidt tot volledige mortaliteit in de larvale fase en dat de larven sterven aan ernstige algehele ontstekingen. Dit komt overeen met het fenotype van mutant muizen die Shp1 missen, en met mensen die mutaties hebben in *PTPN6* en vaak last hebben van neutrofiele dermatose of longemfyseem. We laten zien dat de mutatie in *ptpn6* leidt tot een verlaagd startaantal hematopoëtische stamcellen, maar dat dit gecompenseerd wordt door een verhoogde proliferatie van de stamcellen later tijdens de embryonale

ontwikkeling. Ook laten we zien dat er een verhoogd aantal macrofagen is en een verlaagd aantal neutrofielen. Bovendien hebben de macrofagen en neutrofielen meer moeite om zich te verplaatsen naar de plek van een verwonding.

In hoofdstuk 5 beschrijven we ons onderzoek naar het belang van de oxidatie van Shp2a tijdens regeneratie. Zoals eerder gezegd, weten we dat Shp2a essentieel is voor regeneratie. Echter, we weten ook dat tijdens regeneratie, Shp2a wordt geoxideerd door de ROS. In dit hoofdstuk creëren we een Shp2a die we hebben vastgemaakt aan een Catalase. Catalase verwijdert H_2O_2, een belangrijke ROS. We laten zien dat de Catalase ervoor zorgt dat Shp2a veel minder wordt geoxideerd dan normaal. Vervolgens laten we zien dat regeneratie niet gebeurt als het Shp2a-Catalase eiwit actief is in plaats van normale Shp2a. Deze data laat zien dat de oxidatie van Shp2a een essentiële stap is in het proces van regeneratie. Wij denken dat dit komt doordat oxidatie van Shp2a ertoe leidt dat de negatieve feedback-loop stopt. Wanneer Shp2a vervolgens weer wordt gereduceerd en actief wordt, is zijn signalering een stuk sterker, doordat de negatieve feedback-loop nog uit staat.

In hoofdstuk 6 bediscussiëren we de resultaten die we hebben beschreven in deze thesis en wat dit betekent voor toekomstig onderzoek.

Curriculum vitae

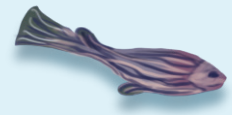

Curriculum vitae

Maaike Allers is geboren op 4 januari 1993 te Nieuwegein. In 2011 ronde zij haar gymnasium opleiding af op het Oosterlicht College in Nieuwegein, met het dubbelprofiel Natuur en Gezondheid en Natuur en Techniek. In september 2011 begon ze aan de bacheloropleiding Biomedische Wetenschappen aan de Universiteit Utrecht, waar ze Cum Laude afstudeerde. Aansluitend volgde zij van 2014 tot 2017 de masteropleiding Cancer, Stem Cells and Developmental Biology aan dezelfde universiteit. Als onderdeel van deze opleiding heeft Maaike een stage van 10 maanden uitgevoerd in het lab van Prof. Dr. Susanne Lens in het Universitair Medisch Centrum Utrecht, waar ze onderzoek deed naar het eiwit Kinesin family member 20A. Vervolgens heeft zij een onderzoeksstage van 6 maanden gedaan bij Somantix BV., gelokaliseerd te Utrecht. Hier werkte Maaike mee aan onderzoek naar stoffen die angiogenese remmen en kwam zij voor het eerst in aanraking met het gebruik van zebravissen voor biomedisch onderzoek. Hierdoor geïnspireerd, heeft Maaike ten laatste nog een onderzoeksstage van 6 maanden uitgevoerd in het lab van dr. Darren Gilmour in het European Molecular Biology Laboratories Heidelberg. Tijdens deze stage deed Maaike onderzoek naar mesenchymale naar epitheliale transities in cellen van het zijlijnorgaan in zebravissen. In de zomer van 2017 begon Maaike aan haar PhD in het lab van Prof. Dr. Jeroen den Hertog in het Hubrecht instituut in Utrecht. Haar PhD onderzoek richtte zich op de rol van 11 specifieke protein tyrosine fosfatases in de regeneratie en embryonale ontwikkeling van zebravissen. Na afloop van haar PhD, werkte Maaike in 2022 tijdelijk als secretaris van de Instanties voor Dierenwelzijn van de Koninklijke Nederlandse Academie van de Wetenschappen. Sinds 2023 werkt Maaike bij de Nederlandse Wetenschappelijke Organisatie als programma coördinator in het domain Exacte en Natuurwetenschappen.

Dankwoord

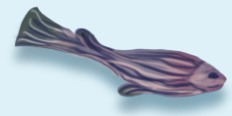

Dankwoord

Ik heb sinds 2017 heel veel over mijzelf en over de wetenschap geleerd. Tijdens mijn PhD-project mocht ik iedere dag met het mooiste proefdiermodel ter wereld werken. Het voor mijn ogen zien ontstaan van een compleet organisme vanuit een enkele eicel, bleef tot de laatste dag prachtig om mee te maken. In dit dankwoord wil ik daarom iedereen van harte bedanken die dit voor mij mogelijk heeft gemaakt.

Graag bedank ik als eerste mijn promotor **Prof. Jeroen Bakkers**. Hartelijk bedankt voor het vertrouwen dat u in mij heeft getoond door de jaren heen.

Veel dank ben ik ook verschuldigd aan mijn promotor **Prof. Jeroen den Hertog**. Ik heb mijn onderzoek uitgevoerd in jouw lab, en zonder jouw steun en advies was dit proefschrift er nooit gekomen. Bedankt voor jouw sturing tijdens het project en het meedenken over wat de resultaten zouden kunnen betekenen. Ik heb me door jouw leiderschap altijd op mijn plek gevoeld in het lab. Jouw snelle reactietijd en uitgebreide feedback op alle geschreven stukken, zijn ook van onschatbare waarde geweest tijdens het schrijven van dit proefschrift.

Van net zulke onschatbare waarde is alle ondersteuning die ik heb gekregen van mijn overige collega's. **Alexander**, je was al bijna klaar toen ik begon, maar ik heb mijn onderzoek mogen bouwen op jouw uiterst sterk onderbouwde en goed gedocumenteerde resultaten. Dankjewel voor je harde werk! **John**, je bent een onmisbare bouwsteen in het Hubrecht instituut. Veel dank voor je altijd vriendelijke ontvangst en natuurlijk voor al je essentiële ondersteuning in het kloneren voor het lab. **Petra**, jij was reeds een ervaren PhD-student toen ik begon in het lab. Heel erg bedankt voor al het werk dat jij al had gedaan in het maken van werkende protocollen, dat heeft mijn onderzoek zeker makkelijker gemaakt. Ik ben erg blij dat we samen hebben kunnen bijdragen aan het publiceren van de interessante resultaten over de Shp1 knock-out. **Maja**, dankjewel voor je rustige aanwezigheid en alle ervaring die jij meebracht. Ik heb een hoop advies van je mogen ontvangen en dat heeft mijn onderzoek zeker vooruit geholpen. **Ouyang**, we lived through our PhD times together, although your experience differed a lot from mine, being on the other side of the world from your home country. Thank you for always being a listening ear. I really liked our dinners with Liyu and Sebastiaan and I am happy I got to know a bit about Chinese culture and cuisine via you. I hope you and Liyu are doing well living at home and hopefully we will get to see each other once more in the future.

Jelmer, je was altijd vrolijk en wist werkelijk alles van het lab. Veel dank voor alles wat je me hebt geleerd, maar ook voor je altijd vriendelijke aanwezigheid! Via jou leerde ik ook **Marloes** beter kennen, Marloes dankjewel voor alle gezelligheid tijdens de evenementen waar Jelmer je weer mee naartoe sleepte. **Wouter**, ook wij hebben onze PhD trajecten haast gelijktijdig doorlopen. Je brengt een enorme berg enthousiasme mee voor elk project wat je aanpakt, in de wetenschap maar ook daarbuiten. Bedankt voor alle energie die jij altijd op iedereen weet over te brengen. **Sasja**, met jou heb ik veruit de meeste tijd doorgebracht binnen en buiten het lab. Wat was het fijn om een collega te hebben met wie het zo goed klikte. Dankjewel voor alle gesprekken en uiteraard je mentale steun. Het begint erop te lijken dat je gelijk had en dat de promotie nu toch echt goed komt. Gelukkig hebben we nog steeds contact en met onze kinderen in dezelfde leeftijd, zullen we elkaar in de toekomst vast en zeker nog eens zien!

Daniëlle, je was mijn eerste student en wat was je een geschenk uit de hemel! Het klikte direct tussen ons, en ik ben erg blij dat ik een rol heb kunnen spelen in hoe jij je eigen pad hebt gevonden. Ik hoop dat we elkaar niet uit het oog verliezen en ik kijk erg uit naar jouw eigen boekje over een paar jaar! **Fereshte**, mijn tweede student, wat heb ik een bewondering voor hoe jij je plek hebt gemaakt in Nederland. Ik hoop dat de toekomst jou en je familie goed gezind is. Je werk ethiek is formidabel en je hebt een hoop nuttige resultaten geboekt. Het einde van ons praktisch werk samen was abrupt en een grote schok door de plotselinge Covid-sluiting, maar je hebt er alsnog een mooie eindverslag van weten te maken. Ik vind het erg gezellig dat we elkaar nog steeds spreken. **Tieme,** je werkte als student voor Maja, maar je vond het geen enkel probleem om ook een aantal van mijn histologie samples mee te nemen. Super bedankt voor je belangloze inzet! **Alle overige studenten**, groot en klein, die bij het Den Hertog lab voorbij zijn gekomen, bedankt voor jullie bijdragen en jullie gezelligheid!

Marieke, Jisca, Pakize en **Ronnie**, tegen de tijd dat jullie bij het lab kwamen werken, was ik veranderd in een weinig sociale brombeer met een slaaptekort en te weinig tijd, mijn excuses daarvoor! Bedankt voor jullie collegialiteit en ik hoop dat het jullie allen goed gaat. **Alle overige collega's** van het Hubrecht, samen maken het instituut, dus ik wil jullie allen bedanken voor jullie vriendelijkheid, inzet en bereidheid om mee te denken over alle onderzoeksprojecten.

Extra nadruk verdienen natuurlijk de medewerkers van de zebravis faciliteit, **Mark, Ben, Miranda, Erma, Rob, Bert** en **Luuk.** Zonder jullie werk om de zebravissen dag en nacht in goede conditie te houden, zou dit onderzoek er nooit geweest zijn. Bedankt voor alles wat jullie doen!

Niels, in korte tijd hebben wij, samen met Jelmer, een prachtig resultaat geboekt met de Catalase-Shp2a fusie eiwitten. Ik hoop dat er ooit nog een mooi paper van komt, om ons werk aan de wereld te laten zien. Dankjewel voor de fijne samenwerking!

Nanneke wij leerden elkaar kennen tijdens onze inzet om het onderzoek met zebravissen nog beter te maken. Ik vond je een hele fijne collega. Nogmaals bedankt voor jouw vertrouwen in mij om de werkzaamheden van Sophie te vervangen tijdens haar verlof, het bleek precies het soort werk te zijn waar ik naar op zoek was. On that note, **Sophie, Willem, Ruben** en **Michiel** ik leerde jullie pas kennen na mijn praktische PhD werkzaamheden, maar wel tijdens het schrijven van dit boekje. Ik heb heel veel van jullie verschillende werkstijlen geleerd. Bedankt voor jullie altijd aanwezige vertrouwen in dat ik dit boekje zou kunnen afronden.

En dat brengt ons naar de tweede helft van het dankwoord. **Mariska**, wat leuk dat we na al die jaren nog steeds bevriend zijn, ondanks dat we toch al jaren een heel stuk bij elkaar uit de buurt wonen. Ik hoop dat we er nog heel wat jaren vriendschap aan vast kunnen plakken. **Linda, Levi** en **Frank**, toen ik aan mijn PhD begon duurden onze filmavondjes nog tot diep in de nacht. Tegenwoordig zijn het vaker theemiddagen inclusief kinderen, maar we lachen nog steeds wat af. Wat is het fijn dat we altijd onze verhalen bij elkaar kwijt kunnen en overal de humor van inzien. Op de momenten dat ik soms niet meer wist waar ik de energie vandaan moest halen, kon ik altijd op jullie rekenen. Ik hoop dat we dit volhouden tot we straks allemaal ver in ons pensioen zijn.

Aan mijn gehele directe familie (hier komen jullie, in random volgorde**) Susanne, André, Karin, Paul, Fenna, Mike, Luca, Cas, Mel, oma Truus, Mary-Ann, Monique, Richard, Stan, Fleur, Mara, Dirk, oma Toos, opa Bart** en **Anneke**, super bedankt voor jullie interesse door de jaren heen en jullie vragen over wanneer het dan af zou zijn… Nu kunnen jullie dan eindelijk het hele boekje lezen, veel leesplezier!

Ik heb ook veel steun mogen ontvangen van mijn schoonfamilie, **Mieke, Menno, Anne-Marie** en **Marjoleine.** Jullie ouderlijk huis is een plek waar we altijd welkom zijn. We zijn ook erg blij dat Floris er al helemaal bij hoort, en dat de baby in een zelfde bad van liefde terecht zal komen. Bedankt voor alle steun, alle oppashulp (dat zal nog wel veel vaker voorkomen) en natuurlijk de praktische tips over PhD's en promoties!

Mijn lieve lieve paranimfen, **Sanne** en **Cas**, wat ben ik blij dat jullie deze promotie samen met mij willen doen. Sanne, jij hebt al sinds de basisschool meer hooi op je vork dan 5 normale mensen aankunnen, maar je hebt toch (meestal) nog tijd voor ons als familie

(en de rest van Nederland). Wat ben ik trots dat jij mijn zus bent. Ik hoop dat je naast alle drukte, ook nog energie blijft hebben om te genieten van alle leuke dingen die je doet. Cas, ik kan met bewondering kijken hoe jij met iedereen een gesprek aan kan knopen en naar het netwerk van vrienden dat je al jaren onderhoudt door half Nederland. Ik ben super trots op hoe je je eigen weg hebt gevonden, ondanks je drie moeders die je in de weg stonden! Ik hoop dat die weg je erg gelukkig maakt.

Papa en **mama**, we kunnen altijd m*et al*les bij jullie terecht. Van advies over werk tot klusjes in huis, we rennen m*et al* onze problemen naar jullie toe. Van kinderen kom je nooit af, zelfs ni*et al*s ze zelf kinderen hebben, dat blijkt maar weer. Super bedankt voor het klussen, het gratis inwonen bij jullie toen we geen huis hadden, het lenen van alle kampeerspullen, de vakanties samen, de ontelbare borrels en diners en tegenwoordig ook ontbijtjes op zondagochtend, alle advies over alle problemen en waarschijnlijk nog wel honderd dingen die ik hier vergeet. En natuurlijk ook heel erg bedankt voor alle zondagen dat jullie op Floris gepast hebben het afgelopen jaar, zodat ik dit proefschrift kon schrijven. Zonder jullie steun was ik nooit zover gekomen. Jullie zijn de beste ouders die ik kan bedenken!

Over beste personen gesproken, lieve **Sebastiaan**, laat ik maar bij het begin beginnen. Toen wij dan toch eindelijk gingen daten, was het voor ons beiden vrij snel duidelijk dat we ware hadden gevonden. Er is niemand anders bij wie ik zo totaal mezelf ben als bij jou. Samen zijn we toch nog wel een stuk volwassener geworden dan we destijds waren, en samen hebben we onze eigen plek in deze wereld gemaakt. Jij hebt een ongelofelijke hoeveelheid moeite bijgedragen aan dit proefschrift, dus eigenlijk verdien je veel meer dan alleen dit stukje tekst. Dankjewel voor al je uitleg over Python, over data analyse en over hoe ik de figuren kon maken. Dankjewel voor alle code die je voor mij hebt geschreven als het mij toch te moeilijk was. Dankjewel voor al het proeflezen van alles. Dankjewel voor je steun als ik niet wist hoe ik met situaties op het werk om moest gaan. Dankjewel voor alle keren dat jij de klusjes in huis opknapte, zodat ik in het weekend kon gaan werken of aan dit proefschrift kon schrijven. Dankjewel voor alle keren dat we voor/na familiebezoek bij het Hubrecht stopten, zodat ik snel mijn experiment kon doen. Dankjewel voor die keren dat je met Floris rond het instituut ging wandelen, zodat ik hem voor en na mijn experiment snel kon voeden. En dankjewel voor alles wat je hebt gedaan, waar ik nu niet aan denk. Je hebt me nooit het gevoel gegeven dat het teveel werk was, je zei altijd dat het prima was, omdat dit belangrijk was voor mij. Je bent een geweldige partner en vader, zonder jou had ik het afmaken van mijn PhD nooit kunnen combineren met het krijgen van een kind. Nu dit avontuur dan toch echt is afgerond, is het tijd om ons gezin uit te breiden met een tweede wonder.

Om af te sluiten, lieve **Floris**, wat zijn we blij met jou en wat houden we allemaal verschrikkelijk veel van je. Jij bent ons eerste wonder en je bent nog leuker en grappiger en slimmer en liever dan we van te voren hadden bedacht dat je zou zijn. Ik kan niet wachten om nog heel veel jaren van je te genieten.